ISTANBUL TECHNICAL UNIVERSITY ★ GRADUATE SCHOOL OF EARTHQUAKE ENGINEERING AND DISASTER MANAGEMENT

THE ASSESSMENT OF THE VARIANT MODAL PUSHOVER ANALYSIS PROCEDURE FOR SPECIFIC BUILDINGS SUBJECTED TO BIDIRECTIONAL GROUND MOTIONS

M.Sc. THESIS

Özge OSMAK

Department of Earthquake Engineering

Earthquake Engineering Programme

DECEMBER 2019

ISTANBUL TECHNICAL UNIVERSITY ★ GRADUATE SCHOOL OF EARTHQUAKE ENGINEERING AND DISASTER MANAGEMENT

THE ASSESSMENT OF THE VARIANT MODAL PUSHOVER ANALYSIS PROCEDURE FOR SPECIFIC BUILDINGS SUBJECTED TO BIDIRECTIONAL GROUND MOTIONS

M.Sc. THESIS

Özge OSMAK
(802171213)

Department of Earthquake Engineering

Earthquake Engineering Programme

Thesis Advisor: Prof. Dr. Ercan YÜKSEL
Thesis Co-Advisor: Assist. Prof. Dr. Melih SÜRMELİ

DECEMBER 2019

ISTANBUL TEKNİK ÜNİVERSİTESİ ★ DEPREM MÜHENDİSLİĞİ VE AFET YÖNETİMİ ENSTİTÜSÜ

İKİ DOĞRULTUDA YER HAREKETİNE MARUZ KALAN ÖZEL BİNALAR İÇİN DEĞİŞTİRİLMİŞ MODAL İTME ANALİZİ PROSEDÜRÜNÜN DEĞERLENDİRİLMESİ

YÜKSEK LİSANS TEZİ

Özge OSMAK
(802171213)

Deprem Mühendisliği Anabilim Dalı

Deprem Mühendisliği Programı

Tez Danışmanı: Prof. Dr. Ercan YÜKSEL
Eş Danışman: Dr. Öğr. Üyesi Melih SÜRMELİ

ARALIK 2019

Özge OSMAK, a M.Sc. student of ITU Graduate School of Science Engineering and Technology student ID 802171213, successfully defended the thesis entitled "THE ASSESSMENT OF THE VARIANT MODAL PUSHOVER ANALYSIS PROCEDURE FOR SPECIFIC BUILDINGS SUBJECTED TO BIDIRECTIONAL GROUND MOTIONS", which she prepared after fulfilling the requirements specified in the associated legislations, before the jury whose signatures are below.

Thesis Advisor :	**Prof. Dr. Ercan YÜKSEL** İstanbul Technical University	....
Co-advisor :	**Assist. Prof. Dr. Melih SÜRMELİ** Bursa Technical University	....
Jury Members :	**Prof.Dr. Engin ORAKDÖĞEN** Istanbul Technical University	....
	Assoc. Prof. Dr. Hasan ÖZKAYNAK Beykent University	....
	Prof.Dr. Z.Canan GİRGİN Yıldız Technical University	....

Date of Submission : 15 November 2019
Date of Defense   : 9 December 2019

To my family,

FOREWORD

I would like to express my gratitude to Prof. Dr. Ercan Yüksel for his invaluable support and attention in the course of completing this study. It has been a great pleasure to study with him.

I would like to thank Dr. Melih Sürmeli for sharing his knowledge and experiences with me, taking time and showing all kinds of support during my graduate education, like in my undergraduate education.

Finally, I am grateful to my family for their effort and support in my life.

December 2019   Özge OSMAK

TABLE OF CONTENTS

ABBREVIATIONS

ADRS	**:**	Modal displacement-modal pseudo acceleration format
AMC	**:**	Adaptive modal combination
APAM	**:**	A displacement-based adaptive procedure based on the effective modal mass combination rule
ASCE	**:**	American Society of Civil Engineers
ATC	**:**	Applied Technology Council
CM	**:**	Center of mass
CMP	**:**	Consecutive modal pushover
CQC	**:**	Complete quadratic combination
CR	**:**	Center of rigidity
CSM	**:**	Capacity spectrum method
CTBUH	**:**	Council of Tall Buildings and Urban Habitat
DAP	**:**	Displacement-based adaptive pushover
DOF	**:**	Degree of freedom
EC8	**:**	Eurocode 8
ELSA	**:**	European Laboratory for Structural Assessment
FAP	**:**	Force-based adaptive pushover
FEMA	**:**	Federal Emergency Management Agency
GLD	**:**	Gravity Load Designed
IRSA	**:**	Incremental response spectrum analysis
MCMP	**:**	Modified consecutive modal pushover
MPA	**:**	Modal Pushover Analysis
NSP	**:**	Nonlinear Static Procedure
NTHA	**:**	Nonlinear Time History Analyses
PEER	**:**	Pasific Earthquake Engineering Research Center
PGA	**:**	Peak ground acceleration
SDOF	**:**	Single Degree of Freedom System
SF	**:**	Scale factor
SPEAR	**:**	Seismic Performance Assessment and Rehabilitation
SRSS	**:**	Square root of the sum of squares
SSAP	**:**	Story shear-based adaptive pushover
VMPA	**:**	Variant modal pushover analyses
VMPA-A	**:**	Adaptive version of VMPA
2D	**:**	Two dimensional
3D	**:**	Three dimensional

LIST OF SYMBOLS

d_b	: Bar diameter
D_n	: Displacement vector for n^{th} mode
D_{mn}	: Target displacement demand at the mth DOF for n^{th} mode
D_{mn_g}	: The displacement demand at the mth DOF due to gravity loading
D_{mn_gx}, D_{mn_gy}	: The displacement demands in X and Y directions at the mth DOF due to gravity loading
$D_{mn\_g\theta}$	: The displacement demand in θ_z direction at the mth DOF due to gravity loading
D_{mn_x}, D_{mn_y}	: Target displacement demand in x and y directions at the mth DOF for n^{th} mode
D_{mn_θ}	: Target displacement demand in θ_z direction at the mth DOF for n^{th} mode
E	: Modulus of elasticity
E_s	: Modulus of elasticity for steel
E_c	: Modulus of elasticity for concrete
EI	: Flexural rigidity
I	: Moment of Inertia
f_c	: Expected compressive strength of concrete
f_y	: Expected yield strength of steel
$f_{y,eq}$	: Equivalent yield strength of beam bars.
f_{ck}	: Characteristic concrete compressive strength
f_{yk}	: Characteristic yield strength of steel
G	: Gravity load
$l_{b,av}$	: Available anchorage length
$l_{b,req}$	: Anchorage length required for full bar anchorage
L_k	: Short length of slab
L_u	: Long length of slab
M	: Mass matrix for 3D structural systems
M_i, M_j	: Bending moments at member ends
M_p	: Moment capacity
P_0	: System loading vector
P_{0n}	: System loading vector for n^{th} mode
Q	: Live load
Q_{0n}	: n^{th} mode compatible force vector obtained from elastic spectral accelerations
Q_n	: Nodal force vector which provides target displacement at the reference DOF for n^{th} mode
R	: Demand parameter of interest

$\boldsymbol{R}_g$	**:** Demand parameter of interest obtained from gravity loads
$\boldsymbol{R}_n$	**:** Demand parameter of interest for the nth mode
$\boldsymbol{R}_{n+g}$	**:** Demand parameter of interest obtained from n^{th} mode horizontal force vectors and gravity loads
$\boldsymbol{s}_n$	**:** The nth mode contribution of effective earthquake force vectors
$\boldsymbol{s}_{nx}$, $\boldsymbol{s}_{ny}$	**:** The nth mode contribution of effective earthquake force vectors for the two horizontal components of ground motion
$\boldsymbol{S}_{an\_e}$	**:** Elastic spectral acceleration for n^{th} mode
$\boldsymbol{S}_{an\_ex}$	**:** Elastic spectral acceleration of x directional earthquake for n^{th} mode
$\boldsymbol{S}_{an\_ey}$	**:** Elastic spectral acceleration of y directional earthquake for n^{th} mode
$\boldsymbol{S}_{an\_px}$	**:** Plastic spectral acceleration of x directional earthquake for n^{th} mode
$\boldsymbol{S}_{an\_py}$	**:** Plastic spectral acceleration of y directional earthquake for n^{th} mode
$\boldsymbol{S}_n$	**:** System stiffness matrix for n^{th} mode
$\ddot{\boldsymbol{u}}_{gx}$, $\ddot{\boldsymbol{u}}_{gy}$	: Horizontal acceleration components of ground motion
$\mathbf{W_p}$	**:** Plastic section modulus
$\mathbf{X,Y,Z}$	**:** Global axis system
$\boldsymbol{\Gamma_{nx}}$, $\boldsymbol{\Gamma_{ny}}$	**:** Modal participation factor of nth mode for the X and Y components of ground motion
σ	**:** Stress
σ_c	**:** Concrete stress
σ_y	: Yield stress of steel
ϕ_p	: Curvature corresponding to Mp
α_n	**:** The loading parameter for n^{th} mode

LIST OF TABLES

LIST OF FIGURES

THE ASSESSMENT OF THE VARIANT MODAL PUSHOVER ANALYSIS PROCEDURE FOR SPECIFIC BUILDINGS SUBJECTED TO BIDIRECTIONAL GROUND MOTIONS

SUMMARY

In this study, variant modal pushover analysis (VMPA) and adaptive version of VMPA (VMPA-A) were applied to evaluate the earthquake performance of asymmetric- plan buildings and high-rise buildings. These methods were implemented through MATLAB based computer programme known as DOC3D software. The 3-storey SPEAR building and the 20-storey SAC building, which are frequently used in the literature, were used as benchmark structures.

Two different approaches to estimate the displacement demands for each mode were applied. The first one is calculation of displacement demand directly from elastic spectral acceleration by using equal displacement rule. In the second approach, mode compatible force vectors are applied to structure and capacity curves of each mode is created. By converting capacity curves to modal pseudo acceleration-displacement relations, the modal capacity curves are obtained. Nonlinear time history analysis (NTHA) is performed to each modal single degree of freedom system (SDOF) and the displacement demands are calculated. The obtained results calculated from the two approaches were compared with Nonlinear Time History Analysis (NTHA) results which was performed by SAP2000 software.

In these verifications, different earthquake record groups were used for each structure. The first group of records for the SPEAR building includes 7 earthquakes from literature. The second for the 20-storey SAC building includes 14 earthquakes from the PEER NGA database. The compared parameters are storey shears, storey displacements, story drifts, column and beam curvatures.

Bi-directional ground motions are taken into account in the VMPA and VMPA-A methods by using hybrid spectrum concept, whose abscissas and ordinates are named as $\Gamma_{nx} S_{dx} + \Gamma_{ny} S_{dy}$ and $\Gamma_{nx} S_{ax} + \Gamma_{ny} S_{ay}$, respectively. As in the S_d- S_a relationship, the slope of this hybrid spectrum corresponding to a given period is equal to the square of

the angular frequency of the respective period. Thus, two horizontal component of ground motions can be considered together with the help of this spectrum.

İKİ DOĞRULTUDA YER HAREKETİNE MARUZ KALAN ÖZEL BİNALAR İÇİN DEĞİŞTİRİLMİŞ MODAL İTME ANALİZİ PROSEDÜRÜNÜN DEĞERLENDİRİLMESİ

ÖZET

Bu çalışmada, planda düzensiz ve yüksek binaların deprem performanslarını değerlendirmek üzere değiştirilmiş modal itme analizi (VMPA) ile yöntemin uyarlamalı versiyonu olan VMPA-A uygulanmıştır. Bu yöntemler MATLAB tabanlı DOC3D yazılımı vasıtasıyla uygulanmıştır. Literatürde sıkça kullanılan 3 katlı SPEAR binası ve 20 katlı SAC binası doğrulama örnekleri olarak kullanılmıştır.

Her bir mod için yerdeğiştirme taleplerini tahmin etmek için iki farklı yaklaşım kullanılmıştır. Bunlardan ilki eşit yerdeğiştirme kuralının uygulanması ile elastik spektral ivme spektrumdan yerdeğiştirme isteminin direkt olarak elde edilmesidir. İkinci yaklaşımda ise, taşıyıcı sisteme her bir titreşim modu ile uyumlu kuvvetler uygulanarak bu modlara ait kapasite eğrileri oluşturulur. Sonrasında kapasite eğrileri modal sözde ivme- yer değiştirme ilişkilerine dönüştürülerek her bir mod için modal kapasite eğrileri elde edilir. Dönüştürülmüş doğrusal olmayan tek serbestlik dereceli sistemlere uygulanan zaman tanım alanında analiz sonucu yerdeğiştirme talepleri hesaplanmaktadır. Her iki yaklaşımdan elde edilen bu sonuçlar SAP2000 yazılımı kullanılarak elde edilen doğrusal olmayan zaman tanım alanında analiz sonuçları ile karşılaştırılmıştır.

Bu doğrulamalarda, her yapı için farklı deprem kayıt grubu kullanılmıştır. SPEAR binası için olan ilk kayıt grubu literatürde yer alan 7 depremi içermektedir. 20 katlı SAC binası için olan ikincisi ise PEER NGA veri tabanından alınan 14 tarihsel depremi içermektedir. Analizler sonucunda karşılaştırılan büyüklükler kat ötelenmeleri, kat ötelenmeleri oranı, kat kesme kuvvetleri ve seçilen kolon ve kirişlerdeki eğrilik değerleridir.

VMPA ve VMPA-A yöntemlerinde çift doğrultuda etkiyen depremin dikkate alınması hibrit spektrum yardımıyla yapılmaktadır. Bu spektrumda apsis ve ordinatı sırasıyla $\Gamma_{nx} S_{dx}+ \Gamma_{ny} S_{dy}$ ve $\Gamma_{nx} S_{ax}+ \Gamma_{ny} S_{ay}$ şeklindedir. S_d- S_a ilişkisindeki gibi bu hibrit

spektrumunun belirli bir periyoda karşı gelen eğimi ilgili periyodun açısal frekansının karesine eşittir. Bu sperktrum yardımıyla deprem hareketinin iki yatay bileşeni birlikte dikkate alınabilmektedir.

1. INTRODUCTION

Nonlinear Time History Analysis (NTHA) is most accurate method used in evaluation of seismic demands of the structure. However, NTHA is a complex and time-consuming process.

Nonlinear Static Procedure (NSP) is a conventional procedure used to determine seismic demands of the structure. An invariant lateral force distribution corresponding to fundamental mode shape is applied to structure. That's why, in high-rise buildings or asymmetric- plan buildings, NSPs are inadequate. So, the applicability of pushover analysis must be extended to structure which is affected by higher modes.

As a multi mode procedure, modal pushover analysis (MPA) (Goel and Chopra, 2005; Chopra and Goel, 2002, 2004a, 2004b; Chopra et al., 2004) is one of the most popular method to estimate sesimic demands of structures whose higher modes are effective. In MPA, an invariant lateral force distribution is applied to structure in each mode to its modal target displacement. The response in each mode is combined by an appropriate modal combination rule to obtain overall building response. However, MPA has some shortcomings: 1) An invariant load pattern compatible with linear-elastic mode shape is applied to structure even though mode shapes change when the inelastic deformation increase. 2) The horizontal components of ground motion are considered separately. Some modal combination methods are used to combine the demand parameters or horizontal components of ground motions. The application of modal combination methods twice may cause errors in results. Several researchers have studied to extend the MPA procedure to overcome the shortcomings of MPA.
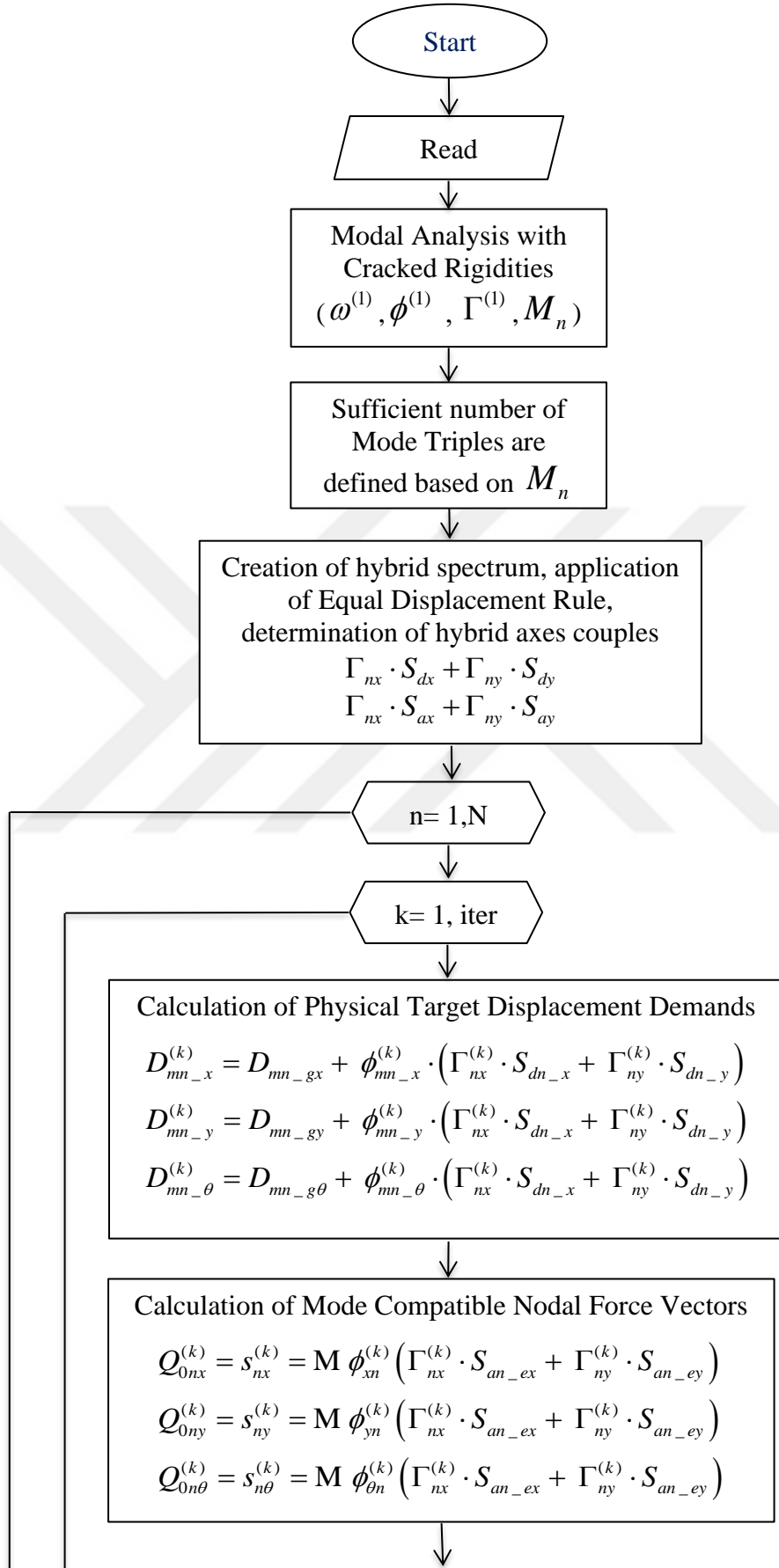
A Variant of Modal Pushover Analyses (VMPA) and adaptive version of VMPA (VMPA) have been proposed by Sürmeli and Yüksel (2015, 2018). In the adaptive version of VMPA procedure, lateral forces are recalculated at each iteration step due to the change in dynamic characteristics. The difference of VMPA from existing MPAs:
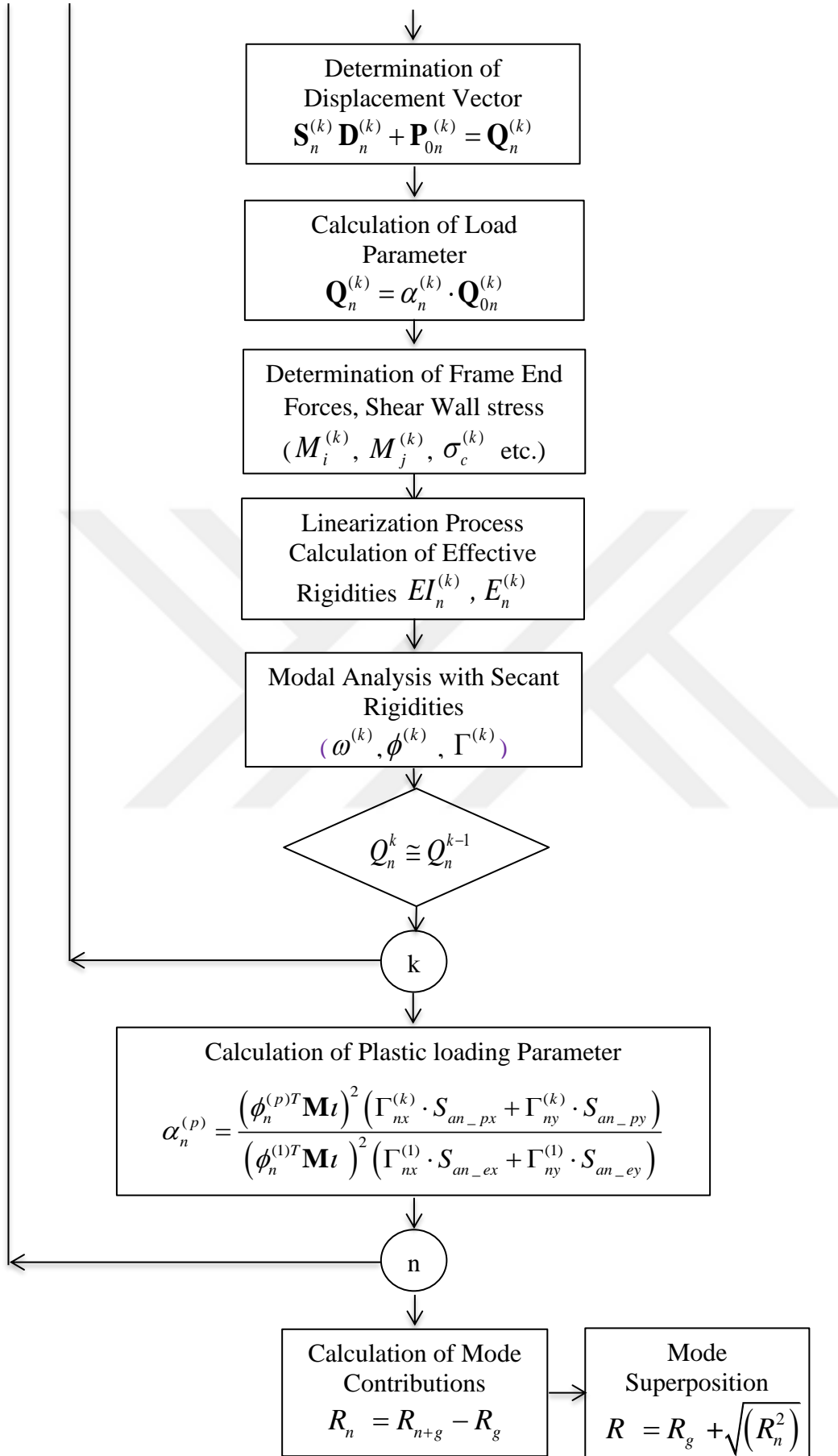
- mode compatible adaptive forces are applied to the structure at each iteration step

- bi-directional ground motions are considered with the hybrid spectrum concept. The methods of determination of seismic demands are applied together with secant stiffness based linearization in the spectral displacement (S_d) – spectral acceleration (S_a) relation. Therefore, the necessity of producing a modal capacity diagram for each mode is eliminated.

In the hybrid spectrum concept, whose absciassas and ordinates are named as $\Gamma_{nx} S_{dx} + \Gamma_{ny} S_{dy}$ ve $\Gamma_{nx} S_{ax} + \Gamma_{ny} S_{ay}$, respectively, horizontal components of an earthquake record are considered simultaneously, and this concept provides a consistency between the force and displacement vectors for each mode. As in the S_d- S_a relationship, the slope of this hybrid spectrum corresponding to a given period is equal to the square of the angular frequency of the respective period.

In this study, VMPA and VMPA-A procedures are applied by using MATLAB based computer programme DOC3D. The flow-chart of the procedure is given in Figure 1.1. First of all, modal analysis are applied with cracked rigidities to obtain initial frequency ($\omega^{(1)}$), mode shapes ($\phi^{(1)}$), modal participation factors ($\Gamma^{(1)}$) and modal mass participation ratios (M_n). Then, sufficient number of mode triples are defined based on M_n (at least 90%) and hybrid spectrum are created for each mode triple. Mode compatible force vectors for each mode (Q_n^k) are applied to the structure. Then secant based iteration process is began to tune the target displacement demands ($D_{mn\_x}, D_{mn\_y}, D_{mn\_\theta}$) until the force vectors obtained at consecutive steps are sufficiently close each other, $Q_n^k \cong Q_n^{k-1}$. Here, Q_n is compatible with the displacement vector. Finally, seismic demand obtained from each mode are combined by using SRSS combination method.

NTHA is apllied by using SAP2000 software and results obtained is accepted as "exact solution" for this thesis.

```
                              ┌──────────┐
                              │   Start  │
                              └────┬─────┘
                                   │
                              ╱────┴─────╲
                              │   Read   │
                              ╲────┬─────╱
                                   │
                          ┌────────┴─────────┐
                          │ Modal Analysis with │
                          │ Cracked Rigidities  │
```

Start

Read

Modal Analysis with
Cracked Rigidities
$(\omega^{(1)}, \phi^{(1)}, \Gamma^{(1)}, M_n)$

Sufficient number of
Mode Triples are
defined based on M_n

Creation of hybrid spectrum, application
of Equal Displacement Rule,
determination of hybrid axes couples

$$\Gamma_{nx} \cdot S_{dx} + \Gamma_{ny} \cdot S_{dy}$$
$$\Gamma_{nx} \cdot S_{ax} + \Gamma_{ny} \cdot S_{ay}$$

n= 1,N

k= 1, iter

Calculation of Physical Target Displacement Demands

$$D_{mn\_x}^{(k)} = D_{mn\_gx} + \phi_{mn\_x}^{(k)} \cdot \left(\Gamma_{nx}^{(k)} \cdot S_{dn\_x} + \Gamma_{ny}^{(k)} \cdot S_{dn\_y} \right)$$

$$D_{mn\_y}^{(k)} = D_{mn\_gy} + \phi_{mn\_y}^{(k)} \cdot \left(\Gamma_{nx}^{(k)} \cdot S_{dn\_x} + \Gamma_{ny}^{(k)} \cdot S_{dn\_y} \right)$$

$$D_{mn\_\theta}^{(k)} = D_{mn\_g\theta} + \phi_{mn\_\theta}^{(k)} \cdot \left(\Gamma_{nx}^{(k)} \cdot S_{dn\_x} + \Gamma_{ny}^{(k)} \cdot S_{dn\_y} \right)$$

Calculation of Mode Compatible Nodal Force Vectors

$$Q_{0nx}^{(k)} = s_{nx}^{(k)} = M \, \phi_{xn}^{(k)} \left(\Gamma_{nx}^{(k)} \cdot S_{an\_ex} + \Gamma_{ny}^{(k)} \cdot S_{an\_ey} \right)$$

$$Q_{0ny}^{(k)} = s_{ny}^{(k)} = M \, \phi_{yn}^{(k)} \left(\Gamma_{nx}^{(k)} \cdot S_{an\_ex} + \Gamma_{ny}^{(k)} \cdot S_{an\_ey} \right)$$

$$Q_{0n\theta}^{(k)} = s_{n\theta}^{(k)} = M \, \phi_{\theta n}^{(k)} \left(\Gamma_{nx}^{(k)} \cdot S_{an\_ex} + \Gamma_{ny}^{(k)} \cdot S_{an\_ey} \right)$$

3

Figure 1.1: Flow-chart of the proposed 3D Analysis Algorithm.

Two alternative methods were considered to estimate displacement demands of the structure. These are equal displacement rule and performing NTHA to modal SDOF.

The basic assumption of equal displacement rule is that the maximum inelastic deformation of a nonlinear single degree of freedom (SDOF) system is approximately equal to the maximum deformation of a linear- elastic SDOF system having the same stiffness as the initial stiffness of the inelastic system.

In the second approach, mode compatible force vectors are applied to structure and capacity of each mode is created. By converting capacity curves to modal pseudo acceleration-displacement relations, the modal capacity curves are obtained. Nonlinear time history analysis (NTHA) is performed to each modal single degree of freedom system (SDOF) and the displacement demands are calculated. In this study, NTHAs are performed to modal SDOF system by using SAP2000.

1.1 Aim of the Study

Developing simple analysis methods with reasonable accuracy is increased in recent years due to complex and time-consuming process of NTHA. In this context, MPA, one of the main well-known pushover procedures, is considered as an alternative to NTHA. The method may be used for 3D structures under bidirectional earthquake loadings. The main deficiencies of MPA are the invariant force distribution and consideration of bidirectional earthquake loading as the component of separate unidirectional loadings. In this thesis, the variant of modal pushover analysis (VMPA) and the adaptive version of VMPA (VMPA-A) are implemented to analyze 3D asymmetric-plan building and high-rise building subjected to bidirectional ground motions.

2. LITERATURE

The Nonlinear Static Procedures (NSPs) are accepted as practical tools to estimate seismic demands in buildings. Different seismic codes such as ATC-40 (1996), CEN (2008), FEMA-356 (2000), FEMA-440 (2005), ASCE/SEI-41 (2007); recommend the implementation of NSPs to evaluate seismic performance of buildings. Two alternative methods are recommended in current standarts to estimate the target displacement demand of the structure. These are the capacity spectrum method (ATC-40) and the displacement coeffient method (FEMA 356).

In NSPs, an invariant lateral force distribution corresponding to fundamental mode shape is applied to the structure. Therefore, the applicability of NSP is limited to low-rise buildings without torsional irregularities. Several researchers have studied to extend the applicability of pushover analysis to structure which is affected by higher modes (Antoniou and Pinho, 2004a, 2004b; Aydınoğlu, 2003; Gupta and Kunnath, 2000; Kalkan and Kunnath, 2006).

MPA procedure is the most well known multi-mode pushover analysis method (Goel and Chopra, 2005; Chopra and Goel, 2002, 2004a, 2004b; Chopra et al., 2004). In this method, a lateral load pattern, which are appropriate with discretre mode shapes, is applied to structure for each mode. The predetermined seismic demand in each mode is combined by a modal combination rule to obtain displacement demand of structure.

A consecutive modal pushover procedure (CMP) is introduced by Poursha et al. (2009) for seismic evaluation of high-rise buildings. In this procedure, lateral load patterns appropriate with linear- elastic mode shapes are applied to structure conceccutively. The procedure was also applied to asymmetric high-rise buildings by Poursha et al. (2011). Modified consecutive modal pushover analyses (MCMP) is proposed by Khoshnoudian and Kashani (2012).

Invariant force distribution is used in the multi-mode pushover analyses mentioned above. Since, the structural members of the building yield, the changes in the dynamic characteristics of the structure occurs. That's why, the lateral force distribution should

be modified in each step. Several adaptive modal pushover methods have been developed to consider the changes in dynamic characteristics. First adaptive modal pushover considers single mode behavior and this procedure is proposed by Bracci et al. (1997). In recent years, several researchers have studied on multi-mode adaptive pushover analysis. (Elnashi (2001), Aydınoğlu (2003,2004,2007), Antonio and Pinho (2004a, 2004b), Kalkan and Kunnath (2006), Shakeri et al. (2010, 2012), Abasnia et al. (2013) and, Sürmeli and Yüksel (2018). The multi-mode adaptive pushover methods can be classified into two groups as the first group, single-run pushover analysis and the second group, multi-run pushover analysis. In the first group, force or displacement distribution is calculated at each incremental step by combining mode contributions based on the instantaneous stiffness condition. In the second group, mode compatible force vectors is applied to structure separately, and the interested demand parameters are combined by an appropriate combination rule.

Force-based adaptive pushover analysis (FAP) was proposed by Elnashi (2001) and Antonioand Pinho (2004a) as a single-run pushover analysis. There is a shortcoming of FAP due to use of quadratic modal combination rule such as SRSS since the resulting forces are always positive at all story levels. To overcome this problem, *displacement-based adaptive pushover analysis* (DAP) was developed by Antonio and Pinho (2004b) as a modified vesion of FAP. In this procedure, the structure is subjected to displacements instead of forces. In this way, the sign reversal of forces at some story level is considered indirectly. When FAP and DAP procedures are compared, in predicting the earthquake demands, DAP procedure is more successful than FAP procedure (Antonio and Pinho 2004b). Another modified version of FAP, *a story shear-based adaptive pushover method* (SSAP) was developed by Shakeri et al. (2010). In the SSAP method, the structure is subjected to forces calculated by subtracting the instantaneous combined modal shear forces of the consecutive stories at each step. The implementation of the SSAP method to asymmetric-plan buildings was proposed by Shakeri et al. (2012). In this method, a lateral force in two translational directions and torques at each step are calculated by subtracting the combined modal storey shears and the combined modal story torques of consecutive storeys.

As a multi-run pushover analysis method, the adaptive modal combination (AMC) method was proposed by Kalkan and Kunnath (2006). This procedure derives its

fundamental shape from the adaptive pushover procedure of Gupta and Kunnath (2000). In the AMC method, the capacity spectrum method and the modal pushover procedure are combined without the necessity of the pre-estimation of target displacement. To estimate the dynamic target point, an energy-based methodology is utilized. In this methodology, inelastic displacement spectra with constant-ductility is used. Abbasnia et al. (2013) propose a displacement-based adaptive procedure based on the effective modal mass combination rule (APAM) to reverse the sign in the load vectors compatible with instantaneous mode shapes. In the estimation of target displacement, the method uses the same methodology with CSM and AMC. The load vector is scaled by relative mode contribution in the modal mass combination rule. The factor varies because of changes in dynamic characteristics. Modified load vectors are combined by summing/subtracting modified load vectors. Each combination is applied to the structure separately, and the envelope of the results is utilized. However, the interactions between the modes because of progressive yielding are not considered through the amalysis process in both AMC and APAM methods.

Aydınoğlu (2003,2004, 2007) proposed an incremental response spectrum analysis (IRSA) procedure. In this procedure, a piece-wise linear incremental analysis procedure is conducted between formation of consecutive plastic hinges. Modal capacity diagram are used to estimate the modal inelastic demands as the backbone curves of modal hysteresis loops. The equal displacement rule with a smoothened elastic response spectrum was mentioned by Aydınoğlu (2003). It is a practical application of the method that uses a non-iterative pushover technique, and between two consecutive plastic hinges, linear analysis is applied using an instantaneous tangent stiffness matrix. Modal displacement or load patterns is applied to structure at each incremental pushover step for the unit value of an unknown incremental scale factor. In the calculation of the increment of the generic response quantity of interest, analysis of response spectrum is utilized. The resulting forces are obtained by adding the increments to previously obtained forces via incremental scale factor. After the calculation of the incremental scale factor of all potential plastic hinges, the smallest factor is chosen as an indicator of obtainment of the next plastic hinge. The other demand parameters are obtained by incremental scale factor.

The application of multi-mode NSPs on asymmetric-plan buildings has become significant in recent years (Chopra and Goel, 2004; Perus and Fajfar, 2005; Marusic

and Fajfar, 2005; Fajfar et al., 2005; Poursha et al., 2011; Kreslin and Fajfar, 2011, 2012; Shakeri et al., 2012). This application requires 3D pushover analysis to account torsional response of the buildings.

2D NTHA is recommended in the design of tall buildings in current tall-building design codes (SEAONC, 2007; LATBSDC, 2008; CTBUH, 2008; PEER, 2010). 3D multi-mode pushover procedures have been recently extended to estimate the seismic demand of buildings subjected to bidirectional ground motion. (Lin and Tsai, 2007, 2008; Reyes, 2009; Reyes and Chopra, 2011a, 2011b; Lin et al., 2012a, 2012b; Bosco et al., 2012, 2013; Manoukas et al., 2012, 2014; Poursha et al., 2014). MPA is one of the pioneering procedures which takes the influence of bidirectional ground motions (Reyes, 2009; Reyes and Chopra, 2011a, 2011b). However, there are two shortcomings of this procedure: 1) The structure is subjected to invariant load pattern compatible withe linear-elastice mode shape. The mode shapes and natural frequencies change when the inelastic deformations increase. When unidirectional ground motion is applied to asymetric-plan buildings, deflection of the structure may not be only in the direction with the same as the direction of ground motion. It may also deflect in the perpendicular direction of ground motion and there could be rotations at the center of mass (CM). Therefore; for a selected node, three DOFs (namely, x and y translational and z rotational displacements) must be considered simultaneously in NSP procedure. Determining the displacements of three DOFs at the selected node simultaneously is not possible when the invariant load patterns are used. The dominant earthquake direction (x or y) of the building is selected as the target DOF by Reyes and Chopra (Reyes and Chopra, 2011a, 2011b). The building is pushed in this direction and the perpendicular direction is kept free. 2) The x and y components of the ground motion are considered separately in the MPA procedure. The demand parameters are combined by a CQC combination rule and an SRSS combination rule is used in the combination of two ground motion components. The combination methods are applied twice so, this may cause error in results. An equivalent single-DOF (E-DOF) system considering multi-directional seismic effects was established by Manoukas et al. (Manoukas et al., 2012, 2014). In this approach, x and y components of ground motion are accepted as proportional to each other with a scale factor ($\ddot{u}_{gx} = \kappa \ddot{u}_{gy}$). Uniaxial pushover analysis is applied in two directions separately to avoid the erroneous results

because of the application of modal combination rule. Scale factor (SF) of $_\kappa$ is assumed as 0.3.

Three-DOF modal systems (representing two modal translations and one modal rotation) were developed by Lin and Tsai (2008) to assess the demands of two-way asymmetric building under bidirectional ground motion. Afterward, Lin and Tsai (2012a, 2012b) established inelastic response spectra which are constructed from the inelastic three-DOF modal systems.

A variant modal pushover analysis (VMPA) is proposed by Sürmeli and Yüksel (2018). In this procedure, bidirectional ground motion is considered simultaneously with hybrid spectrum concept, whose absciassasand ordinates are named as $\Gamma_{nx}\ S_{dx}+ \Gamma_{ny}\ S_{dy}$ ve $\Gamma_{nx}\ S_{ax}+ \Gamma_{ny}\ S_{ay}$, respectively. In the hybrid spectrum concept, full modal capacity curve for each mode does not need to obtained to detemine seismic demands. The adaptive version of VMPA (VMPA-A) is also proposed by Sürmeli and Yüksel (2015, 2018). Change in the dynamic characteristics due to progressive yielding of the structural member is considered in this procedure.

3. CASE STUDIES

The 3-storey SPEAR building and the 20-storey SAC steel building, which are frequently used in the literature, were used as plan irregular and high-rise benchmark structures, respectively. The buildings are modeled with SAP2000 and DOC3D programmes. First of all, eigenvalue analyses are performed to provide the consistency between two programs. Secondly, pushovers analyses were conducted for fundemental modes at X and Y directions to calibrate the nonlinear behavior of the two programs. Finally, NTHAs, admitted as exact solutions, are performed by SAP2000 and the obtained demands are compared with those obtained by VMPA and VMPA-A procedures to investigate the accuracy of the methods.

3.1 SPEAR Building (Plan Irregularity)

Spear building, a full-scale gravity load designed (GLD) building under pseudo dynamic conditions was tested, and subjected to bidirectional seismic loading, at the European Laboratory for Structural Assessment (ELSA) at Ispra, within the European project Seismic Performance Assessment and Rehabilitation (SPEAR) (Stratan and Fajfar, 2003). SPEAR building represents typical existing three-storey building that was designed for gravity loads alone, in the Mediterranean region. This structure was designed using Greece's concrete design code applying between 1954 and 1995, with construction practice and material used in the early 70's, Bhatt and Bento (2011).

The building has asymmetric plan in both X and Y direction and it is regular in elevation. The storey height of the structure is 3m, with 2.5m clear height and the slab thickness is 150mm. Plan and elevation view of the building is shown in Figure 3.1. Gravity loads (G) on slabs are 0.5 kN/m^2 for finishings and 2 kN/m^2 for live loads (Q).

The material properties, cross sectional dimesions, assumptions in modelling and hinge characteristics, the used earthquake records are taken from the study conducted by Stratan and Fajfar (2003).
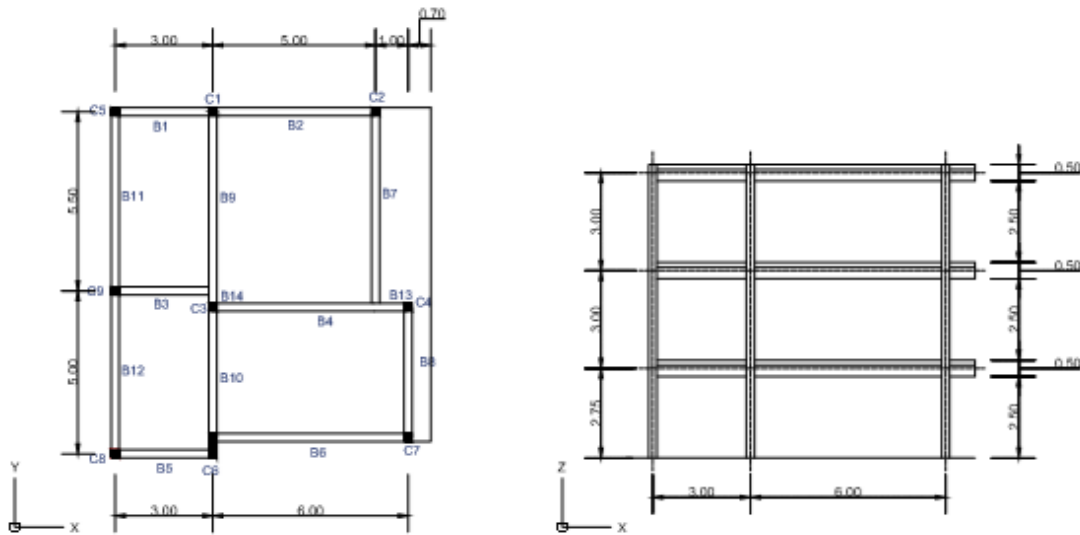
Figure 3.1: Plan and elevation view of SPEAR building.

The building has 9 columns. Only the column C6 has rectangular section of 250x750 mm with strong direction along Y axis. The other columns have square section of 250x250 mm (Figure 3.2). Further details on the structure and column and beam sections can be found in Stratan and Fajfar (2003). The main reasons of the in-plan irregularities are presence of the balcony on the east side of the structure and column C6. Since the bigger dimension of C6 is in the Y direction, center of mass (CM) was shifted away from center of rigidity (CR) and larger eccentricity occurs in this direction. As shown in Figure 3.1, column C8 is at the *stiff edge*, while column C2 is the *flexible edge* of the building.
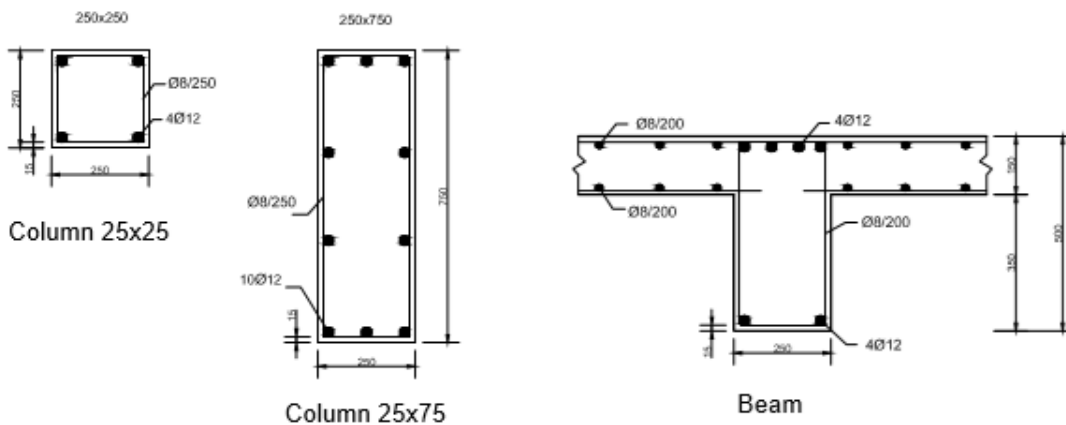
Figure 3.2: Typical column and beam cross-sections.

The confinement effects were ignored for core concrete, due to insufficient transvere reinforcement. The concrete was considered unconfined. The mean compressive strength of unconfined concrete was taken as 25 MPa (f_{ck}) and design yield strength of steel reinforcement is 320 MPa (f_{yk}). Strength degradation of concrete in compression and strain hardening of steel were considered. Expected material strengths are given in Table 3.1 and used for calculation of moment-curvature relations of members.

Table 3.1: Expected material strengths.

Concrete compression strength (f_c)	37.5 N/mm^2 (1.5 f_{ck})
Steel yield strength (f_y)	352 N/mm^2 (1.1 f_{yk})

3.1.1 Modelling of elements

The beams are modelled as T sections and effective widths (b_f) are calculated. Since the effective widths at both ends of the beams are different, beams were divided into two parts. The subscript i corresponds to ith part which is left side of the beams in X direction and bottom side of the beams in Y direction; while subscript j refers to the other part of the corresponding beams.

Because of inadequate construction practice and using of plain bars, insufficient anchorage of reinforcement was generated. In case, a procedure recommended in FEMA356 (2000), the yield strength of the bars is reduced proportionally to the ratio of available anchorage length to the one required for full anchorage:

$$f_{y,eq} = f_y \cdot \frac{l_{b,av}}{l_{b,req}}$$
(3.1)

where f_y (1.1 f_{yk}) is expected yield strength of the steel bar, $l_{b,av}$ is the available anchorage length, $l_{b,req}$ is the anchorage length required for full bar anchorage.

The bar length required for full anchorage was calculated based on Eurocode2 (1999) The bond stress of plain bars is given by

$$f_b = 0.36 \cdot \sqrt{f_c}$$
(3.2)

The required anchorage length was stated as:

$$l_{b,req} = 0.7 \cdot \frac{d_b}{4} \cdot \frac{f_y}{f_b} \tag{3.3}$$

Where d_b is diameter of the steel bar and 0.7 is a coefficient related to the existence of hook.

Table 3.2: Equivalent bar yield strength for insufficient anchorage.

d_b, mm	$l_{b,av}$, mm	$l_{b,req}$, mm	$f_{y,eq}$, N/mm^2	$f_{y,eq}/f_y$
12	220	336	231	0.66
20	220	560	138	0.39

The equivalent yield strength of beam bars has insufficient anchorage (ins, l_b=220 mm) as shown in Table 3.2. The insufficient anchorage lengths are observed generally bottom and montage bars of the beams. Column bar splices are 400 mm length and they would consider as fully anchored (full). Detailed information for beam cross sections are given in Table 3.3.

Table 3.3: Beam effective width and reinforcement details.

Element	b_f (m)	b_w (m)	h (m)	t (m)	Bott. Rein.	Top rein.	Top slab rein.
B1i,B5ij	0.750	0.25	0.5	0.15	2Φ12 ins	2Φ12 ins+2Φ12 full	3Φ8
B1j	0.750	0.25	0.5	0.15	2Φ12 ins	2Φ12 ins+4Φ12 full	8Φ8
B2i	1.250	0.25	0.5	0.15	2Φ12 ins	2Φ12 ins+4Φ12 full	12Φ8
B2j	1.250	0.25	0.5	0.15	2Φ12 ins	2Φ12 ins+2Φ12 full	15Φ8
B3i	1.500	0.25	0.5	0.15	2Φ12 ins	2Φ12 ins+2Φ12 full	8Φ8
B3j	1.500	0.25	0.5	0.15	2Φ12 ins	2Φ12 ins+2Φ12 full	8Φ8
B4i	1.750	0.25	0.5	0.15	3Φ20 ins	2Φ12 ins+4Φ20 full	14Φ8
B4j	1.750	0.25	0.5	0.15	5Φ20 full	2Φ12 full	15Φ8
B6ij	1.500	0.25	0.5	0.15	2Φ12 ins	2Φ12 ins+2Φ12 full	11Φ8
B7i	3.000	0.25	0.5	0.15	2Φ12 ins	2Φ12 ins+3Φ20 full	25Φ8
B7j	1.500	0.25	0.5	0.15	2Φ12 ins	2Φ12 ins+3Φ20 full	7Φ8
B8i	1.250	0.25	0.5	0.15	2Φ12 ins	2Φ12 ins+2Φ12 full	6Φ8
B8j	1.250	0.25	0.5	0.15	2Φ12 ins	2Φ12 ins+2Φ12 full	6Φ8
B9i	1.750	0.25	0.5	0.15	2Φ20 ins	4Φ12 ins+1Φ20 full	13Φ8
B9j	2.000	0.25	0.5	0.15	2Φ20 full	2Φ12 ins+2Φ20 full	9Φ8
B10i	1.250	0.25	0.5	0.15	2Φ12 full	4Φ12 full	6Φ8
B10j	1.250	0.25	0.5	0.15	2Φ12 ins	2Φ12 ins+2Φ12 full+2Φ20 full	8Φ8
B11i	1.375	0.25	0.5	0.15	2Φ12 ins	2Φ12 ins+4Φ12 full	9Φ8
B11j	0.750	0.25	0.5	0.15	2Φ12 ins	2Φ12 ins+4Φ12 full	2Φ8
B12i	0.750	0.25	0.5	0.15	2Φ12 ins	2Φ12 ins+2Φ12 full	2Φ8
B12j	1.250	0.25	0.5	0.15	2Φ12 ins	2Φ12 ins+4Φ12 full	9Φ8
B13i	1.750	0.25	0.5	0.15	3Φ20 full	2Φ12 ins+1Φ20 full	18Φ8
B13j	1.125	0.25	0.5	0.15	3Φ20 ins	2Φ12 ins+3Φ20 full	9Φ8
B14ij	1.750	0.25	0.5	0.15	2Φ20 ins	2Φ12 ins+2Φ12 full+2Φ20 full	19Φ8

Concentrated plasticity model was considered for inelastic flexural behavior of elements. Torsion and shear behavior were accepted as elastic in all cases.

Instead of axial-force (M-N) and biaxial moment (M-M) interaction, a standard moment-curvature analysis was implemented for each element. For columns, to obtain moment-curvature curves, axial force corresponding to gravitational loading was considered.

XTRACT software was used to obtain moment-curvature analysis. Stress-strain models for concrete and steel materials are given in Figure 3.3.
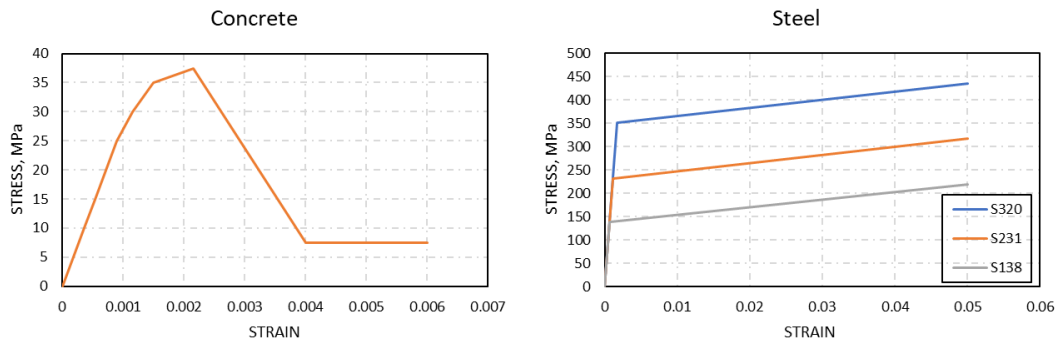
Figure 3.3: Stress-strain relations for steels and concrete.

The yield curvature and ultimate curvature, and yield moments for modelling the one-component concentrated plasticity of the SPEAR building members are presented in Table 3.4 and Table 3.5, and graphically in ANNEX A. Higher moment capacity can be observed under negative bending (top bars are in tension) at beams. Curvature capacity of columns is strongly dependent on the axial force. First storey columns subjected to higher axial force have lower curvature capacity.

Table 3.4: Yield and ultimate curvatures, and yield moments for beams.

Element	Yield Curvature(Φ_y)		Ultimate Curvature(Φ_u)		Yield Moment (kN.m)	
	POS	NEG	POS	NEG	POS	NEG
B1i,B5ij	0.002715	0.004386	0.11030	0.11320	23.84	83.20
B1j	0.002697	0.005330	0.11040	0.09906	23.74	162.20
B2i	0.002677	0.005797	0.11070	0.06623	23.87	211.70
B2j	0.002670	0.005492	0.11060	0.08189	23.84	187.10
B3i	0.002687	0.004902	0.11110	0.11540	23.93	126.30
B3j	0.002687	0.004902	0.11110	0.11540	23.93	126.30
B4i	0.001713	0.006328	0.11300	0.04276	58.58	345.40
B4j	0.004519	0.005070	0.11350	0.11370	246.40	157.50
B6ij	0.002674	0.005103	0.11110	0.10910	23.86	150.10
B7i	0.002772	0.006690	0.11200	0.04437	24.28	368.90
B7j	0.002682	0.006111	0.11130	0.05650	23.92	243.20
B8i	0.002681	0.004720	0.11060	0.11480	23.85	109.50
B8j	0.002681	0.004720	0.11060	0.11480	23.85	109.50
B9i	0.004258	0.005745	0.11300	0.09907	99.16	225.10
B9j	0.001710	0.005345	0.11370	0.06310	39.66	191.20
B10i	0.004081	0.005223	0.11070	0.11480	36.31	121.30
B10j	0.002689	0.006008	0.11090	0.05725	23.98	235.30
B11i	0.002678	0.005279	0.11070	0.10030	23.96	169.30
B11j	0.002707	0.004256	0.11020	0.11300	23.82	75.23
B12i	0.002707	0.004256	0.11020	0.11300	23.82	75.23
B12j	0.002679	0.005355	0.11070	0.09349	23.88	171.10
B13i	0.004349	0.005627	0.11310	0.11260	148.30	229.20
B13j	0.001755	0.005854	0.11230	0.05846	58.69	253.20
B14ij	0.001686	0.006293	0.11300	0.04007	39.31	318.50

Table 3.5: Yield and ultimate curvatures, and yield moments for columns.

Element	Yield Curvature(Φ_y)	Ultimate Curvature(Φ_u)	Yield Moment (kN.m)
C1	0.0120	0.0900	39.1
C2	0.0109	0.0910	38.2
C3	0.0137	0.0515	53.7
C4	0.0114	0.0657	45.1
C5	0.0111	0.1330	25.1
C6X	0.0033	0.0522	178.7
C6Y	0.0111	0.1417	60.7
C7	0.0111	0.1190	29.8
C8	0.0083	0.1300	23.4
C9	0.0111	0.1030	34.2
C10	0.0111	0.1080	31.9
C11	0.0111	0.1110	31.3
C12	0.0123	0.0750	42.2
C13	0.0118	0.0960	36.2
C14	0.0107	0.1500	22.3
C15X	0.0030	0.0630	156.1
C15Y	0.0107	0.1500	53.2
C16	0.0111	0.1330	25.4
C17	0.0107	0.1500	20.9
C18	0.0111	0.1220	28.6
C19	0.0097	0.1264	24.3
C20	0.0111	0.1420	23.8
C21	0.0111	0.1170	30.3
C22	0.0111	0.1300	26.7
C23	0.0089	0.1607	19.1
C24X	0.0022	0.0704	131.7
C24Y	0.0074	0.1630	45.0
C25	0.0092	0.1500	20.7
C26	0.0110	0.1670	18.3
C27	0.0107	0.1500	22.5

3.1.2 Validation of the mathematical model

The test building was modeled by using SAP2000 v21 software and modal results were compared with results in the paper Stratan and Fajfar (2003), taken as the basis for this structure.

Two models of the building were done in SAP2000 program. In the first one, the slabs are modeled by shell elements. The own weight of the structure is automatically calculated by the program. Additional dead loads and live loads are applied on the shell elements to compare the model with Fajfar's modal analysis results. The second model consists of only frame elements. The slab loads are applied to beams as

uniformly distributed (Figure 3.6). This model is same model with DOC3D model. The perspective views of the models are shown in the Figure 3.4.
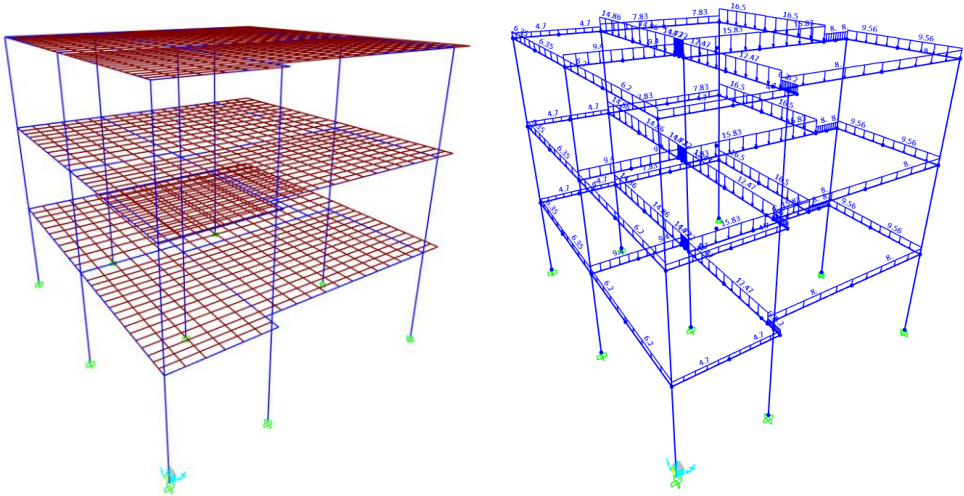
Figure 3.4: The perspective views of the models.

All beams and columns were modeled as frame members. While modelling column with rectangular section, frame member was assigned at the center of the section and connected to beam members with rigid elements. (Figure 3.5)
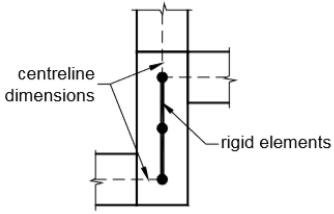
Figure 3.5: Modelling of joint at the 250x750 column.

Since beams were modeled as T shape cross-sections, masses and weights were reduced by coefficients shown in Table 3.6.

Table 3.6: Reduction factors of mass and weigth for beam cross-sections.

Element	Reduction factor of mass and weight	Element	Reduction factor of mass and weight
B1i,B5ij	0.438	B8j	0.318
B1j	0.438	B9i	0.250
B2i	0.318	B9j	0.226
B2j	0.318	B10i	0.318
B3i	0.280	B10j	0.318
B3j	0.280	B11i	0.298
B4i	0.250	B11j	0.438
B4j	0.250	B12i	0.431
B6ij	0.280	B12j	0.318
B7i	0.136	B13i	0.250
B7j	0.280	B13j	0.341
B8i	0.318	B14ij	0.250

Since the effect of the columns is more effective on the rigidity of the structure, the effect of the column reinforcement on the moment of inertia has been considered.

$$n = \frac{E_s}{E_c} = \frac{200}{27.78} = 7.19 \tag{3.4}$$

$$I = I_c + (n-1).A_s.d^2 \tag{3.5}$$

$$k = \frac{I}{I_c} \tag{3.6}$$

$E_s = 200 \ GPa$,

$E_c = 27.78 \ GPa$; $k = 1.05$

- For column with square cross- section
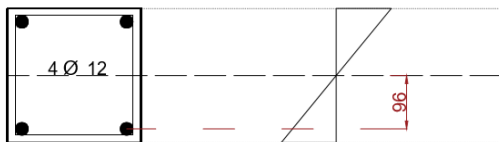
$$I_c = \frac{250.250^3}{12} = 325520833.3 \ mm^4$$

21

$$I = \frac{250.250^3}{12} + 2(7.19 - 1)(226.19)(96)^2 = 351369464.6 \ mm^4$$

$$k = \frac{I}{I_c} = 1.07$$

- For column with rectangular cross- section
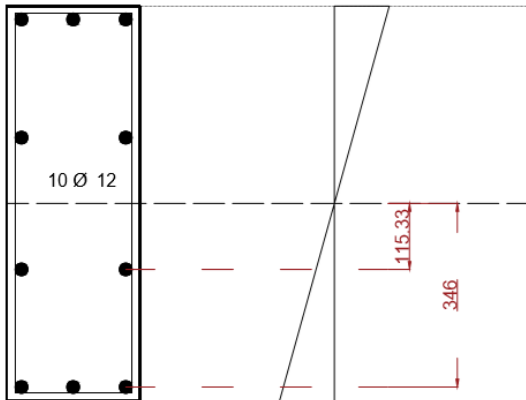
In the strong direction;

$$I_c = \frac{250.750^3}{12} = 8789062500 \ mm^4$$

$$I = \frac{250.750^3}{12} + 2(7.19 - 1)(339.29)(346)^2 + 2(7.19 - 1)(226.19)(115.33)^2 = 9292574314 \ mm^4$$

$$k = 1.05$$

In the weak direction;

$$I_c = \frac{750.250^3}{12} = 976562500 \ mm^4$$

$$I = \frac{750.250^3}{12} + 2(7.19 - 1)(452.39)(96)^2 = 1028177521 \ mm^4$$

$$k = 1.05$$

Comparison of periods, storey masses and center of masses are presented in Table 3.7. One reason for the small differences between the results may be that the beam reinforcement is not considered in the moment of inertia. However, the differences are acceptable.

Table 3.7: Comparison of period, storey masses and center of masses for linear-elastic model.

		Fajfar	SAP2000
	T_1	0.570	0.573
Period	T_2	0.484	0.484
	T_3	0.392	0.390
Mass	Floor 1&2	65.5 t	66 t
	Roof	64.1 t	64 t
Center of mass	Floor 1&2	X=4.53 m Y=5.29 m	X=4.56 m Y=5.27 m
	Roof	X=4.57 m Y=5.33 m	X=4.58 m Y=5.26 m

Since there exists no slab element and the loads can only be applied by uniformly distibured loads in DOC3D programme, triangular or trapezoidal distributed loads are assigned as equivalent uniformly loads by using the formulation shown in Figure 3.6.

All slabs in the structure transfers the loads in two way. Beams on long length carry trapezoidal distributed load and beams on short length carry triangular distributed load.
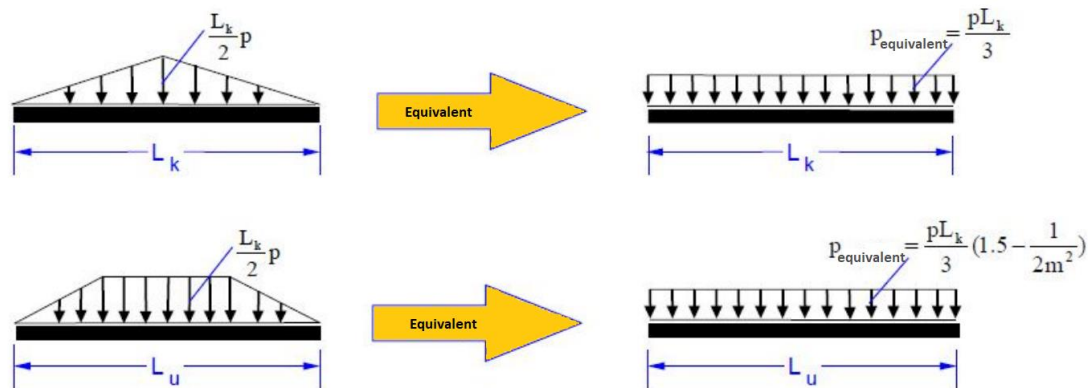
Figure 3.6: Converting triangular and trapezoidal distributed loads to equivalent uniformly distributed loads.

3.1.3 Earthquake records

As stated earlier, the used ground motion selection is taken from the study conducted by Stratan and Fajfar (2003) and they were selected from European Strong Motion Databank (Ambraseys et al., 2002). Seven ground motion records were used in this study. The criterias for selection of records were reported as magnitude (at least 5.8),

peak ground acceleration (at least 1.5 m/s^2), and compatibility to the Eurocode 8 (2002) spectrum.

Acceleration elastic response spectrum defned in Eurocode 8 (2002) is used as the target spectrum (PGA= 0.2g, soil parameter S=1, T_B=0.2s, T_C=0.6s, T_D=2.0s, 5% damping) and ground motion records were scaled to bring the mean of the earthquake spectra to the same level of intensity. The selected records and and scaling factors are presented in Table 3.8 and characteristics of the earthquake records are given in Table 3.9.

Table 3.8: Earthquake records and scaling factors.

Earthquake name	Date	Station Name	Scaling factor
Alkion	24.02.1981	Korinthos – OTE Building	1.074
Alkion	24.02.1981	Xilokastro – OTE Building	0.937
Campano Lucano	23.11.1980	Calitri	0.813
Kalamata	13.09.1986	Kalamata - Prefecture	0.791
Kalamata	13.09.1986	Kalamata – OTE Building	1.047
Montenegro	15.04.1979	Ulcinj – Hotel Albatros	0.991
Montenegro	15.04.1979	Bar – Skupstina Opstine	0.388

Table 3.9: Characteristics of the earthquake records.

Earthquake name	Epicentral Distance	Soil Category	PGA, m/s^2
Alkion	20km	Soft soil	2.26 (X), 3.04 (Y)
Alkion	19km	Alluvium	2.84 (X), 1.67 (Y)
Campano Lucano	16km	Stiff soil	1.53 (X), 1.73 (Y)
Kalamata	9km	Stiff soil	2.11 (X), 2.91 (Y)
Kalamata	10km	Stiff soil	2.35 (X), 2.67(Y)
Montenegro	21km	Rock	1.78 (X), 2.20 (Y)
Montenegro	16km	Stiff soil	3.68 (X), 3.56 (Y)

Nonlinear dynamic analysis for three-dimensional structure requires bidirectional ground motion (vertical component was not considered, Stratan and Fajfar (2003)). The procedure recommended in FEMA 356, (2000) was used in this study. Due to this procedure, two horizontal components of each record are combined with using the Square Root of the Sum of Squares (SRSS) combination method, and scaling procedure is applied to SRSS target spectrum (one-directional EC8 spectrum times $\sqrt{2}$). The error function, defined as the difference between the areas under the SRSS spectrum of a record and the SRSS of the target spectrum in the period range between

TC and TD, minimized by applying scaling procedure for each record separately. The target SRSS spectrum, the mean of SRSS spectra of scaled records, and the mean plus/minus standard deviation are presented in Figure 3.7.
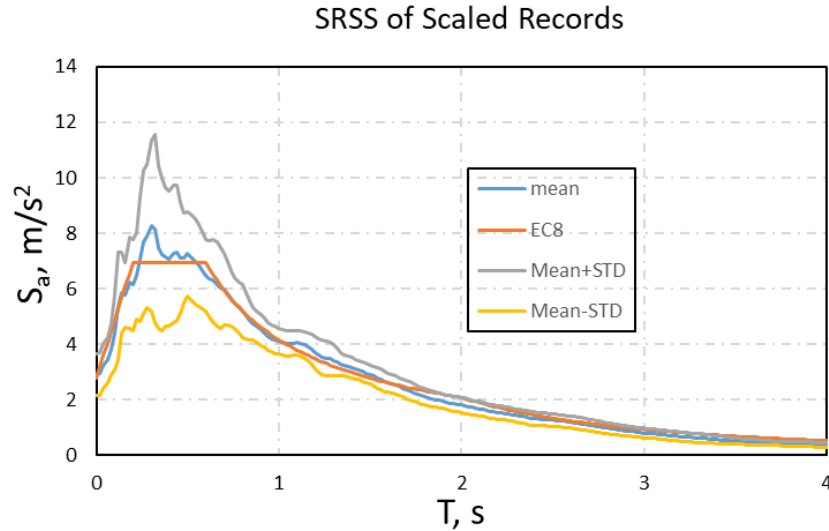
Figure 3.7: Mean of the Square Root of Sum of Squares (SRSS) of scaled records and the target EC8 spectrum.

3.1.4 Analysis

It is clear that the stiffness values of the reinforced concrete structural elements under the effect of the earthquake are different from values predicted during the design phase. For this reason, the cracked rigidities are taken into consideration to determine the structural performance of reinforced concrete bearing systems under the influence of earthquake loads. To determine cracked rigidities, moment curvature relations are idealized as bi-linear. The slope of zero to yield point of these relations are defined as the cracked flexural rigidities. The coefficients used in SAP2000 software to reduce the moment of inertia are given in Table 3.10 for beams and Table 3.11 for columns.

Table 3.10: Scale factors of beams to reduce the moment of inertia.

Element	Scale factor	Element	Scale factor
B1i-B5ij	0.163	B9i	0.257
B1j	0.262	B9j	0.209
B2i	0.326	B10i	0.168
B2j	0.247	B10j	0.273
B3ij	0.177	B11i	0.269
B4i	0.366	B11j	0.152
B4j	0.204	B12i	0.152
B6ij	0.202	B12j	0.207
B7i	0.345	B13i	0.273
B7j	0.265	B13j	0.305
B8ij	0.168	B14ij	0.322

Table 3.11: Scale factors of columns to reduce the moment of inertia.

Element	Scale factor	Element	Scale factor
C1	0.3405	C15-X	0.2131
C2	0.3875	C15-Y	0.1833
C3	0.4335	C16	0.2530
C4	0.4375	C17	0.2160
C5	0.2501	C18	0.2849
C6-X	0.2198	C19	0.2770
C6-Y	0.2016	C20	0.2371
C7	0.2969	C21	0.3019
C8	0.3118	C22	0.2660
C9	0.3407	C23	0.2373
C10	0.3178	C24-X	0.2452
C11	0.3118	C24-Y	0.2242
C12	0.3794	C25	0.2488
C13	0.3392	C26	0.1840
C14	0.2305	C27	0.2325

Modal analysis results (periods and mass participation ratios) of the structure are shown in Table 3.12. Maximum error in periods is 0.1% for mode 6. Maximum error in mass participation ratios in direction Y is about 28% for mode 7. However, the difference in mass participation ratio in direction Y is not important because the first four modes account for 90% of the total mass.

Table 3.12: Comparison of modal participation mass ratios and periods for inelastic model.

	SAP2000				DOC3D			
Mode	Period	U_x	U_y	R_z	Period	U_x	U_y	R_z
1	1.11562	0.83677	0.01800	0.02623	1.11565	0.83672	0.01805	0.02580
2	0.98643	0.03636	0.68569	0.13653	0.98648	0.03641	0.68572	0.13572
3	0.80727	0.00832	0.14167	0.72049	0.80737	0.00832	0.14162	0.72177
4	0.40115	0.08856	0.00220	0.00439	0.40121	0.08854	0.00223	0.00499
5	0.33465	0.00617	0.06782	0.03001	0.33471	0.00620	0.06776	0.03075
6	0.27213	0.00306	0.04738	0.05664	0.27241	0.00288	0.04752	0.05566
7	0.26904	0.01973	0.00026	0.00579	0.26914	0.01989	0.00019	0.00522
8	0.21928	0.00099	0.01123	0.01147	0.21941	0.00100	0.01115	0.01154
9	0.15745	0.00003	0.02574	0.00846	0.15802	0.00003	0.02576	0.00855

Hinges were asigned to both ends of members as bilinear moment-curvature relationship. The definition of some hinge properties in SAP2000 program are presented in Figure 3.8 and Figure 3.9.
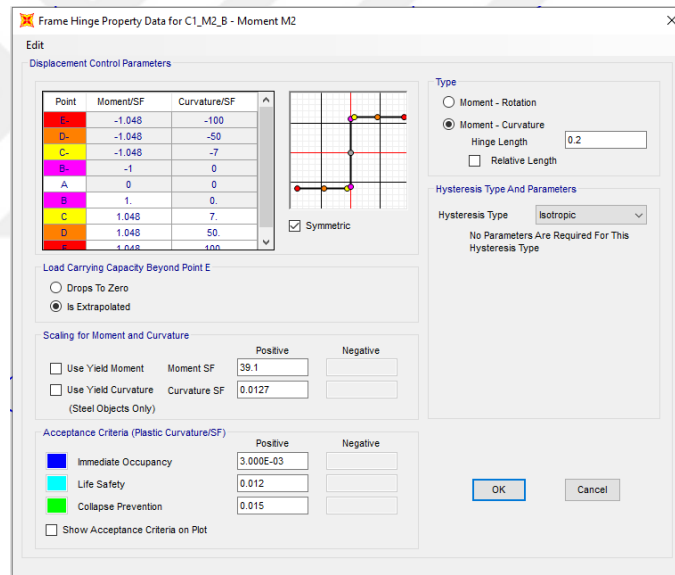
Figure 3.8: Definition of moment-curvature hinge property for columns.
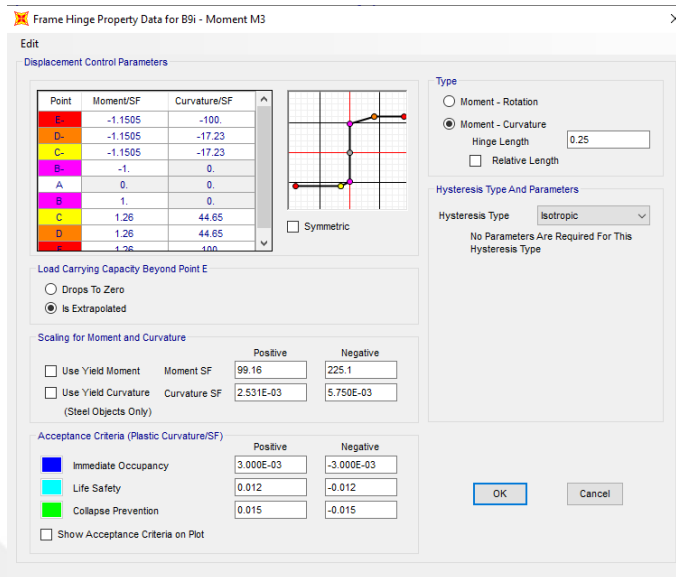
Figure 3.9: Definition of moment-curvature hinge property for beams.

Pushover analysis was applied to structure. The first and second modes that are active in the X and Y directions respectively are considered. The pushover load cases in X and Y directions defined in SAP2000 are given in Figure 3.10 and Figure 3.11.
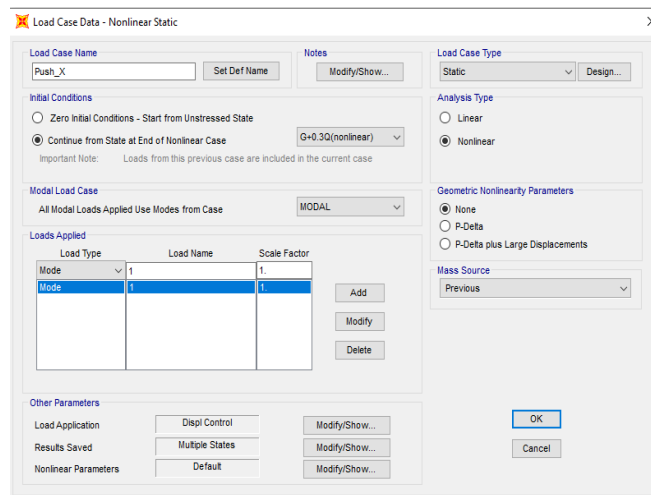
Figure 3.10: Pushover load case in X direction in SAP2000 software.
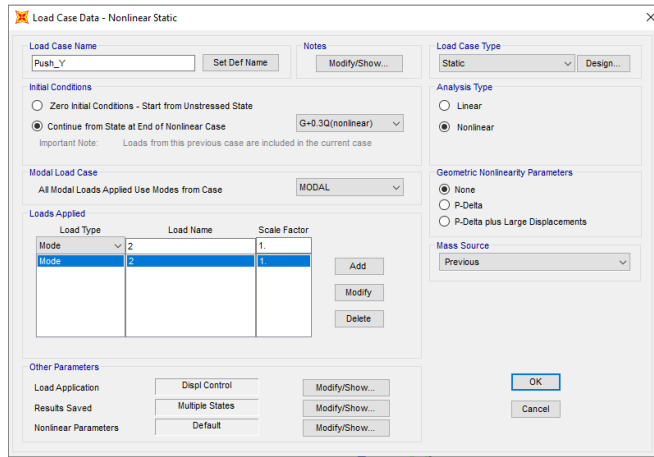
Figure 3.11: Pushover load case in Y direction in SAP2000 software.

Pushover analysis are performed by using SAP2000 and DOC3D, and the capacity curves are compared with each other in Figure 3.12 and Figure 3.13. Although the capacity curves conscide in X and -X directions, there exist minor diffference in Y and -Y directions. Therefore the nonlinear algorithm in DOC3D is validated.
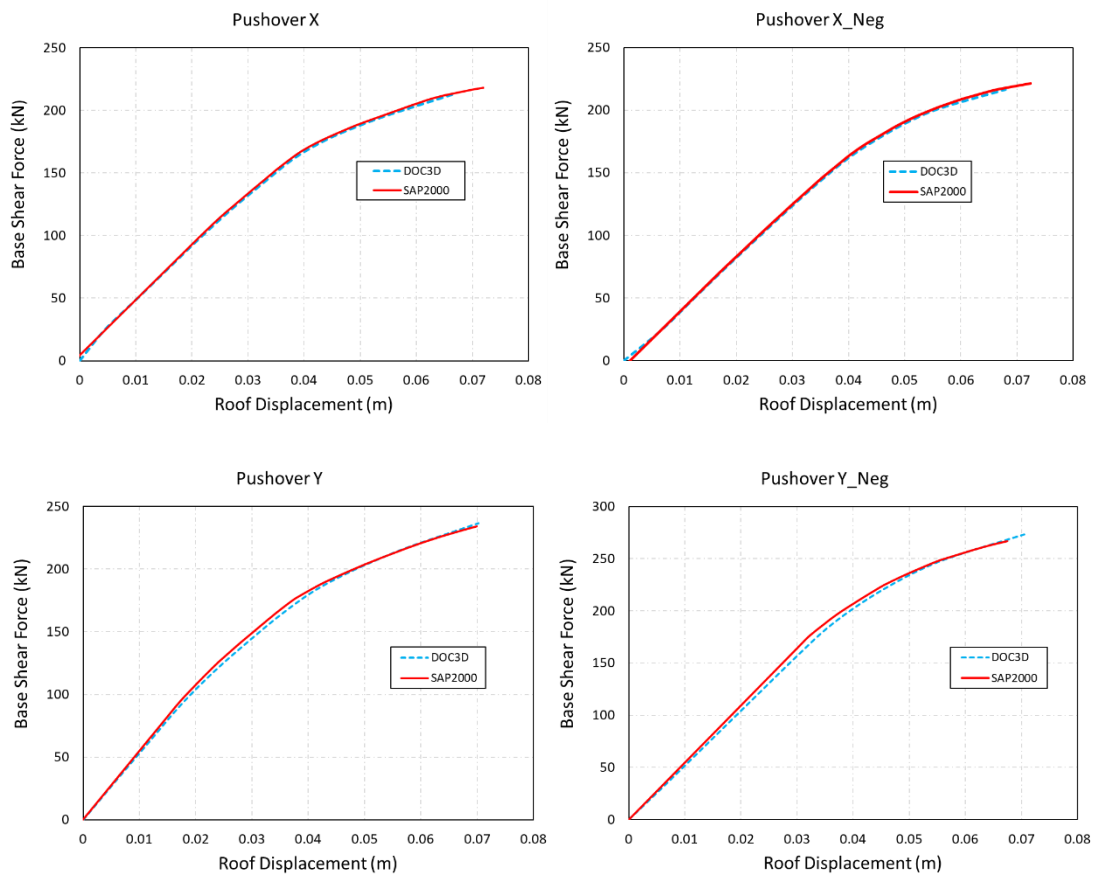
Figure 3.12: Pushover curves in the X and Y directions.

VMPA procedure is applied by using DOC3D. The results of the procedure were compared with results obtained from the NTHA to assess the success of the VMPA procedure. Two different approaches namely, equal displacement rule and application of NTHA to modal SDOF capacity curves are applied to estimate the displacement demands for each mode. The evaluated demand parameters are shear forces, storey displacements, drifts, and the distribution of column and beam curvatures.

Storey shear forces are shown in Figure 3.13. Four different combinations were considered to find maximum shear force. These combinations were created considering the positive or negative effects of Ux, Uy and Rz directions.(+++, -++, +-+, --+)
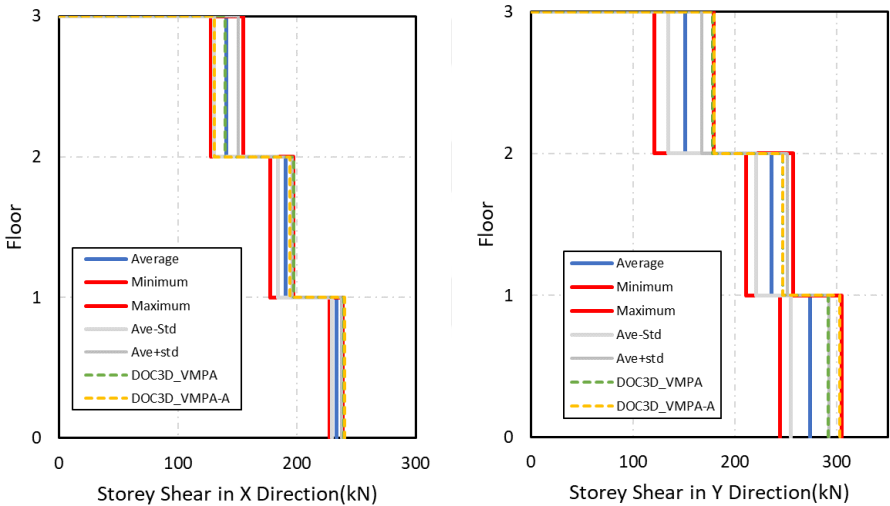
Figure 3.13: Storey shear forces in the X and Y directions.

In the graphics that show storey shear forces, blue line shows average value of NTHA results, red lines show maximum and minimum values, grey lines represent average+STD and average-STD values, green dash line shows the results obtained from VMPA with equal displacement rule, yellow dash line represents the results obtained from VMPA-A with equal displacement rule. When VMPA and VMPA-A results are compared, storey shear forces are almost the same in some floors in both direction. However, VMPA procedure results are better than VMPA-A results. If VMPA is interpreted, it is seen that shear force values in X direction have a maximum 3.9% error on the second floor. On the other hand, in the Y direction, where torsional effect is more, maximum error is 17.7% on the third floor.

Curvature values of columns are shown in Figure 3.14, Figure 3.15 and Figure 3.16. Column C2, C7 and C6 are chosen to compare curvature distribution of columns. Blue line, yellow lines and red lines represent average, average+STD and average-STD, and maximum and minimum values obtained from NTHA, respectively. Green and black dash lines represent VMPA and VMPA-A results, respectively. Graphics at the left handside show the results obtained from equal displacement rules and right handside show the results obtained from application of NTHA to modal SDOF capacity curves approach. In the X direction, for C2 column , VMPA-A results are more consistent than VMPA results. However, in the Y direction, VMPA results are better than VMPA-A. For C7 and C6 column, VMPA procedure is more accurate than VMPA-A.
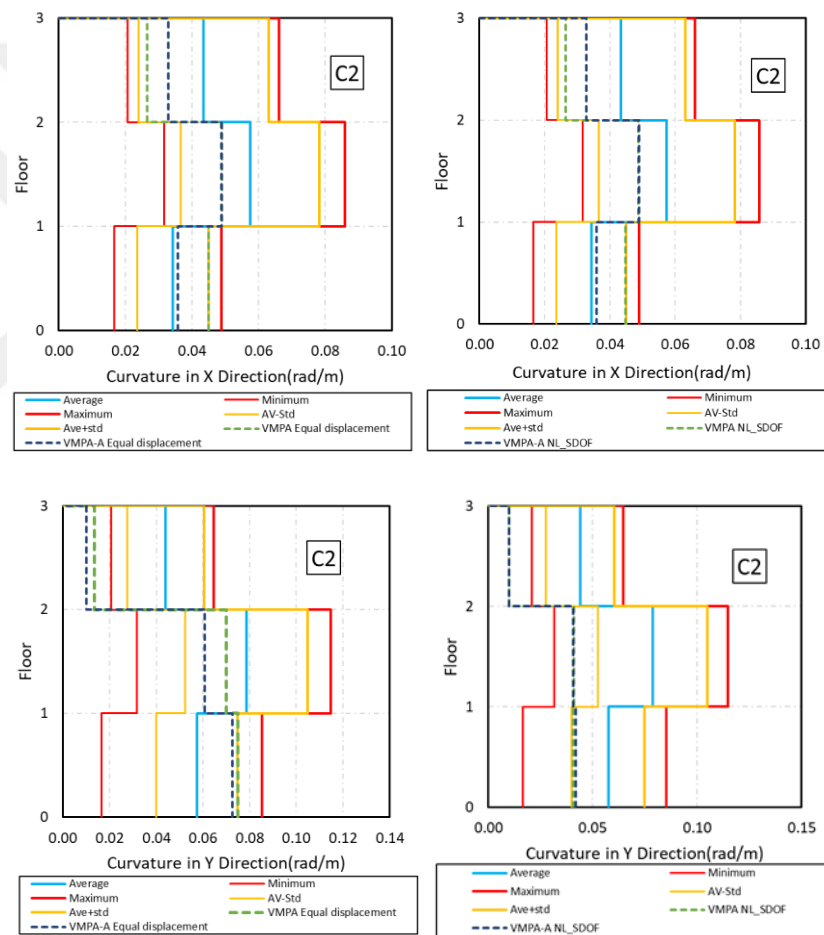
Figure 3.14: Curvature values of column C2 in the X and Y direction.
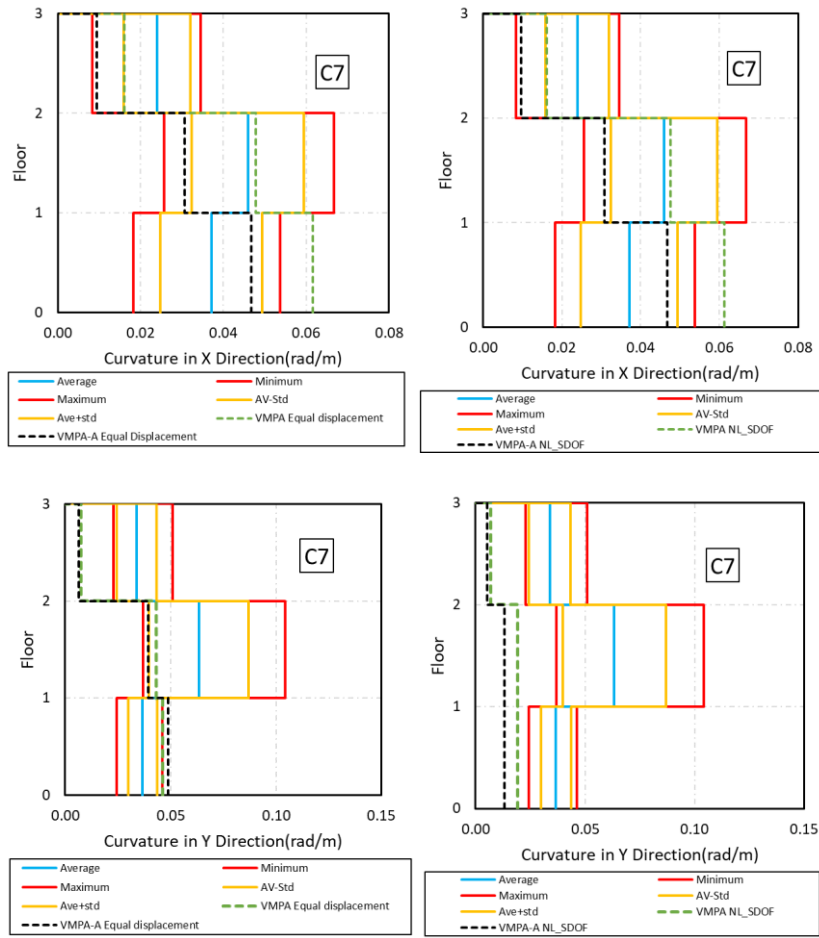
Figure 3.15: Curvature values of column C7 in the X and Y direction.
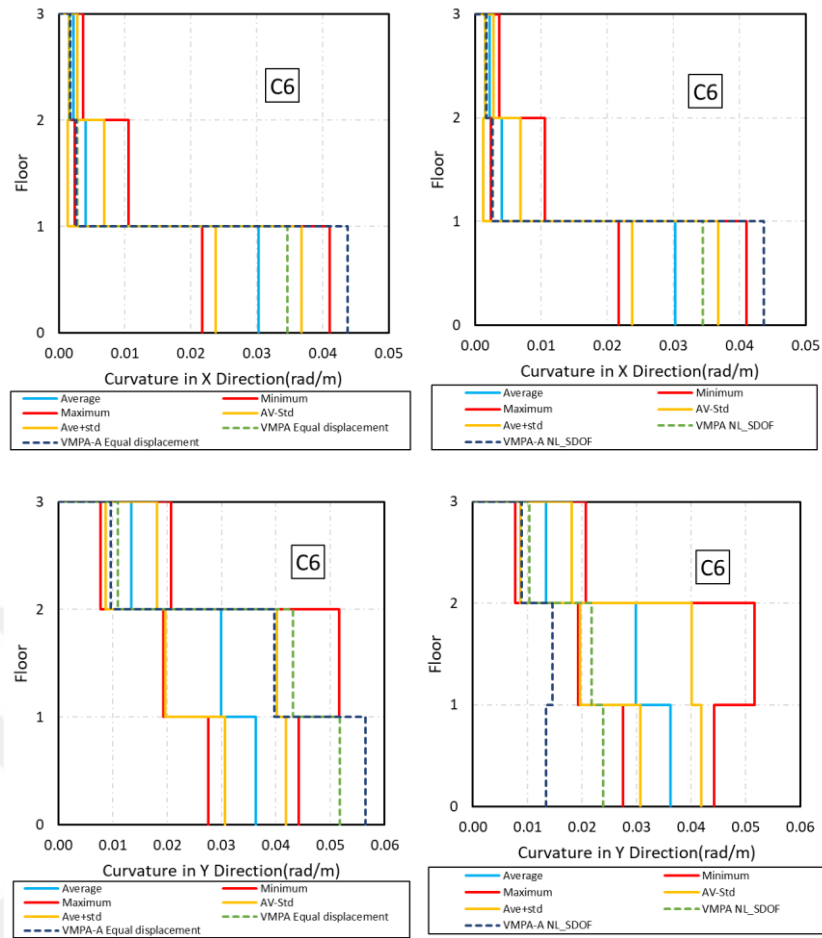
Figure 3.16: Curvature values of column C6 in the X and Y direction.

Curvature values of beams are shown in Figure 3.17, Figure 3.18, Figure 3.19 and Figure 3.20. Blue line, yellow lines and red lines represent average, average+STD and average-STD, and maximum and minimum values obtained from NTHA, respectively. Green and black dash lines represent VMPA and VMPA-A results, respectively. Graphics at the left handside show the results obtained from equal displacement rules and right handside show the results obtained from application of NTHA to modal SDOF capacity curves approach. Eight beams which are close to each corner of the structure in plan, are chosen to compare curvature values with NTHA. B5i, B6j, B1i and B2j are the beams in the X direction, and B12i, B11j, B8i and B7j are the beams in the Y direction. Based on the load direction the moment values at the supports can exceed the negative moments obtained from gravity loads. Since, the positive moment capacity of the beams are very smaller than the negative ones, positive curvatures are considered to evaluate nonlinear behavior. In the X direction, the difference between VMPA and VMPA-A results are small, especially for beam B5i which is close to stiff

edge. For beams B5i and B2j which are close to stiff and flexible edge respectively, the results are not accurate for both procedures.
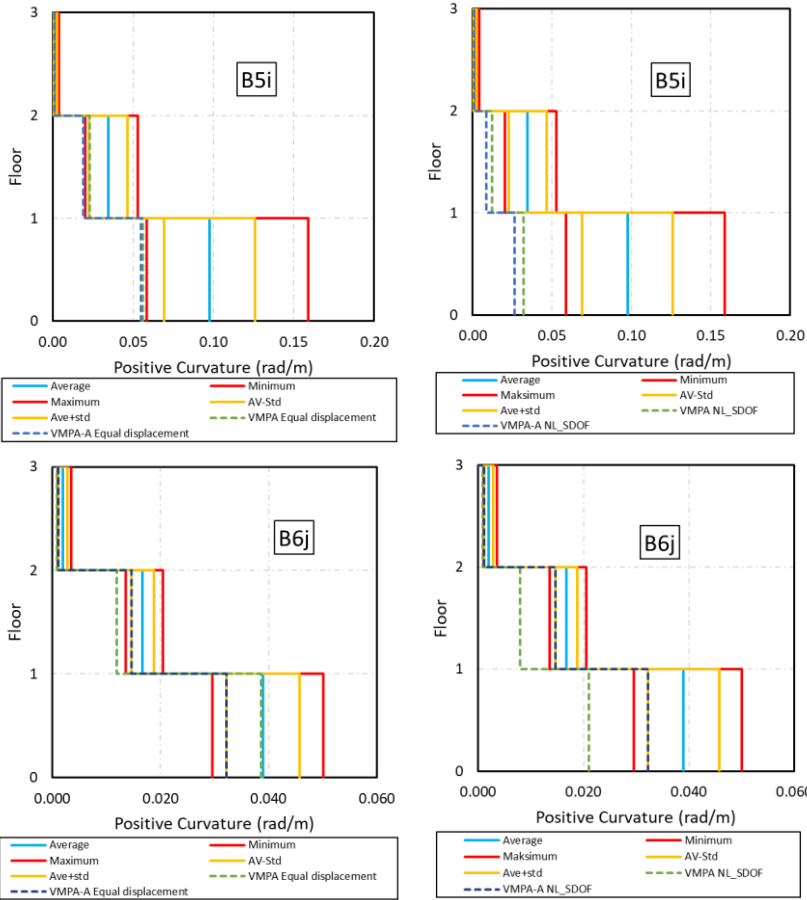
Figure 3.17: Curvature values of beams B5i and B6j in the X direction.
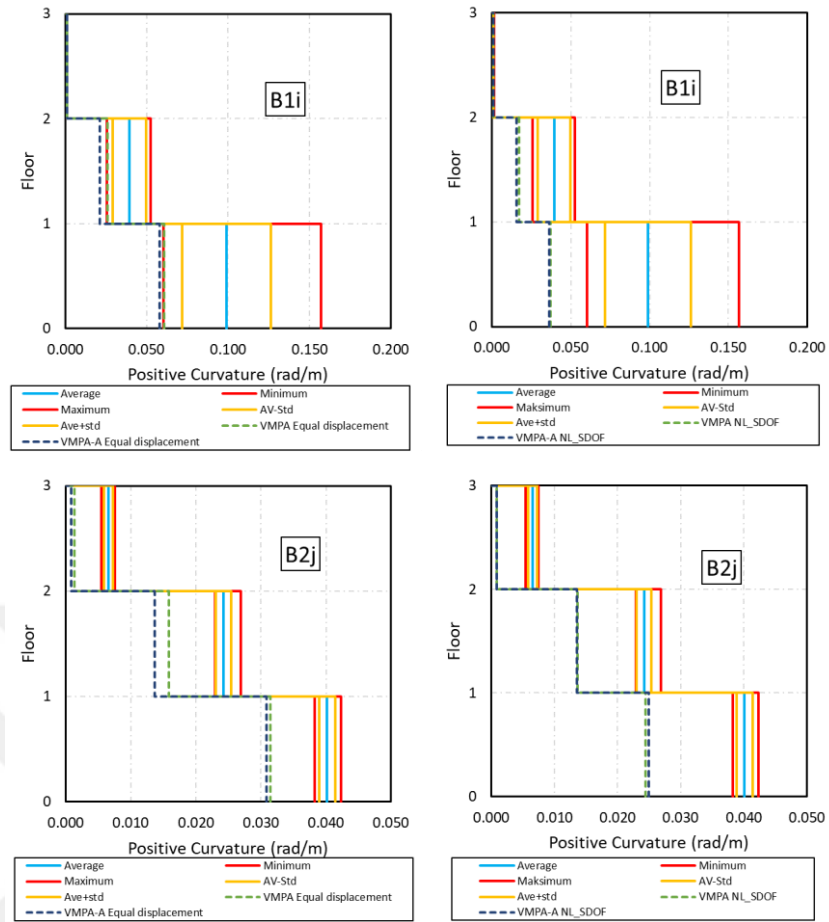
Figure 3.18: Curvature values of beams B1i and B2j in the X direction.

In the Y direction, the results of both procedure are acceptable. In stiff edge (B12i), the results of VMPA-A procedure is almost the same with NTHA results. However, for other beams, VMPA results are more accurate than VMPA-A results.
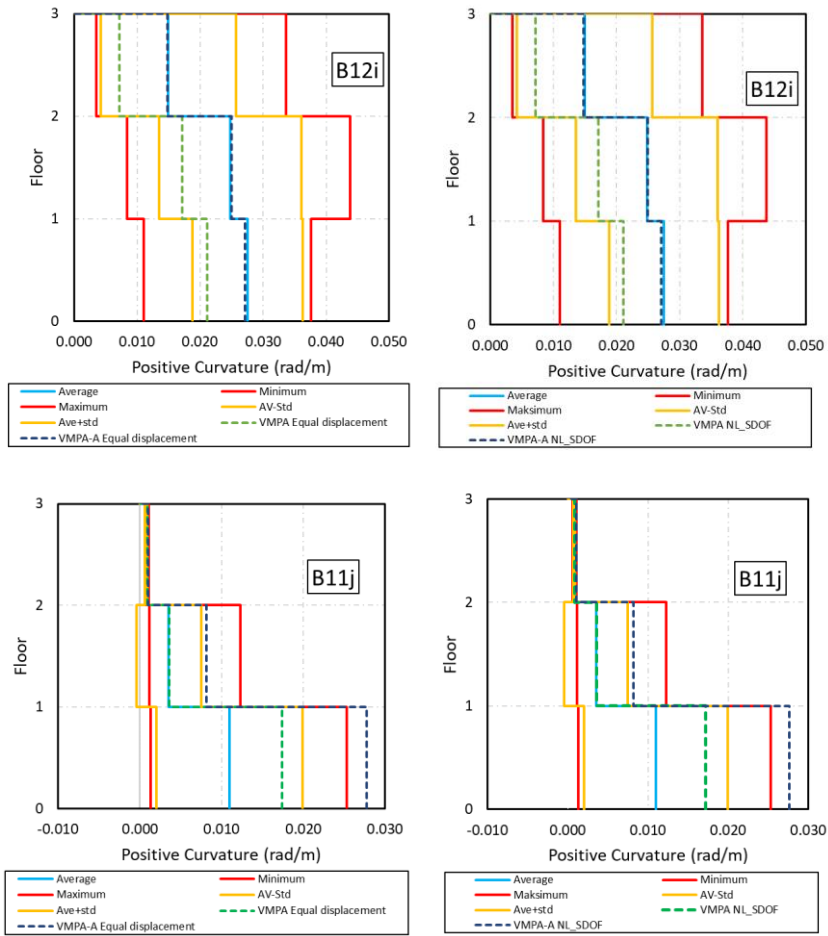
Figure 3.19: Curvature values of beams B12i and B11j in the Y direction.
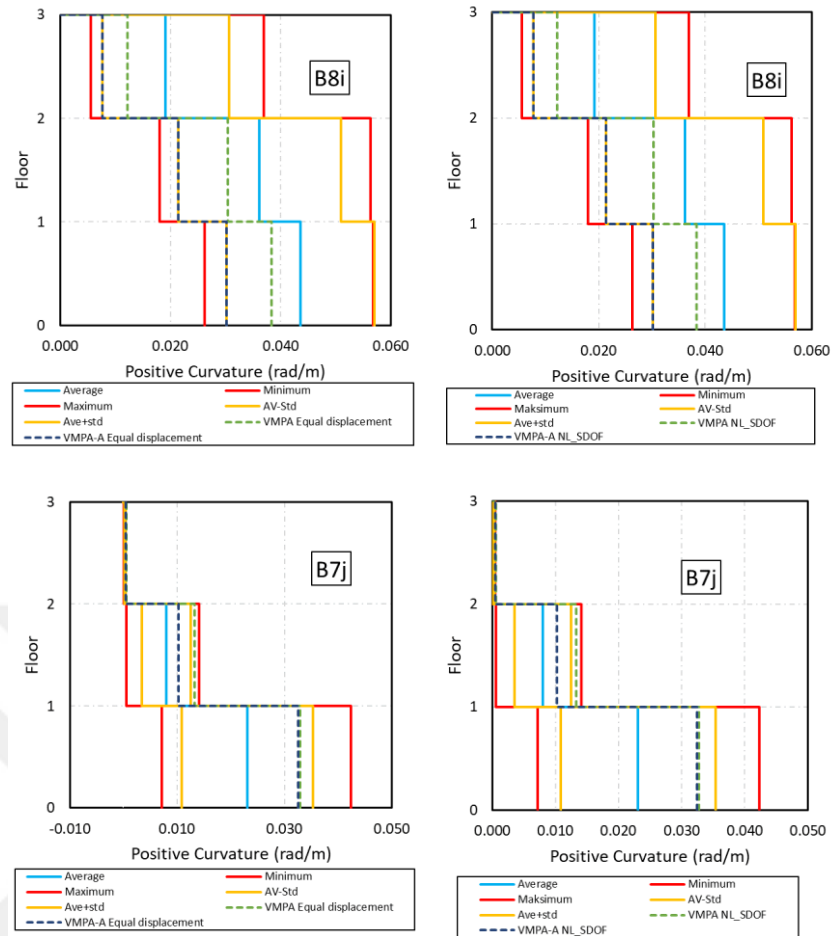
Figure 3.20: Curvature values of beams B8i and B7j in the Y direction.

Since, the VMPA procedure has better results for the SPEAR building, in the evaluation of other seismic demands, only VMPA results are considered.

Storey displacements can be shown in Figure 3.21. In X direction, there is a huge difference between two approaches. The application of NTHA to modal SDOF capacity curves concept approach is more conservative than equal displacement rule. These two approaches coincide in Y direction. In Y direction, the application of NTHA to modal SDOF capacity curves concept is more consistent at the center point, on the other hand, in X direction, storey displacements at the flexible edge have better results than other points.
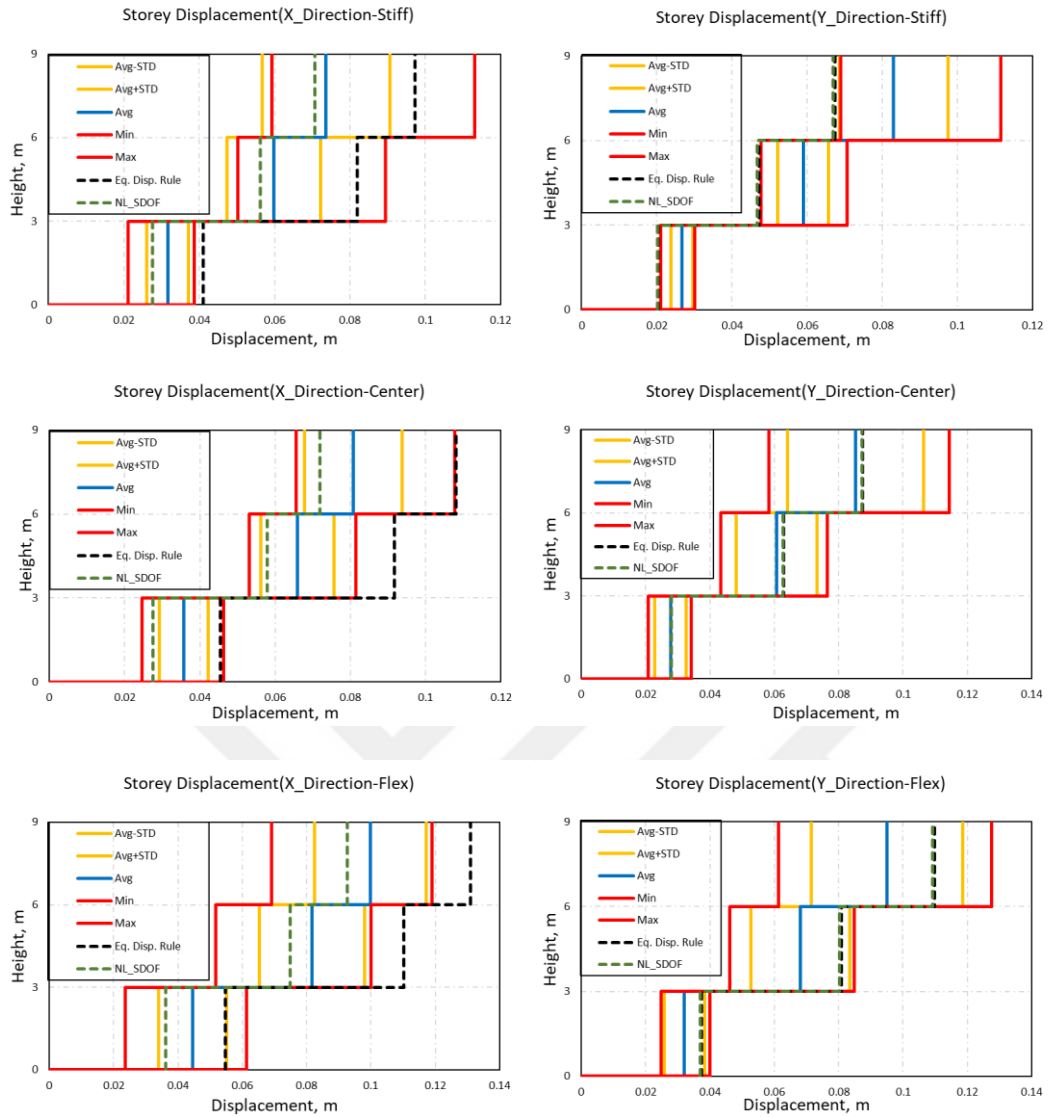
Figure 3.21: Storey displacement demands at the center of mass, stiff and flexible edges in the X and Y direction.

Storey drifts are presented in Figure 3.22. Storey drifts at center point in the Y direction have about 6% error for both approaches. However, in the X direction, the approaches have different results and NTHA to modal SDOF capacity curves approach is more consistent than equal displacement rule.
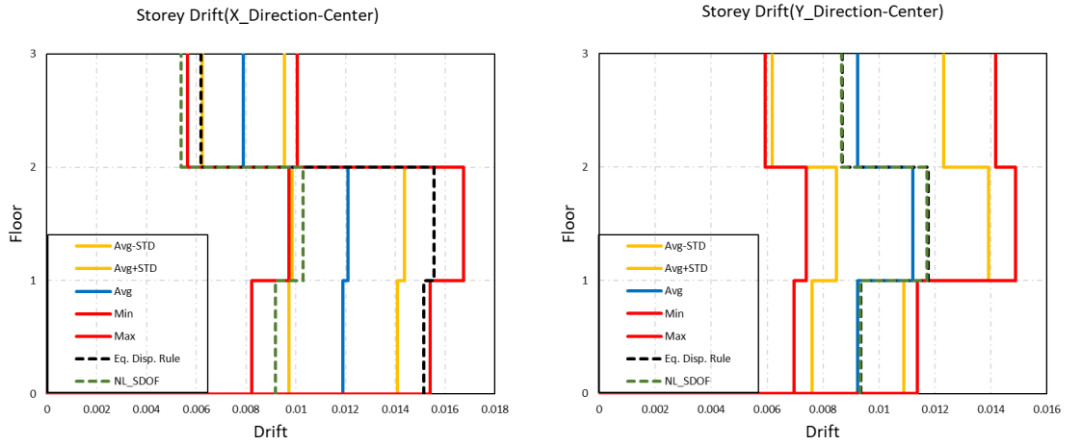
Figure 3.22: Storey drifts at the center of mass in X and Y direction.

3.1.5 Results

VMPA and VMPA-A are used here for a typical existing three-storey building, which has an asymmetric-plan, to verify the methods against NTHA results by comparing some demand parameters. The following conclusions are drawn from the study:

1) When storey forces are considered, VMPA procedure is more accurate than VMPA-A procedure, escipacially in the direction that torsional effect is higher. The error rate of the floor forces is acceptable for VMPA. Due to the torsion effect in the Y direction is greater, the error rate is higher.

2) When the curvature values of column C2 which is corresponding to stiff edge, are examined, in the X direction, the results obtained by equal displacement rule and application of NTHA to modal SDOF capacity curves method are the same, and VMPA-A procedure is more consistent than VMPA procedure. On the other hand, in the Y direction, VMPA procedure is more consistent than VMPA-A procedure escipacially for the results obtained from equal displacement rule. For column C7, in the X direction, VMPA procedure has better results than VMPA-A, except first floor, and in the Y direction, at all floors, VMPA with equal displacement rule method has more convenient results. For column C6 which has rectangular cross section, VMPA-A procedure has larger error at first floor for both direction and approaches.

3) In the X direction, the difference between beam curvature results of VMPA and VMPA-A procedures are small, especially at beam B5i which is close to

stiff edge. For beams B5i and B2j which are close to stiff and flexible edge respectively, the results are not accurate for both procedures. In the Y direction, the results of both procedure are acceptable. In stiff edge (B12i), the results of VMPA-A procedure is almost the same with NTHA results. However, for other beams, VMPA results are more accurate than VMPA-A results.

4) Storey displacements in the Y direction of both approaches give similar results. When the results are examined, it is seen that the difference between NTHA results and VMPA is increased as moving from center point to stiff and flexible edge. On the other hand, in the X direction results of the both approach have different story displacement values and application of NTHA to modal SDOF capacity curves method has a better result due to the implementation of the method.

5) When storey drifts at the center of the mass are compared, in the Y direction, both approaches have similar results and maximum error is at the third floor with 6%. In the X direction, the difference between the results of two approaches are larger, at first and second floor application of NTHA to modal SDOF capacity curves method has better results and maximum error occur at second floor with about 15%, however, at the third floor equal displacement rule approach results are better than the other, and error value is about 21%.

3.2 20-Storey SAC Building

Twenty storey SAC building, which was designed for Los Angeles (LA) region (Gupta and Krawinkler (1999)), is a steel structure and selected as a benchmark structure for this study. The structure is 30.48 m by 36.58 m in plan, 80.77 m in elevation. There are 5 bays in the N-S direction and 6 bays in the E-W direction. The bays are 6.10 m in both directions. The outer bays of the structure contain Moment Resisting Frames (MRFs) and the interior bays includes gravity frames. Loads on the slabs are assumed to be transferred by secondary beams on the beams in N-S direction. Plan and elevation view of the 20-storey SAC buildings shown in Figure 3.23.

The yield strength of columns and beams are taken as 345 MPa and 248 MPa, respectively.
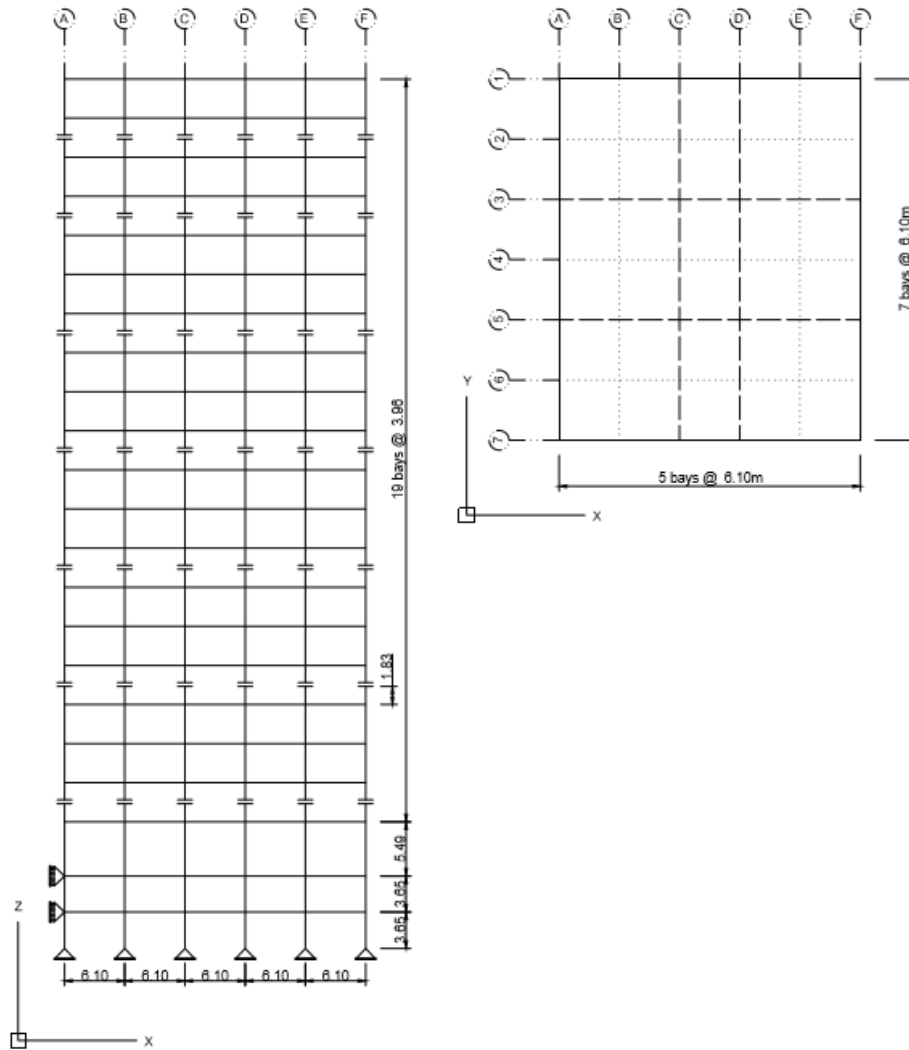
Figure 3.23: Elevation and plan view of the 20-storey SAC buildings.

3.2.1 Modelling of elements

The corner columns have tube cross section and others have I-shape cross section. The column sizes change at splices which are 1.83 m above some floor levels. Cross section of beams and columns are given in Table 3.13 and Table 3.14 for each floor.

Table 3.13: Cross sections of columns and beams for MRFs.

Floor	Columns		Beams
	Exterior	Interior	
-2/-1	15X15X2.00	W24X335	W14X22
-1/1	15X15X2.00	W24X335	W30X99
1/2	15X15X2.00	W24X335	W30X99
2/3	15X15X2.00, 15X15X1.25	W24X335, W24X335	W30X99
3/4	15X15X1.25	W24X335	W30X99
4/5	15X15X1.25	W24X335	W30X99
5/6	15X15X1.25, 15X15X1.00	W24X335, W24X229	W30X108
6/7	15X15X1.00	W24X229	W30X108
7/8	15X15X1.00	W24X229	W30X108
8/9	15X15X1.00, 15X15X1.00	W24X229, W24X229	W30X108
9/10	15X15X1.00	W24X229	W30X108
10/11	15X15X1.00	W24X229	W30X108
11/12	15X15X1.00, 15X15X1.00	W24X229, W24X192	W30X99
12/13	15X15X1.00	W24X192	W30X99
13/14	15X15X1.00	W24X192	W30X99
14/15	15X15X1.00, 15X15X0.75	W24X192, W24X131	W30X99
15/16	15X15X0.75	W24X131	W30X99
16/17	15X15X0.75	W24X131	W30X99
17/18	15X15X0.75, 15X15X0.75	W24X131, W24X117	W27X84
18/19	15X15X0.75	W24X117	W27X84
19/20	15X15X0.75, 15X15X0.50	W24X117, W24X84	W24X62
20/Roof	15X15X0.50	W24X84	W21X50

Table 3.14: Cross sections of columns and beams for gravity frames.

Floor	Columns	Beams	
		Long span	Short span
-2/-1	W14x550	W21X50	W14X22
-1/1	W14x550	W24X68	W16X26
1/2	W14x550	W21X50	W14X22
2/3	W14x550, W14x455	W21X50	W14X22
3/4	W14x455	W21X50	W14X22
4/5	W14x455	W21X50	W14X22
5/6	W14x455, W14X370	W21X50	W14X22
6/7	W14X370	W21X50	W14X22
7/8	W14X370	W21X50	W14X22
8/9	W14X370, W14X311	W21X50	W14X22
9/10	W14X311	W21X50	W14X22
10/11	W14X311	W21X50	W14X22
11/12	W14X311, W14X257	W21X50	W14X22
12/13	W14X257	W21X50	W14X22
13/14	W14X257	W21X50	W14X22
14/15	W14X257, W14X176	W21X50	W14X22
15/16	W14X176	W21X50	W14X22
16/17	W14X176	W21X50	W14X22
17/18	W14X176, W14X109	W21X50	W14X22
18/19	W14X109	W21X50	W14X22
19/20	W14X109	W21X50	W14X22
20/Roof	W14X109, W14X43	W21X44	W12X16

Loads on slabs were transferred to beams in the N-S direction with secondary beams. Loads were determined by using a trial and error method. G+0.3Q load combination values for each storey are given in Table 3.15. Mass of structural members were considered as zero. After analysing the structure, storey masses were compared with storey masses given in Ohtori et al. (2004). The difference between the storey masses are approximately 10 tonnes (Table 3.15), and this difference can be acceptable.

Table 3.15: Comparison of storey massses.

Floor	Storey masses	
	Ohtori et al.	SAP2000
20th floor	584 t	574.78 t
2nd-19th floor	552 t	543.42 t
1st floor	563 t	553.84 t
Ground floor	532 t	522.48 t

Storey masses are considered as a point mass for modal analysis (5% eccentricity is applied). Rotational mass values were calculated by using following equation;

$$\left(\frac{a^2 + b^2}{12} \right).m \tag{3.7}$$

Where a and b are the lengths of the structure in the X and Y direction, and m is the storey mass value.

Translational mass and rotational mass of the storeys are given in Table 3.16.

Table 3.16: Translational and rotational masses of each storey.

Floor	Translational mass	Rotational mass
20th floor	574.78 t	108720.12 tm^2
2nd-19th floor	543.42 t	102788.35 tm^2
1st floor	553.84 t	104759.30 tm^2
Ground floor	522.48 t	98827.53 tm^2

Modal participation mass ratios and periods were obtained after modal analysis of elastic model. Comparison of modal participation mass ratios and periods are given in Table 3.17. The difference between the results of SAP2000 and DOC3D model are acceptable. Since the outputs of two program have approximate results, it was accepted that the modeling was done correctly and nonlinear analysis procedure can be started.

Table 3.17: Comparison of participation mass ratios and periods for elastic model.

	SAP2000				DOC3D			
Mode	Period	U_x	U_y	R_z	Period	U_x	U_y	R_z
1	3.95791	0.79889	0.00000	0.00000	3.96745	0.80109	0.00000	0.00001
2	3.58730	0.00000	0.80518	0.00000	3.54904	0.00000	0.80588	0.00000
3	2.10011	0.00000	0.00000	0.81983	2.03491	0.00000	0.00000	0.81960
4	1.38353	0.10991	0.00000	0.00000	1.38760	0.10979	0.00000	0.00001
5	1.26121	0.00000	0.10748	0.00000	1.24776	0.00000	0.10711	0.00000
6	0.81157	0.03629	0.00000	0.00000	0.81391	0.03601	0.00000	0.00003
7	0.74803	0.00000	0.00000	0.09652	0.73654	0.00000	0.03542	0.00000
8	0.74432	0.00000	0.03567	0.00000	0.72989	0.00001	0.00000	0.09780
9	0.57326	0.01893	0.00000	0.00000	0.57495	0.01861	0.00000	0.00000

Concentrated plasticity model was considered for inelastic flexural behavior of elements. A standart moment curvature analysis was implemented for each member instead of biaxial moment (M-M) and moment-axial force (M-N) interaction. For columns, axial force corresponding to gravitational loading was considered to obtain moment curvature relationship. XTRACT software was used to obtain moment curvature analysis. For beams, following equations were used to obtain moment curvature relationships.

$$M_p = \sigma_y.W_p \tag{3.8}$$

Where, σ_y is the yield strength of steel material, W_p is the plastic section modulus and M_p is the moment capacity of the cross-section.

$$\phi_p = \frac{M_p}{EI} \tag{3.9}$$

Where, ϕ_p is the curvature corresponding to M_p.

Moment capacity and yield curvature of beams are shown in Table 3.18, and moment capacity and yield curvature of columns in both direction X and Y are given in ANNEX B and moment curvature relationship of beams and columns are given in ANNEX C.

Table 3.18: Moment capacity and yield curvature of beams.

Element	Moment Capacity	Yield Curvature
W14x22	135	0.00814
W30x99	1270	0.00382
W30x108	1410	0.00378
W27x84	992	0.00418
W24x62	622	0.00482
W21x50	447	0.00546
W24x68	719	0.00472
W21x44	388	0.00552
W16x26	180	0.00717
W12x16	81.7	0.00953

3.2.2 Earthquake records

Fourteen ground motion records were selected from the PEER ground motion database (2006). The selection criteria is to match the average spectrum of X and Y components of ground motions with target ASCE/SEI 7-16 (2017) spectrum. For Los Angles region, the spectral characteristics are given as S_{ds}=1.58, S_{d1}=0.79 and T_L= 8 sec in ASCE/SEI 7-16 (2017). The average Spectrum in X and Y directions and target spectrum is given in Figure 3.24.
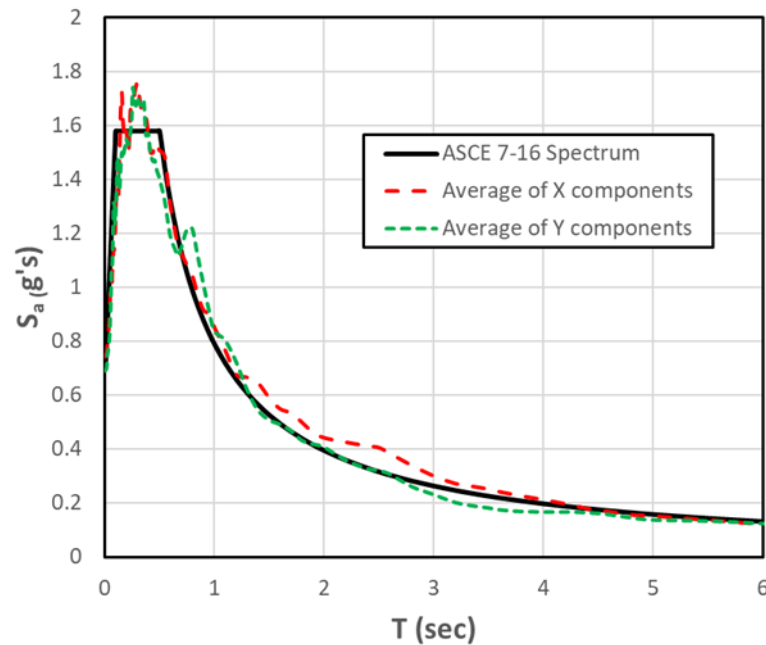
Figure 3.24: The average spectrum of selected records and target spectrum.

The selected records and scaling factors are presented in Table 3.19.

Table 3.19: Earthquake records and scaling factors.

Earthquake name	Year	Station Name	Mechanism	Scaling factor
Imperial Valley-06	1979	El Centro Array #8	Strike slip	1.8196
Loma Prieta	1989	Hollister – South & Pine	Strike slip	1.7744
Kobe_ Japan	1995	Amagasaki	Strike slip	1.7043
Kocaeli_ Turkey	1999	Duzce	Strike slip	1.6296
Chi-Chi_ Taiwan	1999	CHY036	Strike slip	1.9495
Chi-Chi_ Taiwan	1999	TCU129	Strike slip	1.7822
Manjil_ Iran	1990	Abbar	Strike slip	1.8207
Cape Mendocino	1992	Ferndale Fire Station	Strike slip	1.7617
Iwate_ Japan	2008	WITH24	Strike slip	1.9274
Iwate_ Japan	2008	Kurihara City	Strike slip	1.6732
El Mayor-Cucapah_ Mexico	2010	El Centro Array #10	Strike slip	1.8825
El Mayor-Cucapah_ Mexico	2010	El Centro Array #11	Strike slip	1.5443
Darfield_ New Zealand	2010	Christchurch Cathedral College	Strike slip	1.9372
Darfield_ New Zealand	2010	Papanui High School	Strike slip	1.871

3.2.3 Analysis

Hinges were asigned to both ends of members as bilinear moment curvature relationship. Definition of column and beam hinge properties are shown in Figure 3.25 and Figure 3.26.
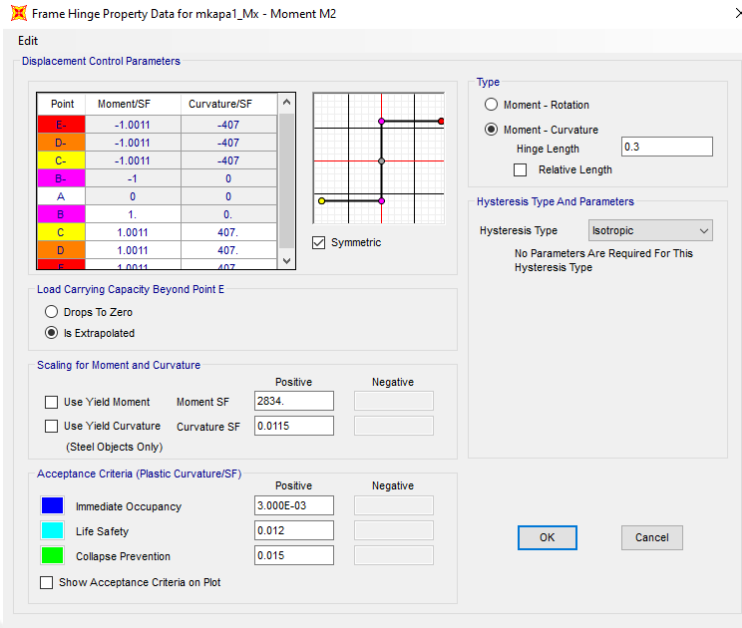
Figure 3.25: Definition of moment-curvature hinge property for column.
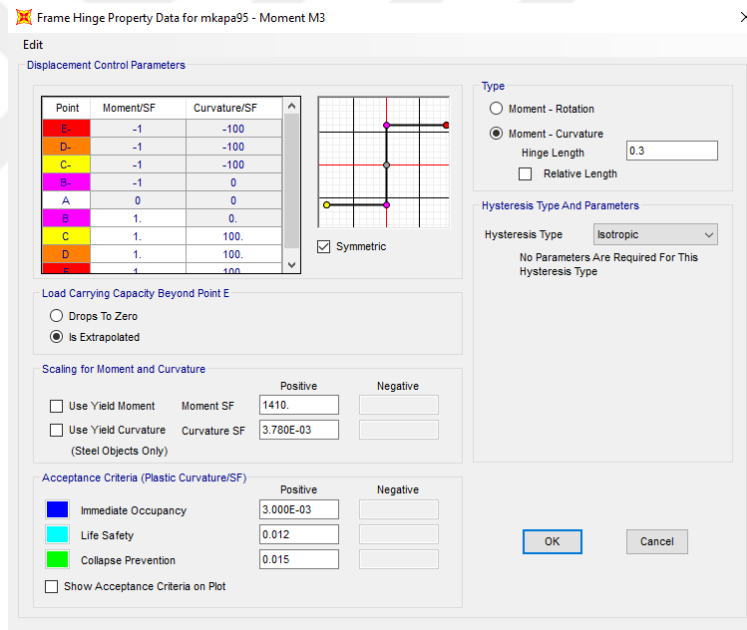
Figure 3.26: Definition of moment-curvature hinge property for column.

Pushover analysis was applied to structure in the X and Y direction that the first two modes of the structure are effective. The application of pushover analysis in the X and Y direction are shown in Figure 3.27 and Figure 3.28.
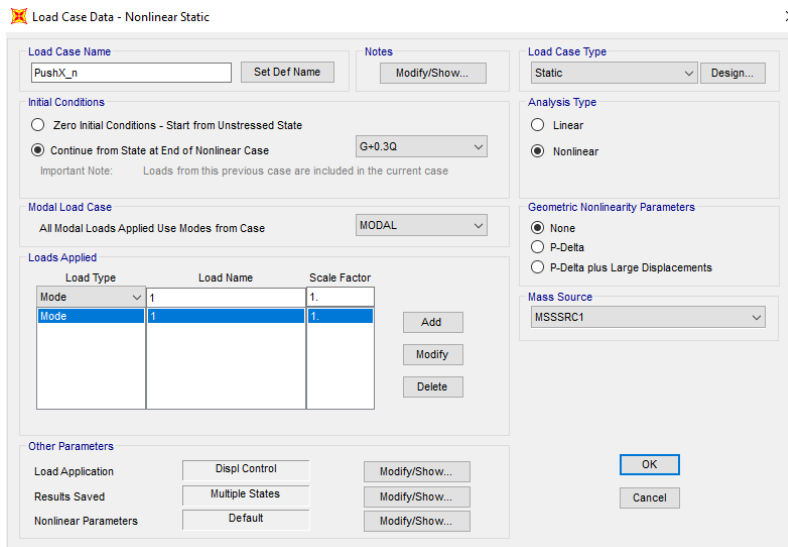
Figure 3.27: Definiton of NSP in X direction in SAP2000 software.
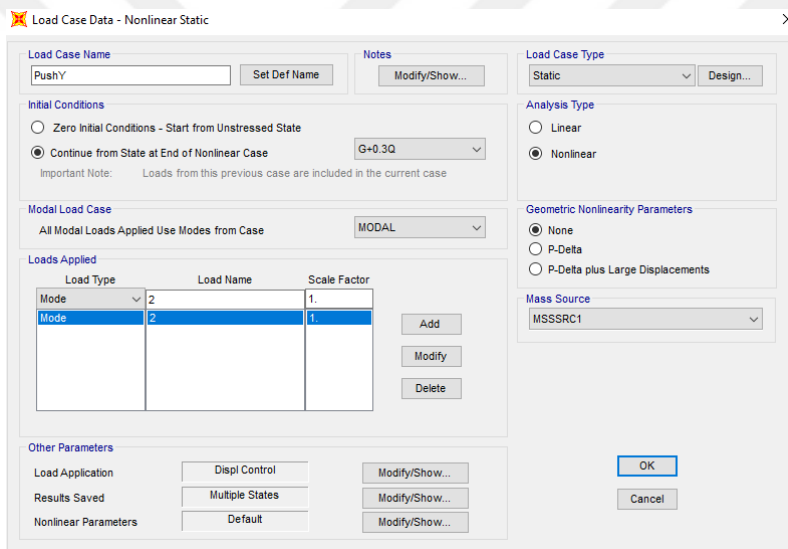
Figure 3.28: Definiton of NSP in X direction in SAP2000 software.

Pushover curves of the structure are presented in Figure 3.29. It can be seen that SAP2000 and DOC3D results are the same in both direction.
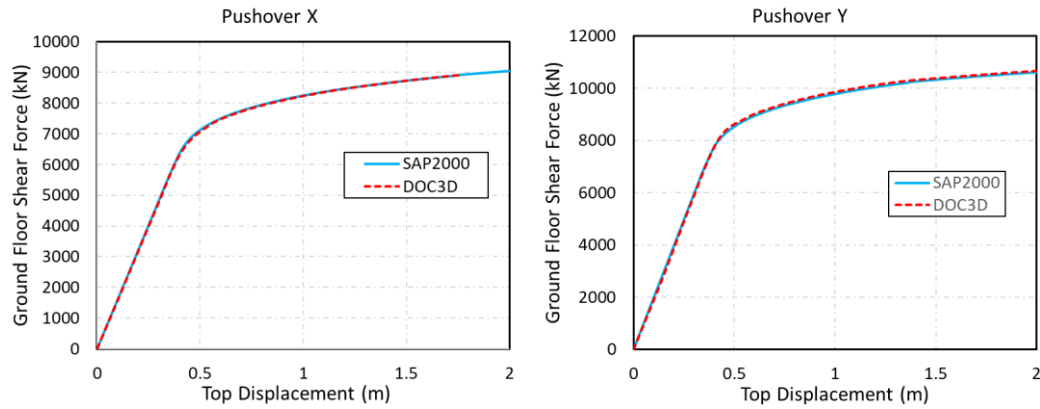
Figure 3.29: Pushover curves in the X and Y directions.

To determine seismic demands of the structure, VMPA and VMPA-A procedures were applied by using DOC3D matlab programme, the results are compared with NTHA by using SAP2000 software.

In the storey shear and curvature graphs, first two storeys represent basement floors and in the storey displacement and storey drift graphs, basement floors were not considered, storey numbers are started from first floor.

Storey shear forces are given in Figure 3.30. It shows that the results obtained from VMPA-A procedure is more accurate than others, and the results obtained from VMPA with equal displacement rule approach has larger error than other approach.
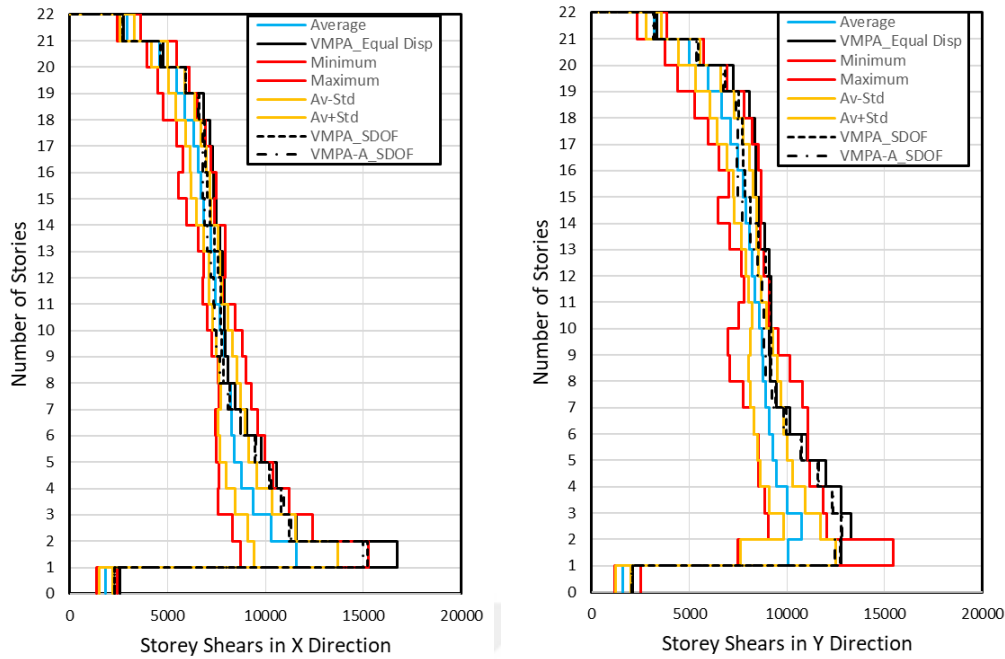
Figure 3.30: Storey shear forces in the X and Y direction.

The curvatures of bottom sections of columns are presented in Figure 3.31 and Figure 3.32. For corner column (A1), VMPA-A procedure is more consistent than others in the X direction. However, when Y direction is considered, the consistency of approaches changes floor by floor.
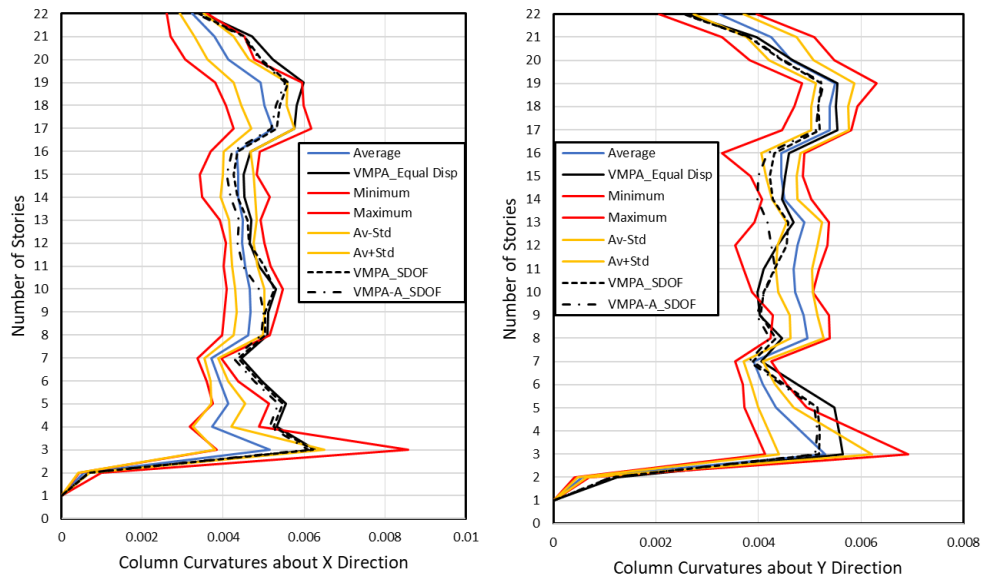
Figure 3.31: Curvature values of the corner column (A1).

When the curvature values of the mid-columns (C1 for direction X and A4 for direction Y) of the MRFs are considered, it can be seen that all approaches have approximately

the same results. On the other hand, in the X direction, VMPA-A procedure is more accurate, but after third floor, curvature values are not consistent with exact solution.
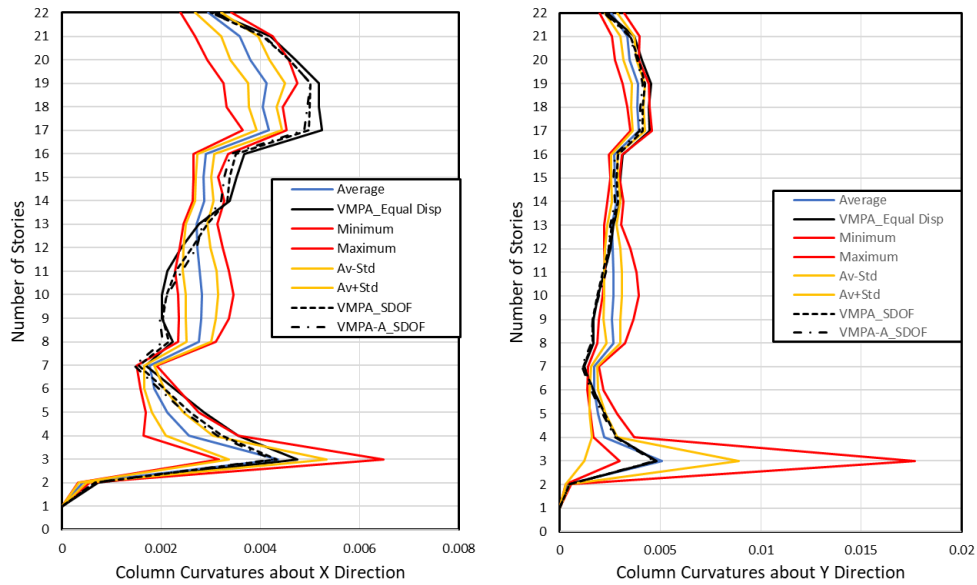
Figure 3.32: Curvature values of the mid-column of the MRFs in both X and Y direction, C1 and A4 respectively.

Curvature values for beams in the X direction are given in Figure 3.33 and Figure 3.34, and curvature values for beams in the Y direction are given in Figure 3.35 and Figure 3.36. In the figures, right section shows the maximum values and left section shows the minimum curvature values. VMPA-A procedure is more accurate than other procedures for all selected beams. In the X direction, there are difference between results, and VMPA procedure with equal displacement rule results are not in acceptable range. In the Y direction, all results are in acceptable range and the difference between them are small. However, VMPA-A solution is more convenient than others.
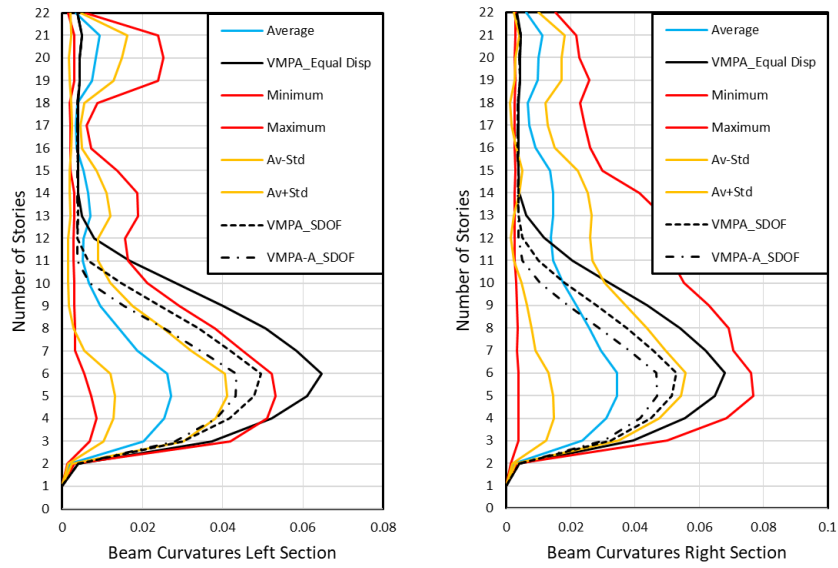
Figure 3.33: Curvature values of the beams located at x=0 and x=6.1 m when y=0.
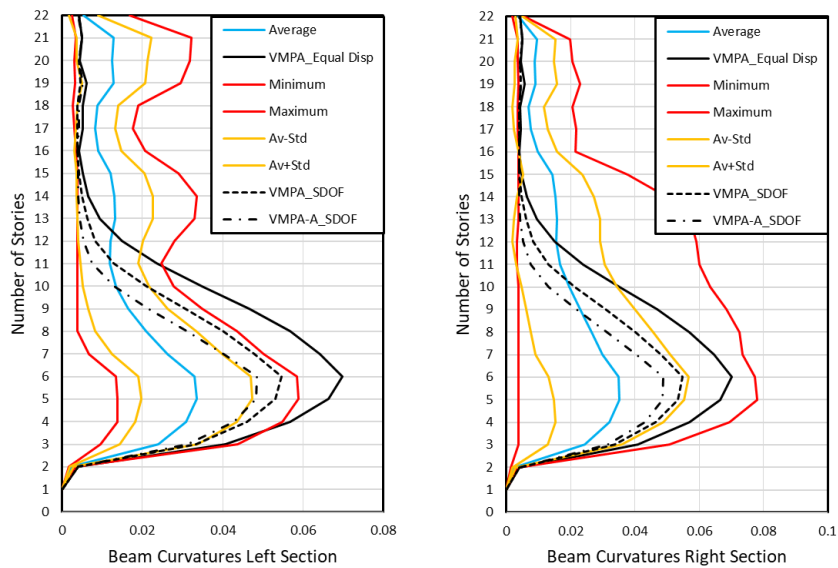
Figure 3.34: Curvature values of the beams located at x=12.2 and x=18.3 m when y=0.
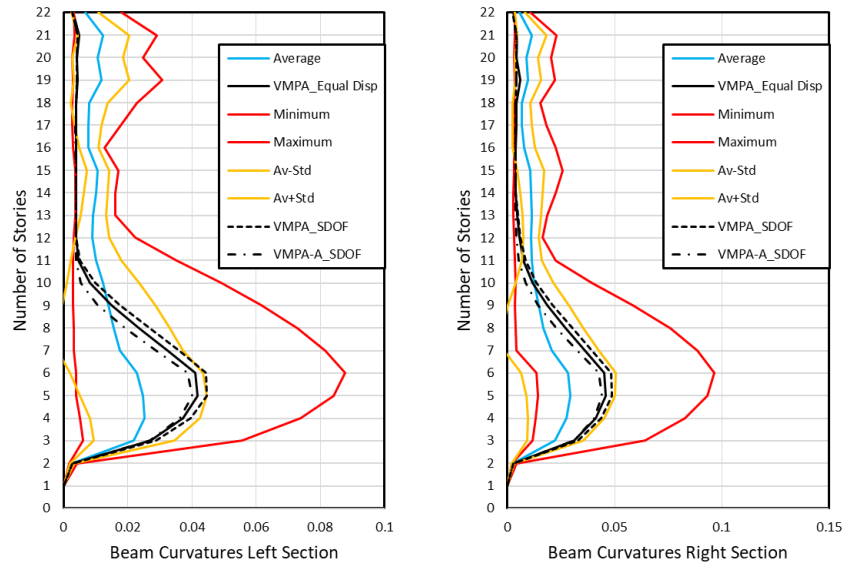
Figure 3.45: Curvature values of the beams which located at y=12.2 and y=18.3 m when x=0.
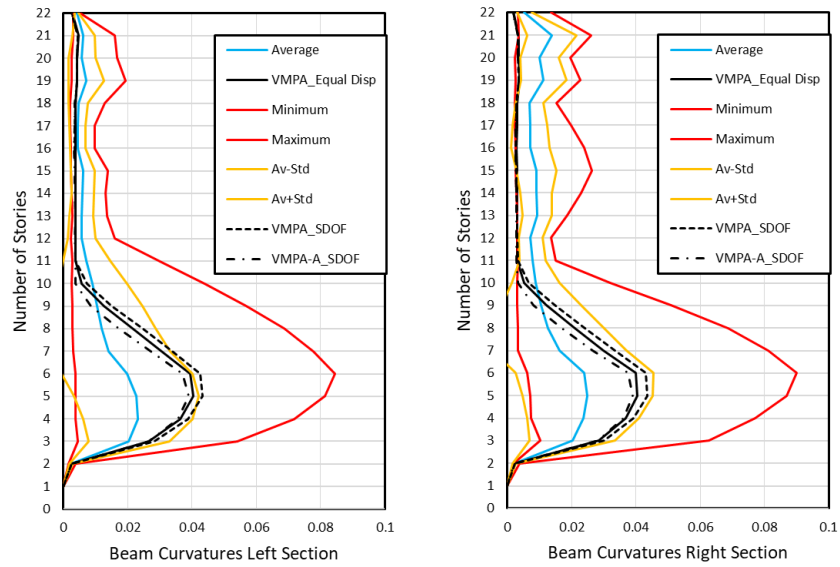
Figure 3.56: Curvature values of the beams which located at y=30.5 and y=36.6 m when x=0.

Storey displacement values are shown in Figure 3.37. According to figure, the results obtained from VMPA-A procedure are close to the results obtained from NTHA.
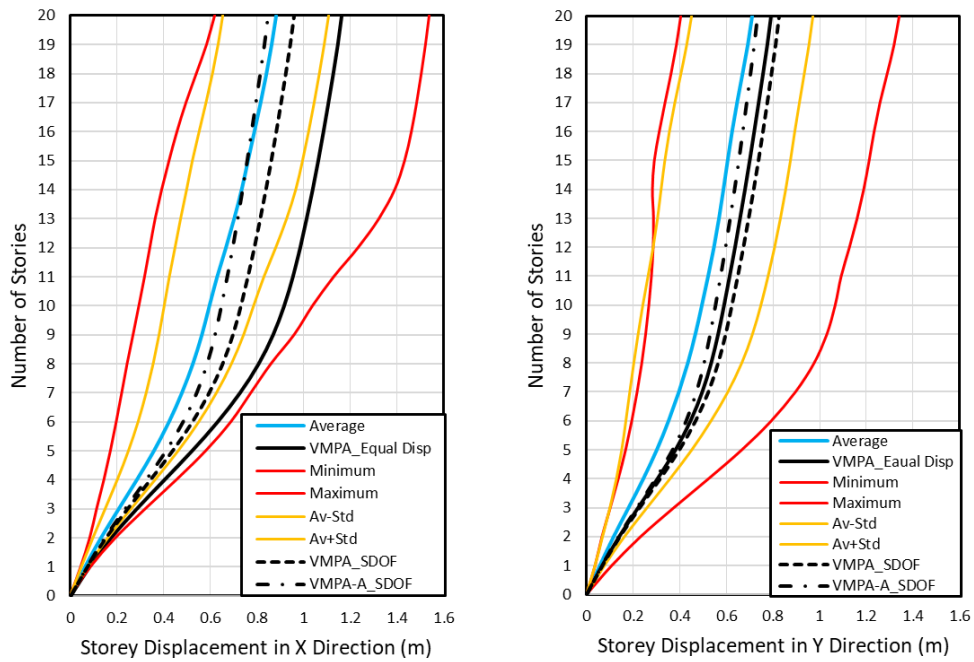
Figure 3.37: Storey displacements of the SAC20 buildings in X and Y directions.

Storey drift values are presented in Figure 3.34. In the X direction, VMPA-A procedure has better results up to seventh floor. After nineth floor, VMPA procedure with equal displacement rule approaches has more accurate results than others. In the Y direction, at lower floors VMPA-A procedure is accurate. Towards the upper floors VMPA with equal displacement rule approach has better results.
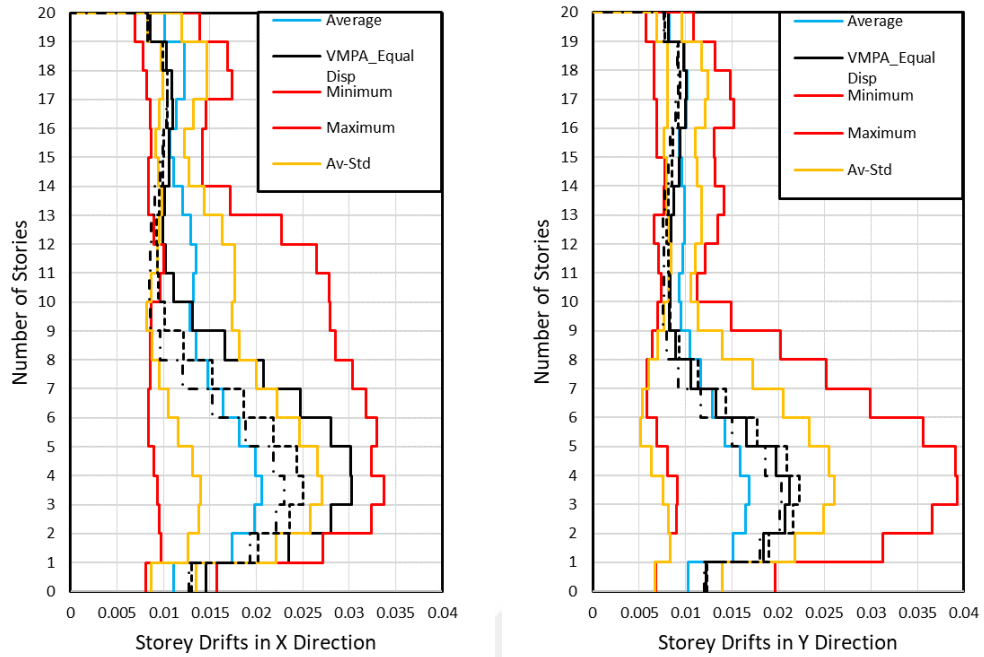
Figure 3.38: Storey drifts of the structure in X and Y directions.

3.2.4 Results

VMPA and VMPA-A are used here for a high-rise building to verify the methods against NTHA results by comparing some demand parameters. The following conclusions are drawn from the study:

1) For SAC building, in the X direction shear force results obtained from VMPA procedure with equal displacement rule are in acceptable range except basement floors. In the Y direction, relative difference of the results obtained from VMPA procedure with equal displacement rule are changing floor by floor.

2) For SAC building, curvature values of column in both direction are not consistent. Relative difference of the procedures are inconsitent, VMPA procedure is inadequate to calculate column curvatures for high-rise buildings. Curvature results of beams in the X direction which is the same direction with dominant period, for left section, results obtained from VMPA procedure with equal displacement rule are not in acceptable range. Curvature results of beams in the Y direction are in acceptable range for all approaches.

3) For SAC building, storey displacements are in acceptable range in both directions. However, in the X direction, application of NTHA to modal SDOF

capacity curves approach has more convenient results than equal displacement rule.

4) VMPA-A procedure with application of NTHA to modal SDOF capacity curves approach has more accurate results for all demand parameters in both direction X and Y. However, VMPA procedure with equal displacement rule can be recommended due to convenience in application and time.

5) The results obtained from VMPA procedure with equal displacement rule are more inconvenient than others in the X direction. However, in the Y direction VMPA procedure with application of NTHA to modal SDOF capacity curves approach has more inconvenient than other although the results of all procedures are considered.

4. CONCLUSIONS

In this study, a variant modal pushover analysis (VMPA) and adaptive version of VMPA (VMPA-A) are utilized to evaluate seismic performans of an asymmetric plan building and a high-rise building.

Two example buildings namely, SPEAR building and 20-story SAC Steel building have been analyzed to assess the success of the mentioned procedures by comparing the analysis result with those of NTHAs. The following conclusions can be drawn from these study:

1- Pushover curves obtained from DOC3D is validated by using SAP2000 software for the two structures.

2- For asymmetric plan building, shear force results obtained from VMPA and VMPA-A procedures are in acceptable range, and the results obtained from VMPA procedure with equal displacement rule has better results.

3- For SPEAR building, column curvature results are inconsistent escipacially in the Y direction. The procedures are inadequate to calculate column curvatures. Curvature results of the beams in the X direction which is the same direction with dominant period, are inconvenient. The result in the Y direction are in acceptable range.

4- For SPEAR building, in the X direction, storey displacement values obtained from VMPA procedure with equal displacement rule are in acceptable range only in the stiff edge. When the flexibility increase, inconsistency in the results increase. On the other hand, VMPA procedure with application of NTHA to modal SDOF capacity curves approach has acceptable results for stiff, center and flexible point. In the Y direction, the result at all point are in acceptable range.

5- For 20-storey SAC Steel building, in the X direction shear force results obtained from VMPA procedure with equal displacement rule are in acceptable

range except basement floors. In the Y direction, relative difference of the results obtained from VMPA procedure with equal displacement rule change floor by floor.

6- For 20-storey SAC Steel building, curvature values of column in both direction are not consistent. Relative difference of the procedures are inconsitent, VMPA procedure is inadequate to calculate column curvatures for high-rise buildings. Curvature results of beams in the X direction which is the same direction with dominant period, for left section, results obtained from VMPA procedure with equal displacement rule are not in acceptable range. Curvature results of beams in the Y direction are in acceptable range for all approaches.

7- For 20-storey SAC Steel building, storey displacements are in acceptable range in both directions.

8- For SPEAR building, VMPA procedure with application of NTHA to modal SDOF capacity curves approach is more convenient than others. However, equal displacement rule approach can be prefered since the results are conservative and application of equal displacement method is practical.

9- For 20-storey SAC Steel building, generally, VMPA-A procedure with procedure with application of NTHA to modal SDOF capacity curves approach has better results especially at lower floors. At the upper floors, all approaches have the results that are closed to each other.

10- In both structure, in the Y direction, the results obtained by equal displacement rule and application of NTHA to modal SDOF capacity curves approaches are almost the same results since the equal displacement rule approach already provides the seismic demands.

REFERENCES

Abbasnia, R., Davoudi, A. T. & Maddah M.M. (2013). An adaptive pushover procedure based on effective modal mass combination rule, *Engineering Structures, 52*, 654-666.

Ambraseys, N., Smit, P., Sigbjornsson, R., Suhadolc, P. & Margaris, B. (2002). Internet-site for European Strong-motion Data. European Commission, *Research-Directorate General, Environment and Climate Programme.* Available from: http://www.isesd.hi.is/ESD_Local/frameset.htm

Antonio, S. & Pinho, R. (2004a). Advantages and limitations of adaptive and non-adaptive force-based pushover procedures, *Journal of Earthquake Engineering, 8*(4), 497-522.

Antonio, S. & Pinho, R. (2004b). Development and verification of a displacement-based adaptive pushover procedure, *Journal of Earthquake Engineering, 8*(5), 643-661.

ASCE/SEI 7-16. (2017). Minimum Design Loads and Associated Criteria for Buildings and Other Structures, *ASCE*, California.

ASCE/SEI 41.06. (2007). Seismic Rehabilitation of Existing Buildings, the latest generation of performance-based seismic rehabilitation methodology, *ASCE*, California.

ATC-40. (1996). Seismic evaluation and retrofit of concrete buildings, *Applied Technology Council*, Volume 1, Redwood City, CA.

Aydınoğlu, M.N. (2003). An incremental Response Spectrum Analysis Procedure Based on Inelastic Spectral Displacements for Multi-Mode Seismic Performance Evaluation, *Bulletin of Earthquake Engineering*, 1, 3-36.

Aydınoğlu, M.N. (2004). An Improved Pushover Procedure for Engineering Practice: Incremental Response Spectrum Analysis (IRSA) in Performance-Based Seismic Design Concepts and Implementation. In *Proceedings of International Workshop, Bled, Slovenia, June 28-July 1* (edited by P. Fajfar and H. Krawinkler): Report PEER 2004/05, University of California, Berkeley, LA.

Aydınoğlu, M.N. (2007). A Response Spectrum-Based Nonlinear Assessment Tool for Practice: Incremental Response Spectrum Analysis (IRSA), *ISET Journal of Earthquake Technology, 44*(1), 169-192.

Bhatt C., &Bento R. (2011). Assessing the Seismic Response of Existing RC Buildings Using the Extended N2 Method, *Bulletin of Earthquake Engineering, 9*(4), 1183-1201.

Bosco, M., Ghersi, A. & Marino, M. (2012). Corrective eccentricities for assessment by the nonlinear static method of 3D structures subjected to

bidirectional ground motions, *Earthquake Engineering and Structural Dynamics, 41*, 1751-1773.

Bosco, M., Ghersi, A., Marino, E. M. & Rossi P. P. (2013). Comparison of nonlinear static methods for the assessment of asymmetric buildings, *Bulletin of Earthquake Engineering*, *11*, 2287-2308.

Bracci, J.M., Kunnath, S.K. & Reinhorn, A.M. (1997). Seismic Performance and Retrofit Evaluation for Reinforced Concrete Structures, *Journal of Structural Engineering*, *ASCE*, *123*(1), 3-10.

CEN. (2008). Eurocode 8: design of structures for earthquake resistance. Part 1: general rules seismic actions and rules for buildings. EN 1998-1, *CEN*, Brussels, December.

Chopra, A.K. & Goel, R.K. (2002). A modal pushover analysis procedure for estimating seismic demands for buildings, *Earthquake Engineering and Structural Dynamics, 31*, 561-582.

Chopra, A.K. & Goel, R.K. (2004a). A modal pushover analysis procedure to estimate seismic demands for unsymmetric-plan buildings, *Earthquake Engineering and Structural Dynamics, 33*, 903-927.

Chopra, A.K. & Goel, R.K. (2004b). Evaluation of Modal and FEMA Pushover Analyses: SAC Buildings, *Earthquake Spectra*, *20*(1), 225-254.

Chopra, A.K., Goel, R.K. & Chintanapakdee, C. (2004). Evaluation of a Modified MPA Procedure Assuming Higher Modes as Elastic to Estimate Seismic Demands, *Earthquake Spectra, 20*(3), 757-778.

CTBUH. (2008). Recommendations for the seismic design of high-rise buildings, *Council on Tall Buildings and Urban Habitat*, Chicago.

Elnashai, A.S. (2001). Advanced inelastic static (pushover) analysis for earthquake applications, *Structural Engineering and Mechanics, 12*(1), 51-69.

EN 1998-1 Eurocode 8. (2002) Design of structures for earthquake resistance. Part 1: General rules, seismic actions and rules for buildings, CEN.

EN 1992-1-1 Eurocode 2. (1999). Design of concrete structures. Part 1-1 : General rules and rules for buildings, CEN.

Fajfar, P., Marusic, D. & Perus, I. (2005). Torsional Effects in the Pushover-based Seismic Analysis of Buildings, *Journal of Earthquake Engineering, 9*(6), 831-854.

Stratan, A. & Fajfar, P. (2003) Seismic Assessment of the Spear Test Structure, *IKPIR Report*, University of Ljubljana.

FEMA 356. (2000). *Prestandard and Commentary for the Seismic Rehabilitation of Buildings*.Washington, D.C.: Federal Emergency Management Agency.

FEMA 440. (2005). *Prestandard and Commentary for the Seismic Rehabilitation of Buildings Improvement of Nonlinear Static Seismic Analysis Procedures*. Washington, D.C.: Federal Emergency Management Agency.

Goel, R.K. & Chopra, A.K. (2005). Extension of Modal Pushover Analysis to Compute Member Forces, *Earthquake Spectra, 21*(1), 125-139.

Gupta, A. & Krawinkler, H. (1999). *Seismic Demands for Performance Evaluation of Steel Moment Resisting Frame Structures* (SAC Task 5.4.3 Report No. 132). Stanford, CA.: The John A. Blume Earthquake Engineering Center

Gupta, B. & Kunnath, S.K. (2000). Adaptive Spectra-Based Pushover Procedure for Seismic Evaluation of Structuresi, *Earthquake Spectra, 16*(2), 367-391.

Kalkan, E. & Kunnath, S.K. (2006). Adaptive Modal Combination Procedure for Nonlinear Static Analysis of Building Structures, *Journal of Structural Engineering ASCE, 132*, 1721-1731.

Khoshnoudian, F. & Kashani, M.M.B. (2012) Assessment of modified consecutive modal pushover analysis for estimating the seismic demands of tall buildings with dual system considering steel concentrically braced frames, *Journal of Constructional Steel Research, 72*, 155-167.

Kreslin, M. & Fajfar, P. (2011). The extended N2 method taking into account higher mode effects in elevation, *Earthquake Engineering and Structural Dynamics, 40*, 1571-1589.

LATBSDC. (2008). An alternative procedure for seismic analysis and design of tall buildings located in the Los Angeles region. *Los Angeles Tall Buildings Structural Design Council*, Los Angeles, CA.

Lin, J. L. & Tsai K. C. (2007). Simplified seismic analysis of asymmetric building systems, *Earthquake Engineering and Structural Dynamics, 36*, 459-479.

Lin, J.L. & Tsai, K. C. (2008). Seismic analysis of two-way asymmetric building systems under bidirectional seismic ground motions, *Earthquake Engineering Structural Dynamics*, *37*, 305-328.

Lin, J. L., Tsai, K. C. & Yang, W.C. (2012a). Inelastic responses of two-way asymmetric-plan structures under bidirectional ground excitations-part I: modal parameters, *Earthquake Spectra, 28*(1), 105-139.

Lin, J. L., Tsai, K. C. & Yang, W.C. (2012b). Inelastic responses of two-way asymmetric-plan structures under bidirectional ground excitations-part II: response spectra, *Earthquake Spectra, 28*(1), 141-157.

Manoukas, G., Athanatopoulou, A. & Avramidis, I. (2012). Multimode pushover analysis for asymmetric buildings under biaxial seismic excitation based on a new concept of the equivalent single degree of freedom system, *Soil Dynamics and Earthquake Engineering, 38*, 88-96.

Manoukas, G. & Avramidis, I. (2014) Evaluation of a multimode pushover procedure for asymmetric in plan buildings under biaxial seismic excitation, *Bulletin of Earthquake Engineering, 12*, 2607-2632.

Marusic, D. & Fajfar, P. (2005). On the inelastic seismic response of asymmetric buildings under bi-axial excitation, *Earthquake Engineering and Structural Dynamics*, *34*, 943-963.

Ohtori, Y., Christenson, R.E., Spencer Jr., B.F., & Dyke, S.J., (2004). Benchmark Control Problems sor Seismically Excited Nonlinear Buildings, *Journal of Engineering Mechanics,* 130 (4).

PEER. (2010). ATC 72-1, Modeling and Acceptance Criteria for Seismic Design and Analysis of Tall Buildings, *Applied Technology Center (ATC), Building Seismic Safety Council (BSSC), National Institute of Building Sciences (NIBS), Federal Emergency Management Agency (FEMA), Pacific Earthquake Research Center (PEER)*, University of California Berkeley, CA.

PEER. (2010). Guidelines for Performance-Based Seismic Design of Tall Buildings (Report No. 2010/5). Tall Buildings Initiative (TBI), University of California, Berkeley, CA: PEER Report.

PEER. (2006). PEER NGA Database*, Pacific Earthquake Engineering Research Center*, University of California, Berkeley, CA. Available from: http://peer.berkeley.edu/nga/

Perus, I. & Fajfar, P. (2005). On the *inelastic* torsional response of single-storey structures under bi-axial excitation, *Earthquake Engineering and Structural Dynamics, 34*, 931-941.

Poursha, M., Khoshnoudian, F. & Moghadam, A.S. (2009). A consecutive modal pushover procedure for estimating the seismic demands of tall buildings, *Engineering Structures, 31*, 591-599.

Poursha, M., Khoshnoudian, F. & Moghadam, A.S. (2011). A consecutive modal pushover procedure for nonlinear static analysis of one-way unsymmetric-plan tall building structures, *Engineering Structures, 33*, 2417-2434.

Poursha, M., Khoshnoudian, F. & Moghadam, A.S. (2014). The extended consecutive modal pushover procedure for estimating the seismic demands of two-way unsymmetric-plan tall buildings under influence of two horizontal components of ground motions, *Soil Dynamics and Earthquake Engineering, 63*, 162-173.

Reyes, J.C. (2009). *Estimating seismic demands for performance-based engineering of buildings*. (Ph.D. Dissertation). Department of Civil and Environmental Engineering, University of California, Berkeley, CA.

Reyes, J.C. & Chopra, A.K. (2011a). Evaluation of three-dimensional modal pushover analysis for unsymmetric-plan buildings subjected to two components of ground motion, *Earthquake Engineering and Structural Dynamics, 40*(13), 1475-1494.

Reyes, J.C. & Chopra, A.K. (2011b). Three-dimensional modal pushover analysis of buildings subjected to two components of ground motion, including its evaluation for tall buildings, *Earthquake Engineering and Structural Dynamics, 40*, 789-806.

SEAONC. (2007). Recommended administrative bulletin on the seismic design and review of tall buildings using non-prescriptive procedures, *Structural Engineers Association of Northern California*, San Francisco.

Shakeri, K., Shayanfar, M.A. & Kabeyasawa, T. (2010). A story shear-based adaptive pushover procedure for estimating seismic demands of buildings, *Engineering Structures, 32*: 174-183.

Shakeri, K., Tarbali, K. & Mohebbi, M. (2012). An adaptive modal pushover procedure for asymmetric-plan buildings, *Engineering Structures, 36*, 160-172.

Stratan, A., & Fajfar, P. (2003). Seismic Assessment of the Spear Test Structure, *Institute of Structural Engineering, Earthquake Engineering and Construction IT* (IKPIR).

Sürmeli, M. & Yüksel, E. (2015). A variant of modal pushover analyses (VMPA) based on a non-incremental procedure, *Bulletin of Earthquake Engineering*, *13,* 3353-3379.

Sürmeli, M. & Yüksel, E. (2018). An adaptive modal pushover analysis procedure (VMPA-A) for buildings subjected to bi-directional ground motions, *Bulletin of Earthquake Engineering*, *16,* 5257-5277.

XTRACT V3.05. (2006). Cross-sectional X sTRuctural Analysis of ComponenTs. *Imbsen Software Systems*. Sacremento, CA 85827, USA.

ANNEX A. Moment-curvature idealisation of elements for SPEAR building

66
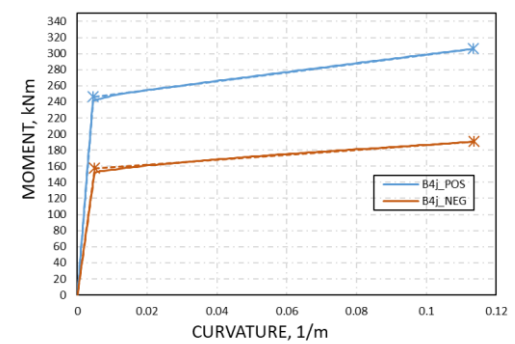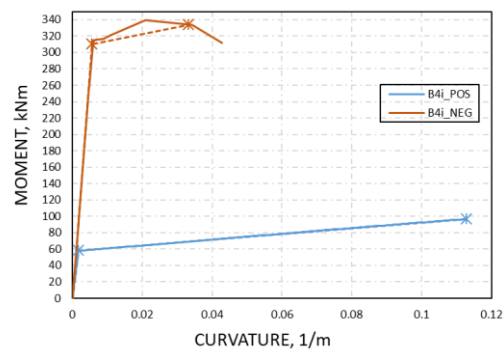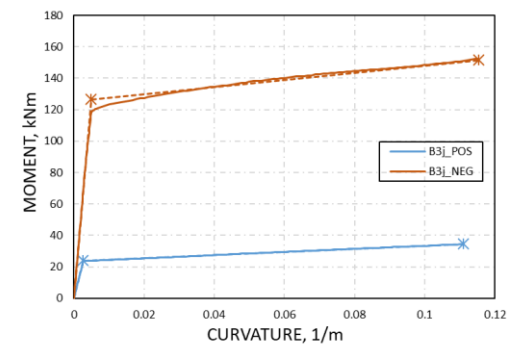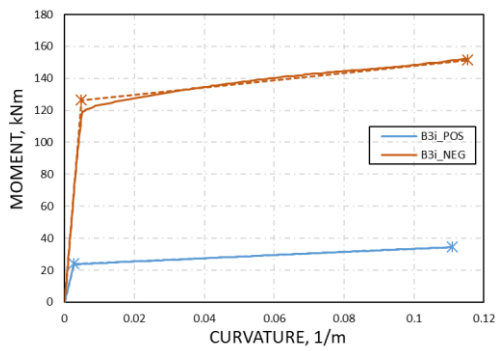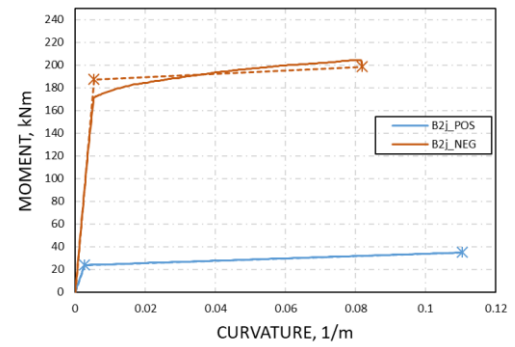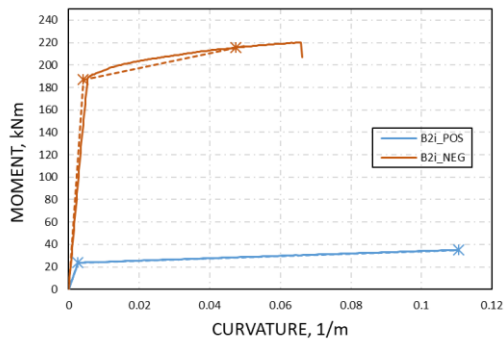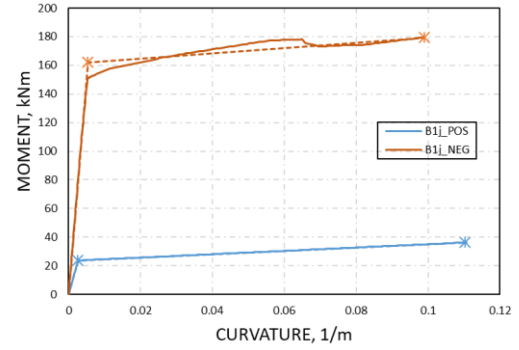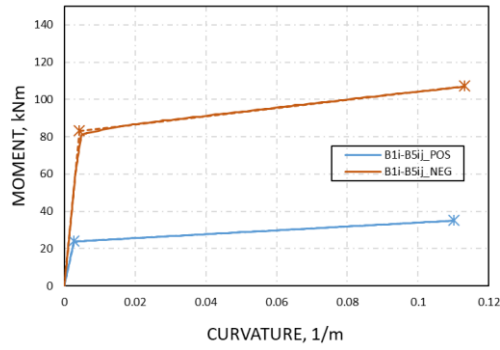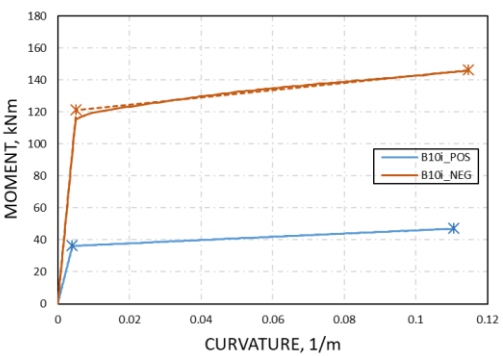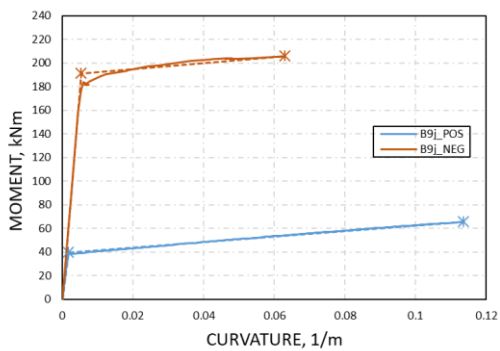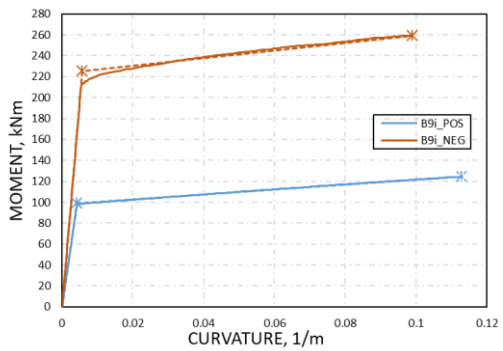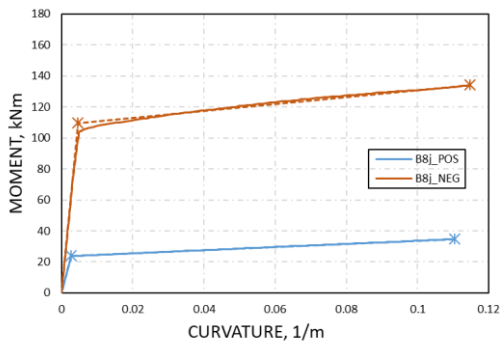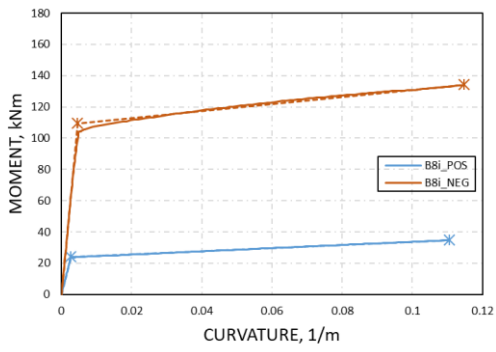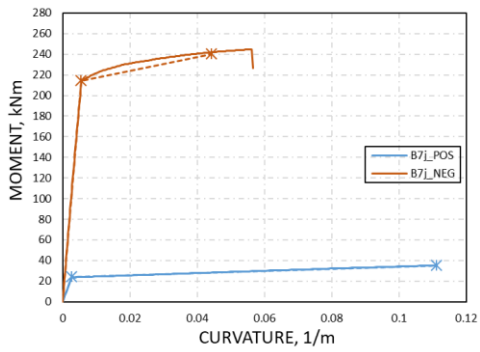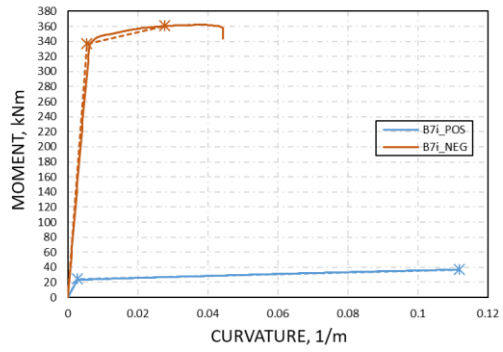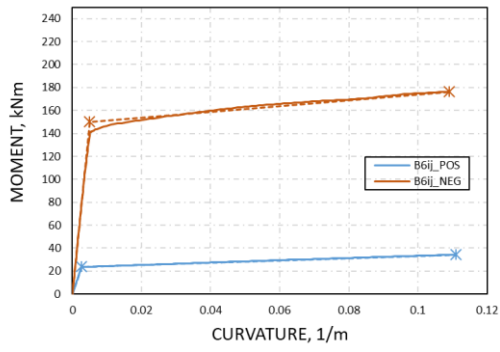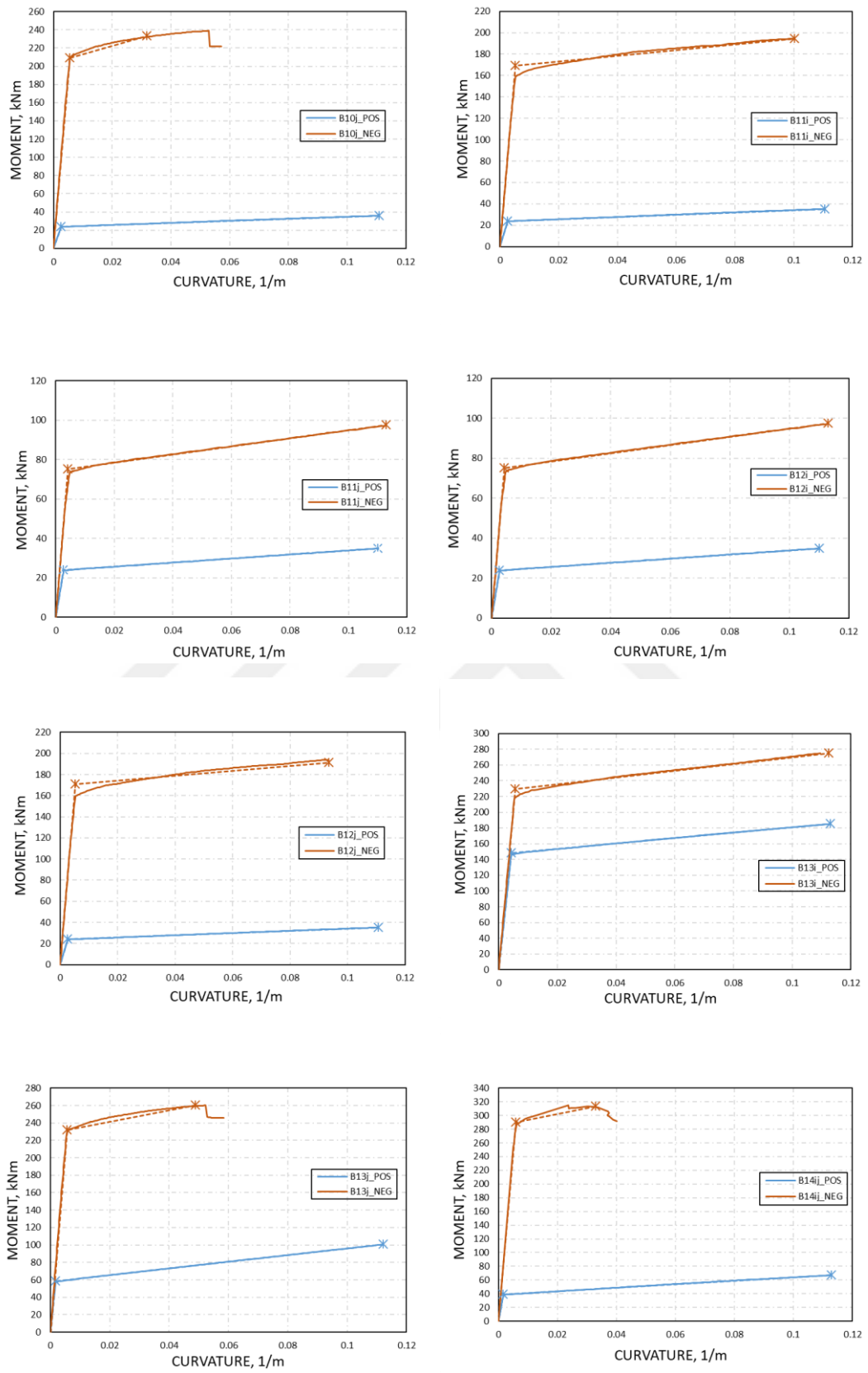
Figure A.1: Moment curvature bilinear idealisations for beams.
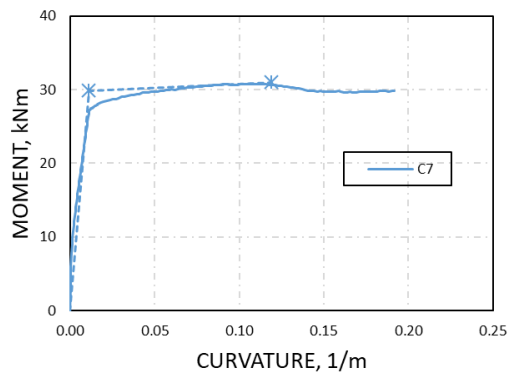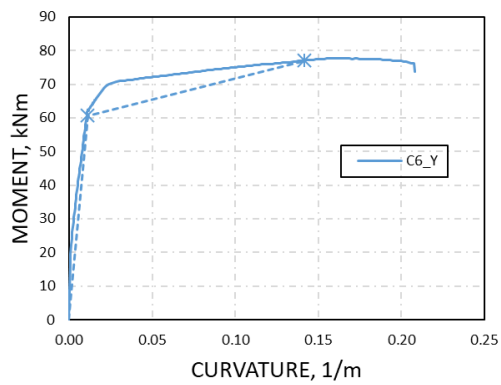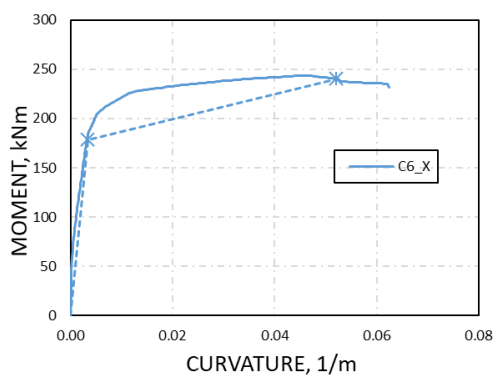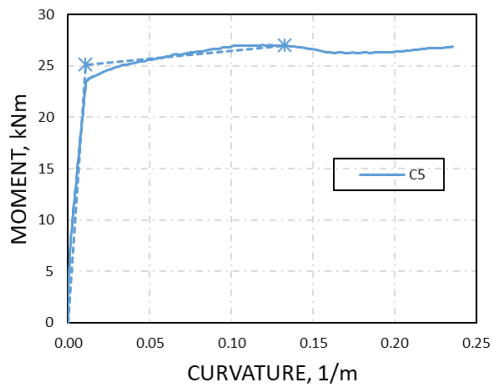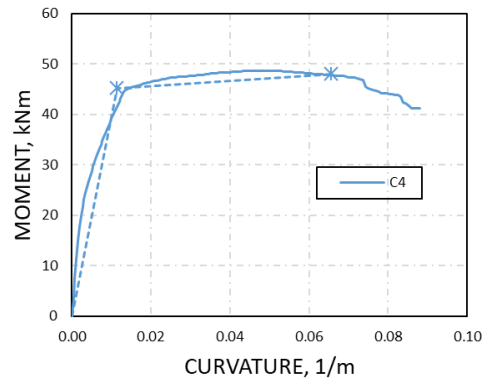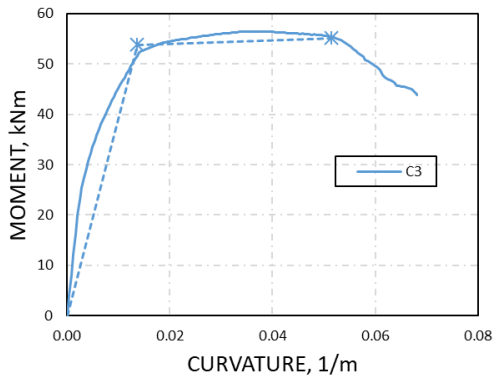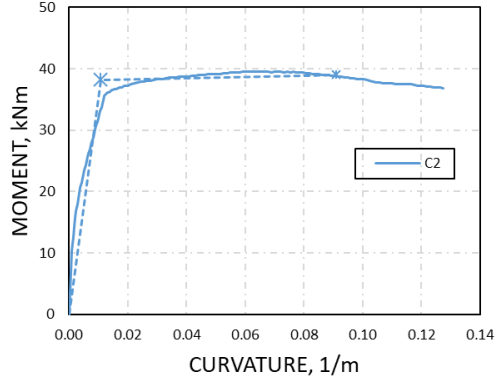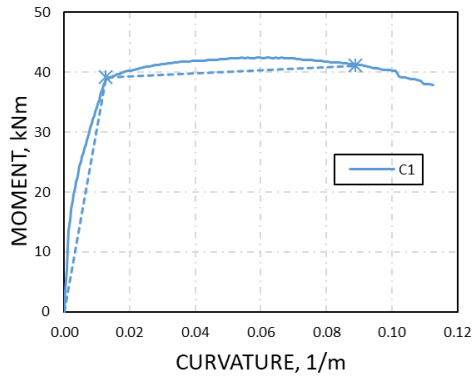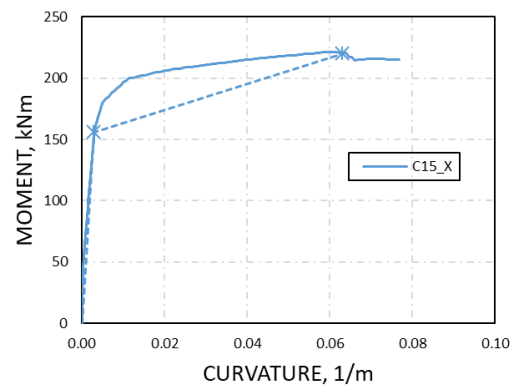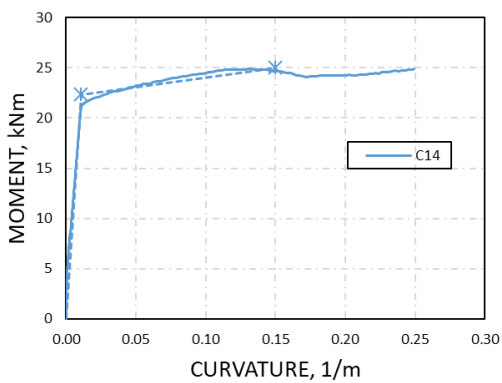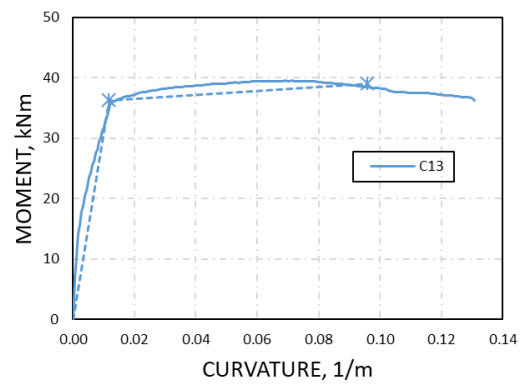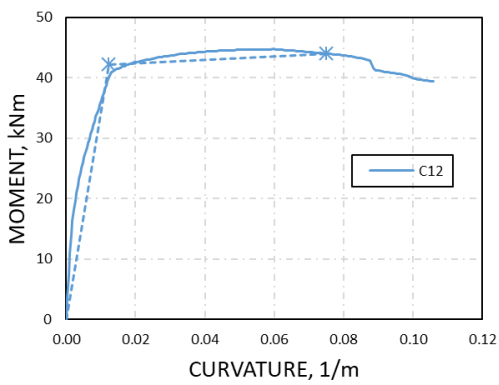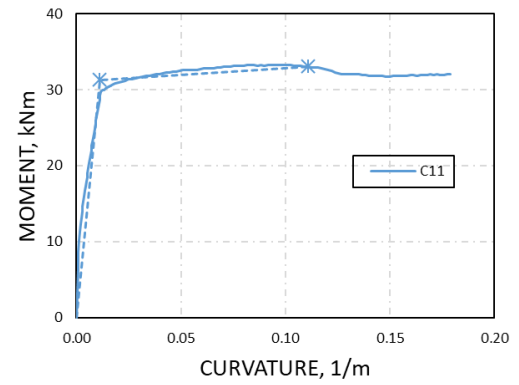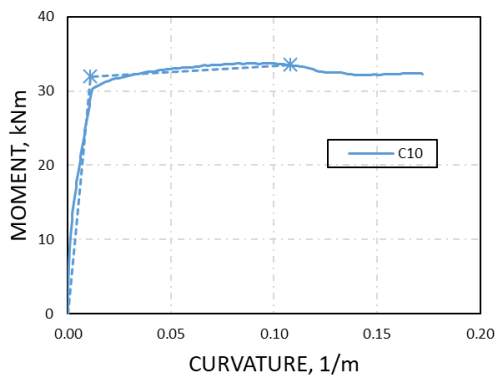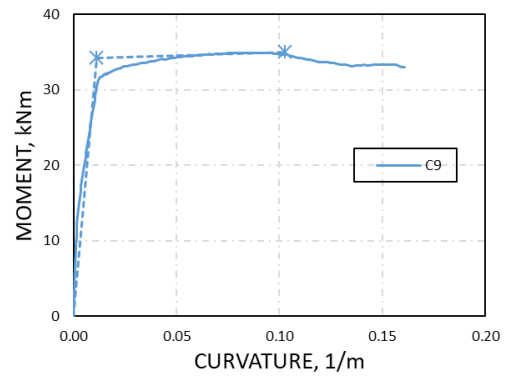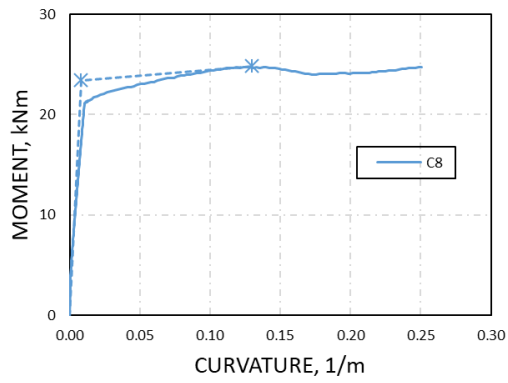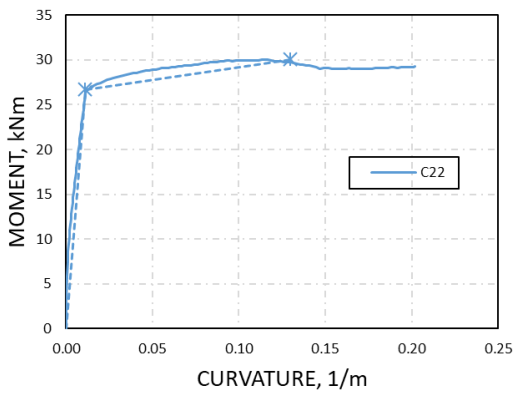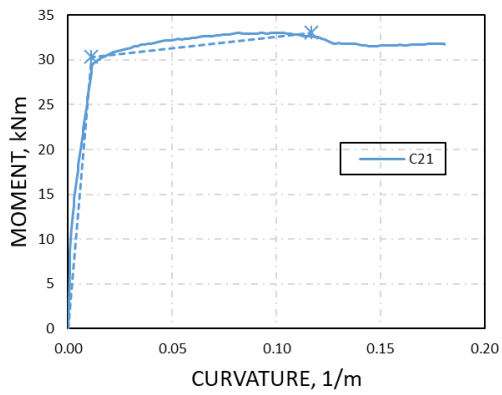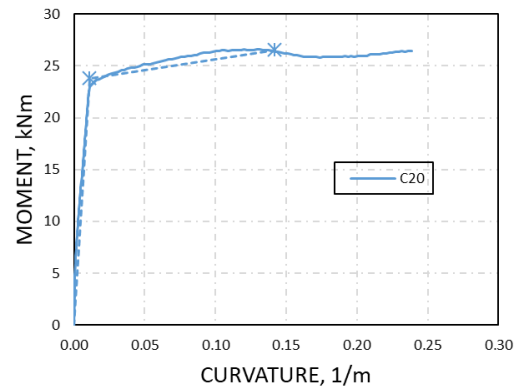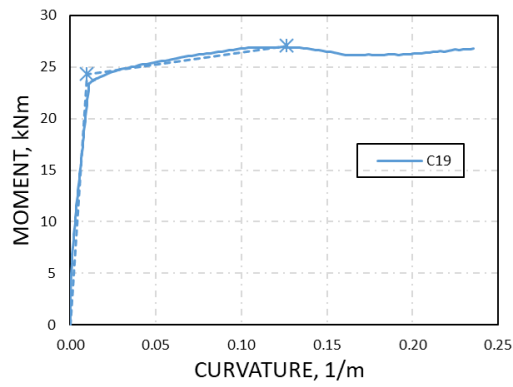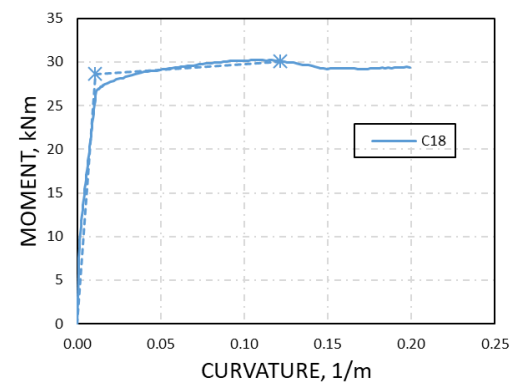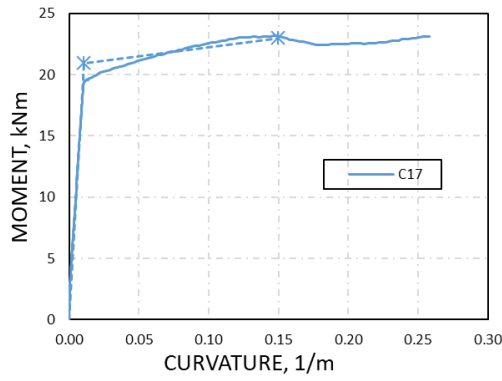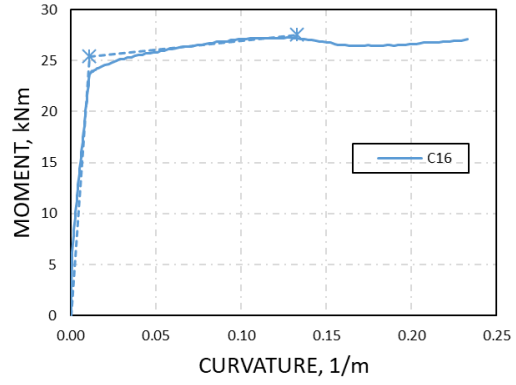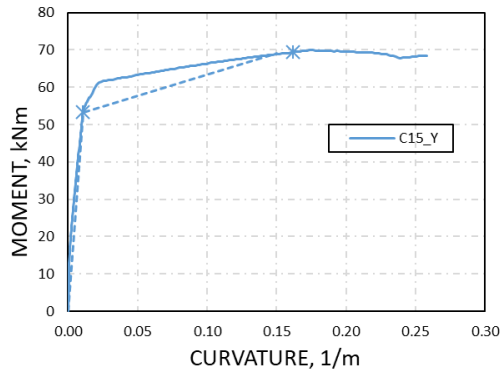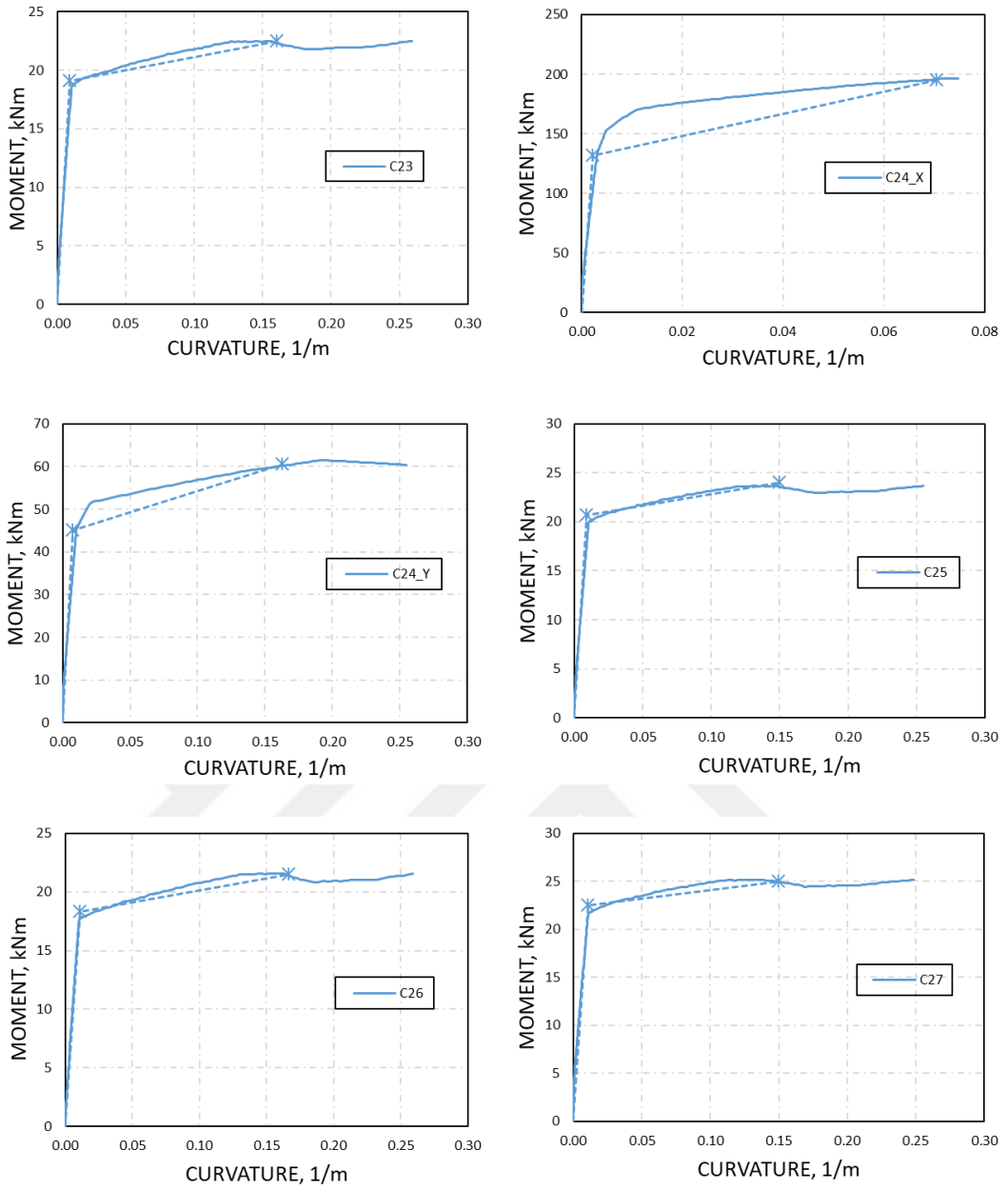
Figure A.2: Moment curvature bilinear idealisations for columns.

ANNEX B. Axial force, moment capacity and yield curvature of columns for 20-story SAC building

Table 20: Axial force, moment capacity and yield curvature of columns.

Story	Element	Axial Force	Moment Capacity (X)	Yield Curvature (X)	Moment Capacity (Y)	Yield Curvature (Y)
Base and ground	A-1	2179	2834	0.0115	2834	0.0115
1st and 2nd	A-1	2032	2838	0.0115	2838	0.0115
2nd and 3rd	A-1	1927	1954	0.0109	1954	0.0109
4rd and 5th	A-1	1721	1962	0.0109	1962	0.0109
5th and 6th	A-1	1621	1617	0.0107	1617	0.0107
7th and 8th	A-1	1424	1625	0.0107	1625	0.0107
8th and 9th	A-1	1324	1629	0.0108	1629	0.0108
10th and 11th	A-1	1119	1636	0.0108	1636	0.0108
11th and 12th	A-1	1016	1639	0.0108	1639	0.0108
13th and 14th	A-1	803	1645	0.0109	1645	0.0109
14th and 15th	A-1	696	1275	0.0107	1275	0.0107
16th and 17th	A-1	482	1280	0.0107	1280	0.0107
17th, 18th and 19th	A-1	317	1282	0.0107	1282	0.0107
19th and 20th	A-1	154	885.5	0.0105	885.5	0.0105
Base and ground	B-1	1970	1328	0.0155	5656	0.00571
1st and 2nd	B-1	1932	1328	0.0155	5659	0.00571
2nd and 3rd	B-1	1892	1328	0.0155	5662	0.00572
4rd and 5th	B-1	1779	1329	0.0155	5670	0.00572
5th and 6th	B-1	1705	850.3	0.0157	3720	0.00584
7th and 8th	B-1	1522	851	0.0157	3738	0.00587
5878th and 9th	B-1	1416	851.4	0.0157	3747	0.00588
10th and 11th	B-1	1180	852.4	0.0157	3765	0.00591
11th and 12th	B-1	1058	700.4	0.0159	3112	0.00597
13th and 14th	B-1	810	701.2	0.0159	3128	0.00600
14th and 15th	B-1	680	453.3	0.0160	2054	0.00614
16th and 17th	B-1	409	453.9	0.0160	2068	0.00618
17th, 18th and 19th	B-1	227	397.8	0.0161	1833	0.00622
19th and 20th	B-1	79	181	0.0230	1255	0.00636
Base and ground	C-1	4397	1310	0.0153	5334	0.00538
1st and 2nd	C-1	4012	1314	0.0153	5401	0.00545
2nd and 3rd	C-1	3760	1317	0.0154	5442	0.00549
4rd and 5th	C-1	3285	1320	0.0154	5511	0.00556
5th and 6th	C-1	3060	844.7	0.0156	3526	0.00554
7th and 8th	C-1	2636	846.5	0.0156	3599	0.00565
5878th and 9th	C-1	2438	847.3	0.0156	3629	0.00570
10th and 11th	C-1	2057	848.9	0.0157	3681	0.00578
11th and 12th	C-1	1870	697.7	0.0158	3027	0.00581
13th and 14th	C-1	1500	699	0.0158	3072	0.00589
14th and 15th	C-1	1319	451.7	0.0160	1994	0.00596
16th and 17th	C-1	967	452.6	0.0160	2032	0.00607
17th, 18th and 19th	C-1	687	396.9	0.0161	1811	0.00615
19th and 20th	C-1	380	180.5	0.0230	1247	0.00632

Table 21: Axial force, moment capacity and yield curvature of columns (continued).

Story	Element	Axial Force	Moment Capacity (X)	Yield Curvature (X)	Moment Capacity (Y)	Yield Curvature (Y)
Base and ground	A-2	3620	5464	0.00552	1318	0.0154
1st and 2nd	A-2	3348	5503	0.00555	1319	0.0154
2nd and 3rd	A-2	3166	5527	0.00558	1320	0.0154
4rd and 5th	A-2	2807	5573	0.00563	1323	0.0154
5th and 6th	A-2	2629	3600	0.00565	846.5	0.0156
7th and 8th	A-2	2277	3652	0.00573	848	0.0156
8th and 9th	A-2	2105	3675	0.00577	848.7	0.0157
10th and 11th	A-2	1764	3714	0.00583	850	0.0157
11th and 12th	A-2	1595	3061	0.00587	698.7	0.0158
13th and 14th	A-2	1262	3095	0.00594	699.8	0.0159
14th and 15th	A-2	1098	2020	0.00604	452.3	0.0160
16th and 17th	A-2	775	2048	0.00612	453	0.0160
17th, 18th and 19th	A-2	450	1825	0.00619	397.4	0.0161
19th and 20th	A-2	283	1251	0.00634	180.6	0.0230
Base and ground	A-3	3882	5422	0.00547	1316	0.0153
1st and 2nd	A-3	3605	5466	0.00552	1318	0.0154
2nd and 3rd	A-3	3415	5493	0.00554	1319	0.0154
4rd and 5th	A-3	3041	5544	0.00560	1321	0.0154
5th and 6th	A-3	2855	3563	0.00559	845.6	0.0156
7th and 8th	A-3	2485	3622	0.00569	847.1	0.0156
5878th and 9th	A-3	2301	3648	0.00573	847.9	0.0156
10th and 11th	A-3	1936	3695	0.00580	849.3	0.0157
11th and 12th	A-3	1754	3042	0.00584	698.1	0.0158
13th and 14th	A-3	1391	3083	0.00592	699.3	0.0158
14th and 15th	A-3	1208	2007	0.00600	452	0.0160
16th and 17th	A-3	843	2043	0.00610	452.9	0.0160
17th, 18th and 19th	A-3	568	1819	0.00617	397.1	0.0161
19th and 20th	A-3	291	1250	0.00634	180.6	0.0230
Base and ground	A-4	3939	5413	0.00546	1315	0.0153
1st and 2nd	A-4	3660	5458	0.00551	1317	0.0154
2nd and 3rd	A-4	3469	5486	0.00554	1319	0.0154
4rd and 5th	A-4	3093	5537	0.00559	1321	0.0154
5th and 6th	A-4	2905	3554	0.00558	845.4	0.0156
7th and 8th	A-4	2530	3615	0.00568	846.9	0.0156
5878th and 9th	A-4	2343	3643	0.00572	847.7	0.0156
10th and 11th	A-4	1972	3691	0.00580	849.2	0.0157
11th and 12th	A-4	1785	3038	0.00583	698	0.0158
13th and 14th	A-4	1413	3080	0.00591	699.3	0.0158
14th and 15th	A-4	1227	2005	0.00599	451.9	0.0160
16th and 17th	A-4	855	2042	0.00610	452.8	0.0160
17th, 18th and 19th	A-4	575	1818	0.00617	397.1	0.0161
19th and 20th	A-4	294	1250	0.00634	180.6	0.0230
Base, Ground,1st and 2nd	C-3	9660	3146	0.0116	5576	0.00710
2nd, 3rd, 4th and 5th	C-3	8354	2531	0.0119	4373	0.00731
5th, 6th, 7th and 8th	C-3	6927	2005	0.0121	3399	0.00751
8th, 9th, 10th and 11th	C-3	5499	1661	0.0124	2815	0.00781
11th, 12th, 13th and 14th	C-3	4072	1357	0.0126	2342	0.00827
14th, 15th, 16th and 17th	C-3	2644	903.6	0.0130	1560	0.00876
17th, 18th, 19th and 20th	C-3	1217	519.5	0.0140	994.6	0.00964
20th	C-3	503	96.21	0.0256	359.7	0.01010

ANNEX C. Moment-curvature idealisation of elements for 20-story SAC building
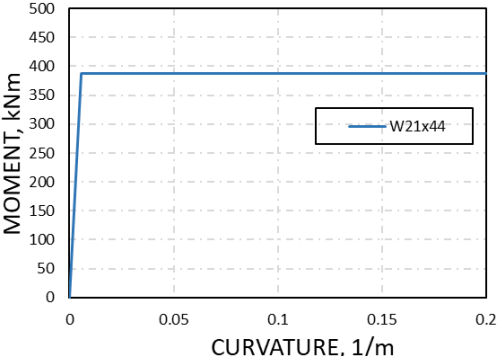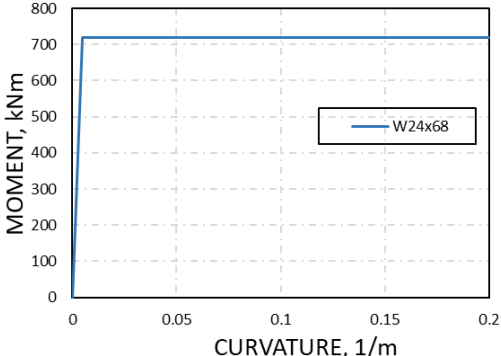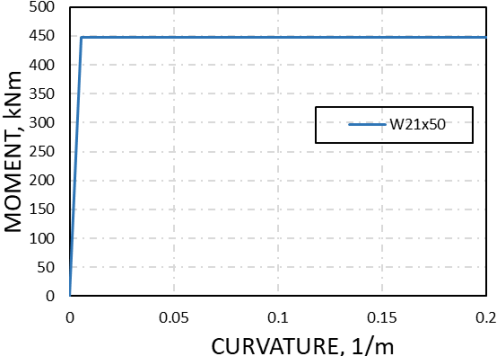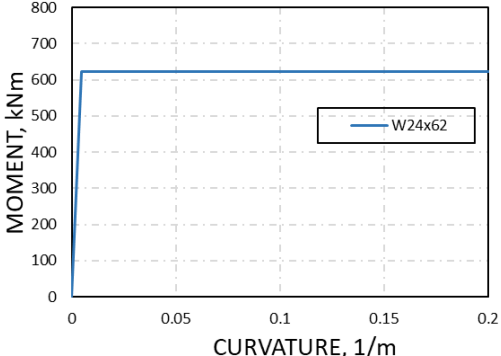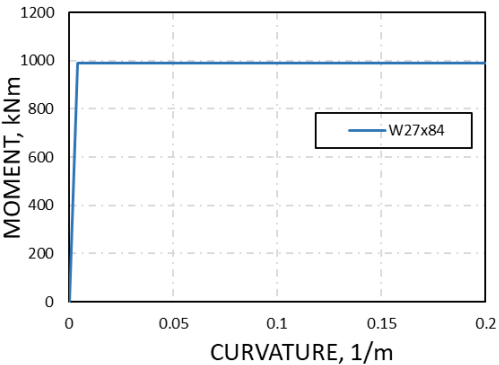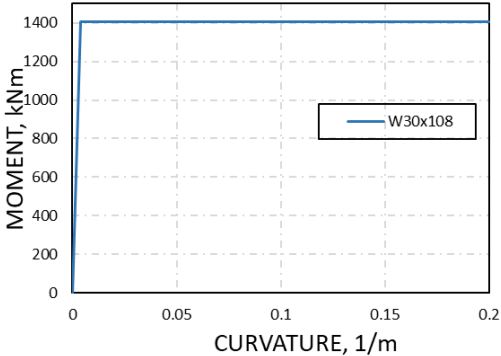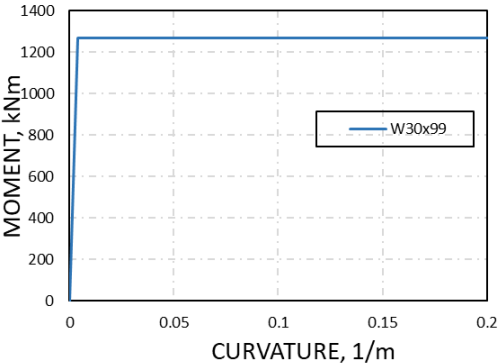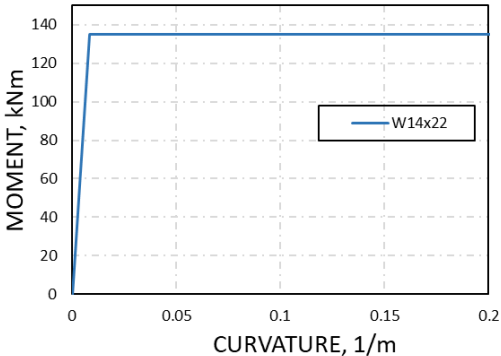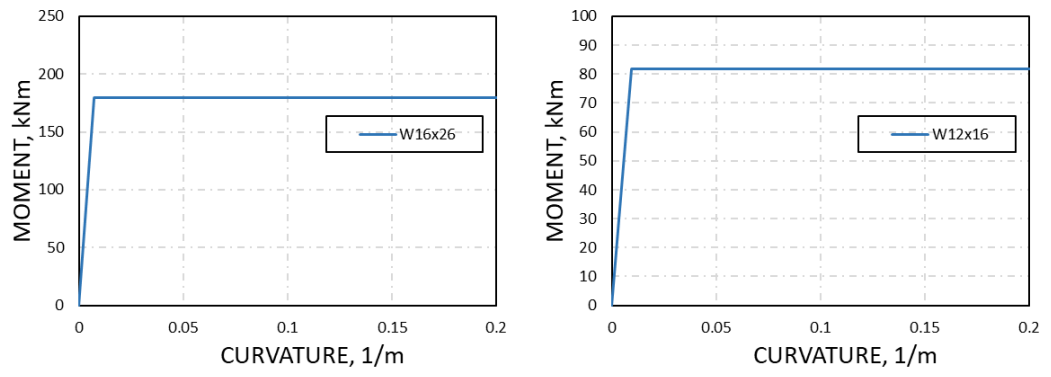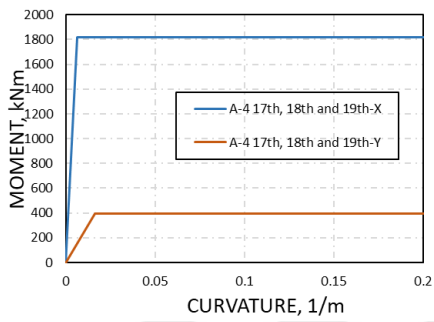
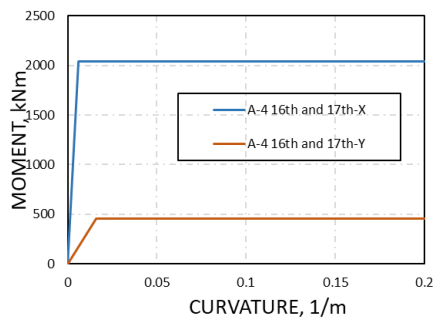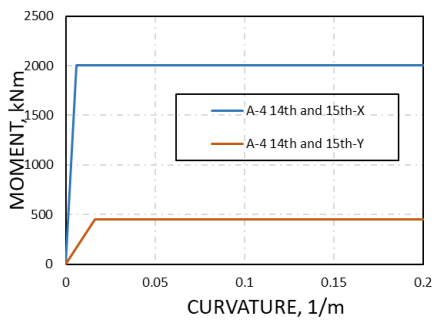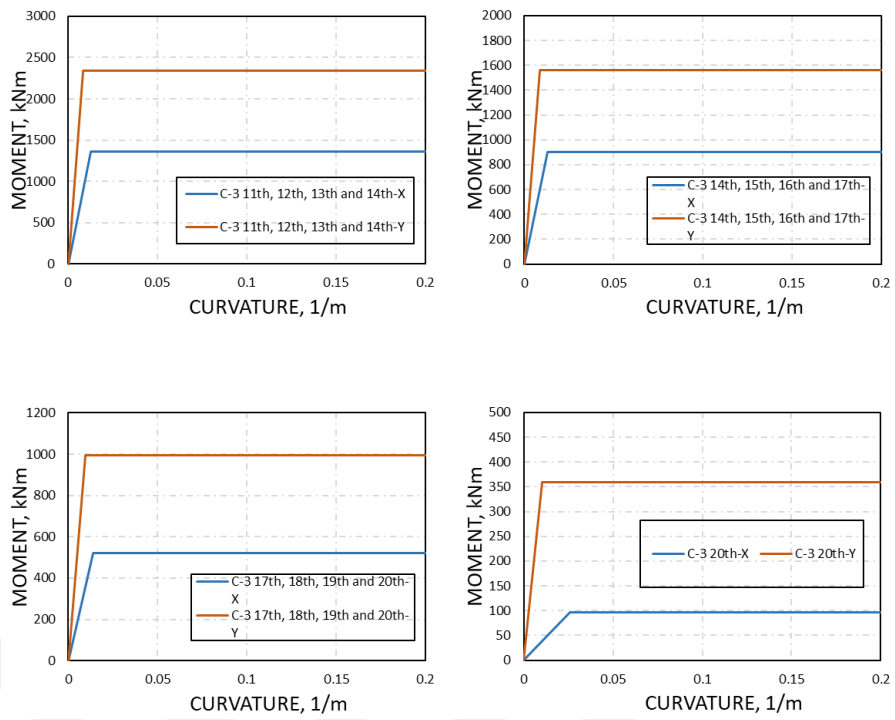**Figure C.1:** Moment curvature relationship for beams.
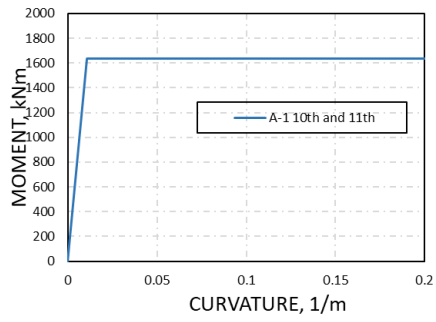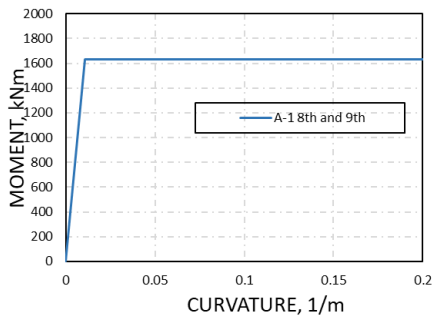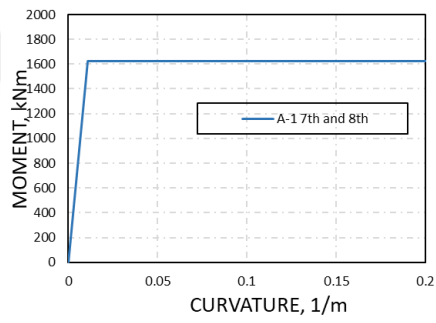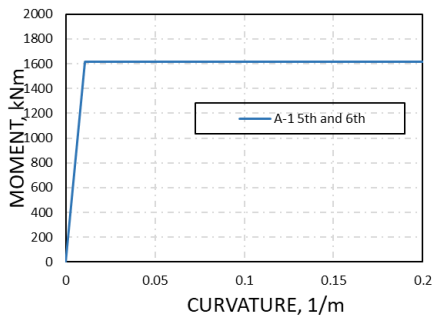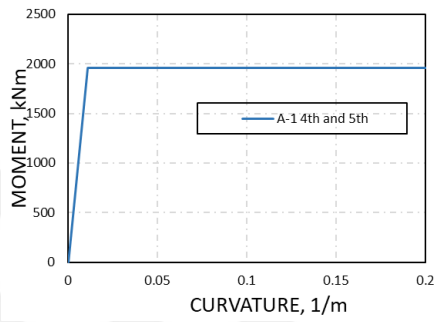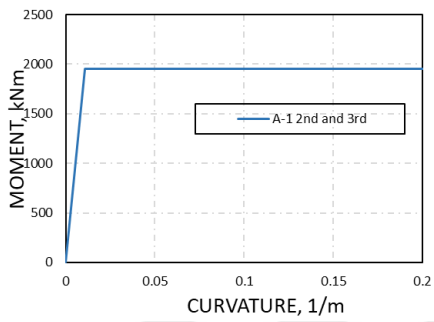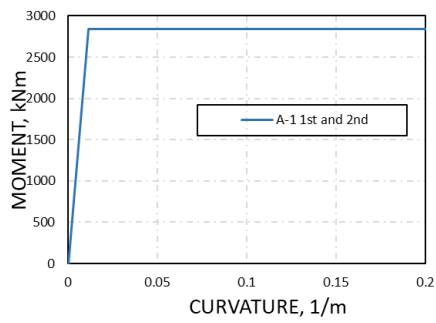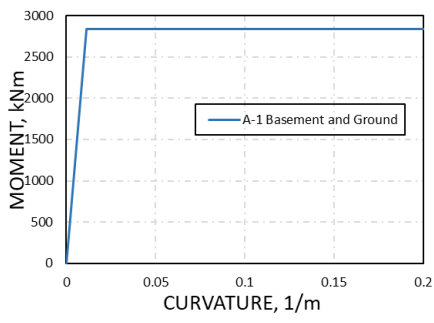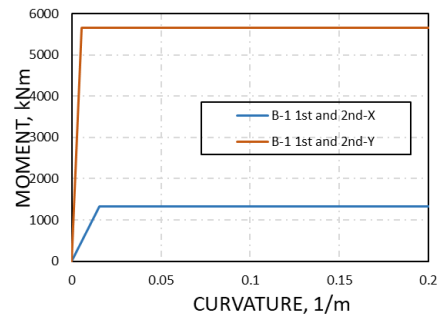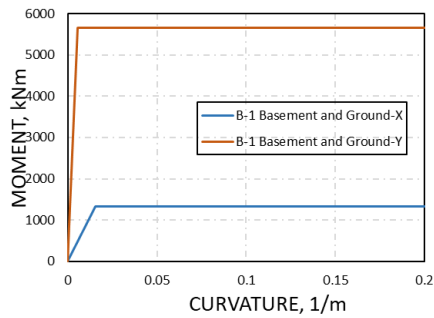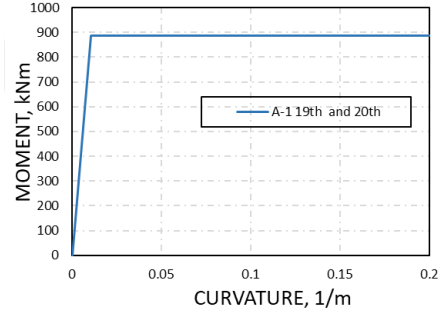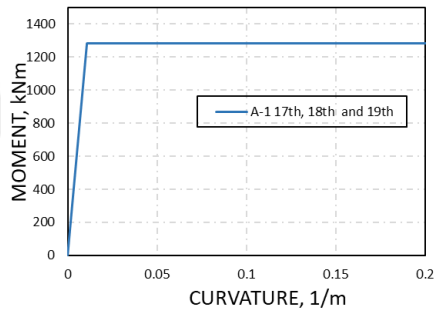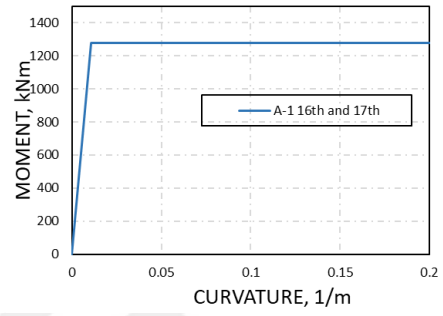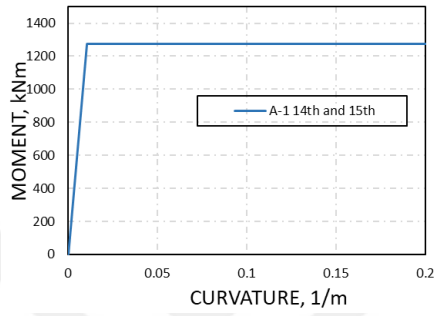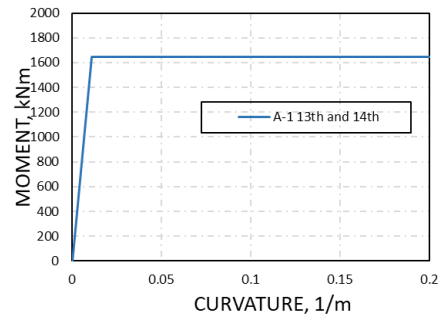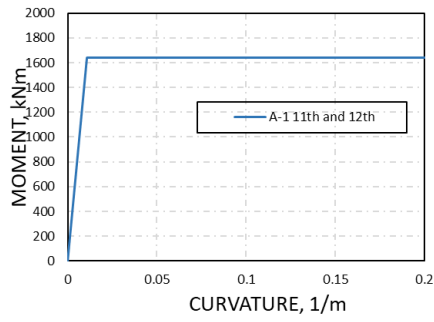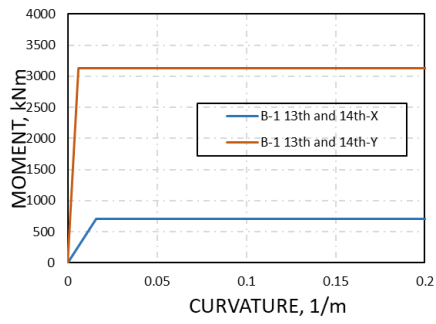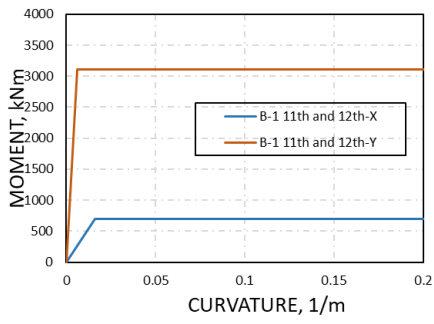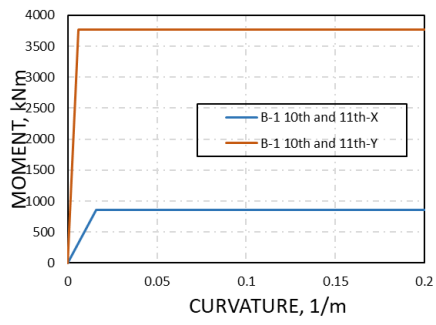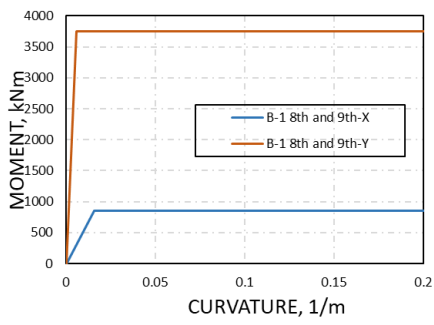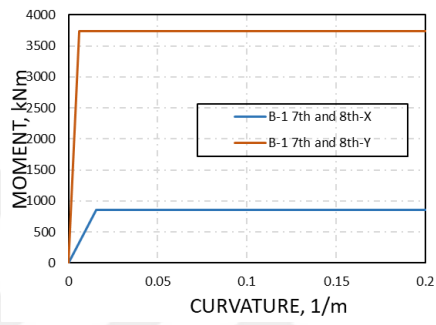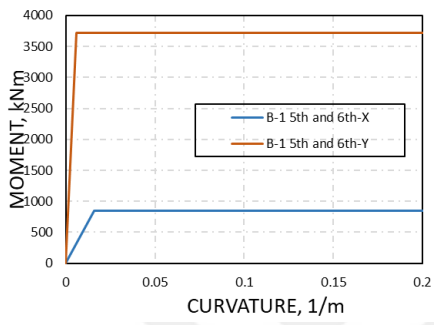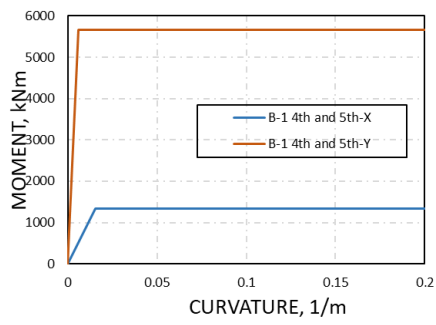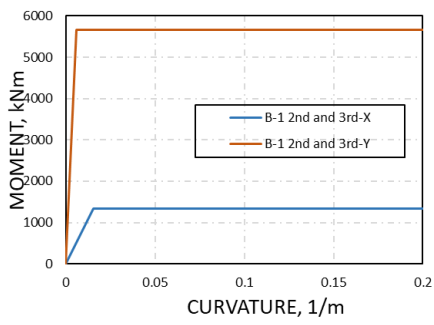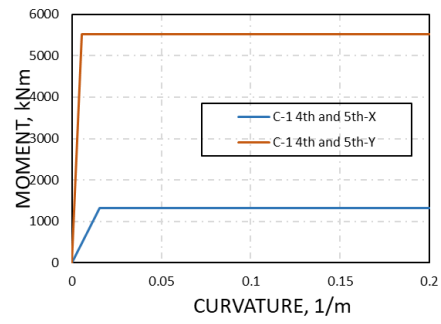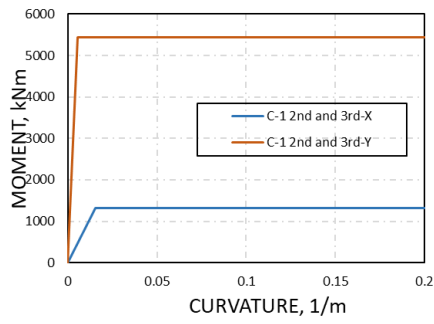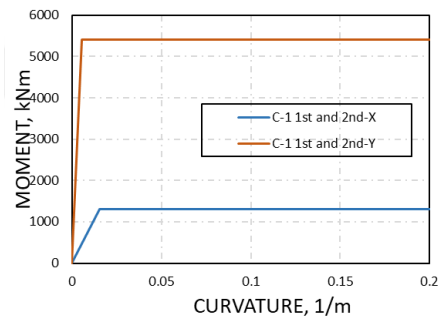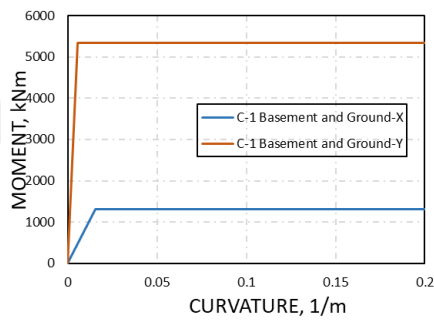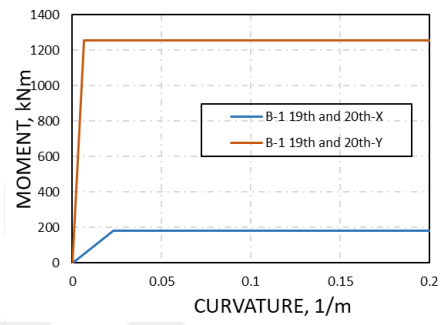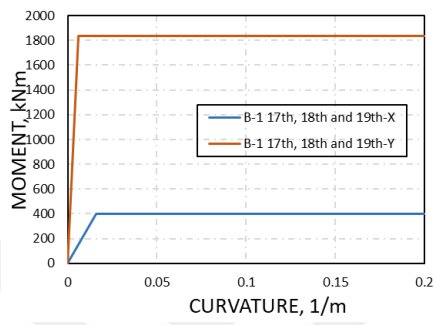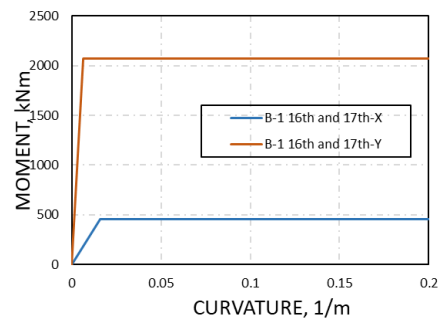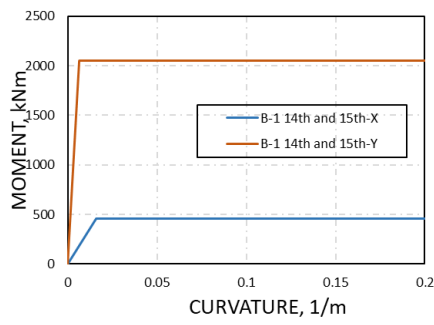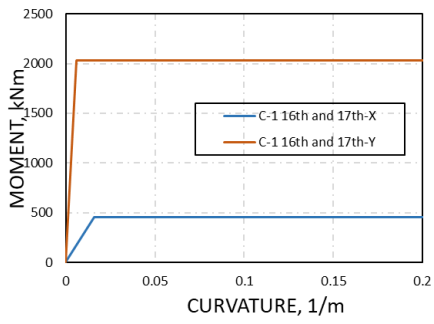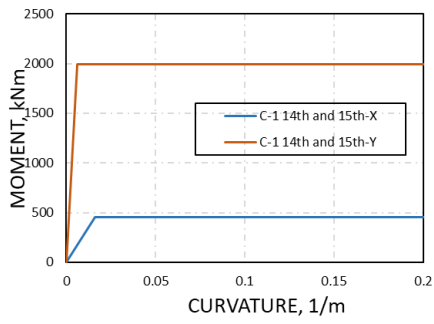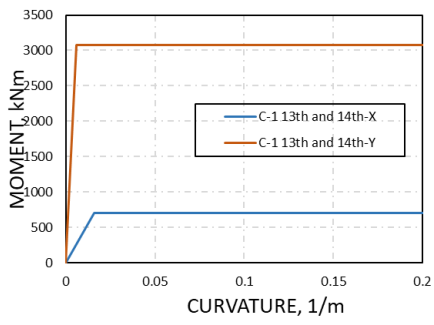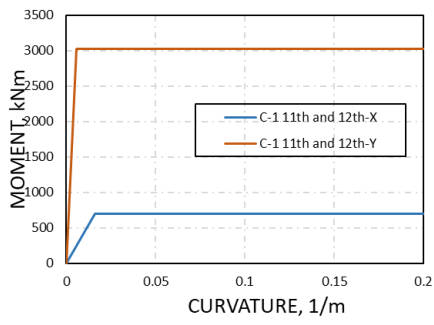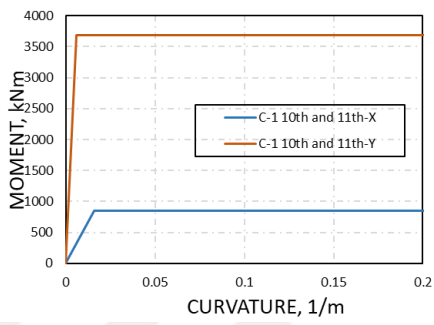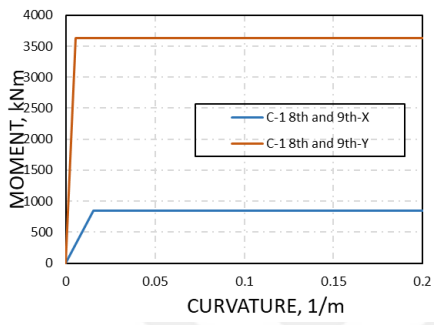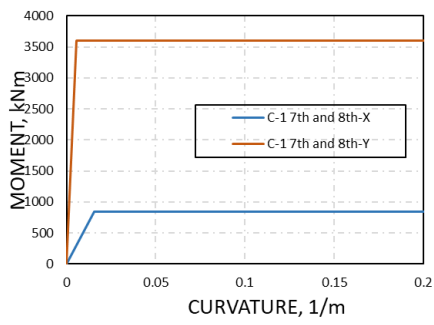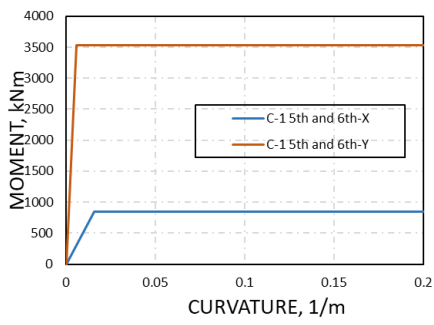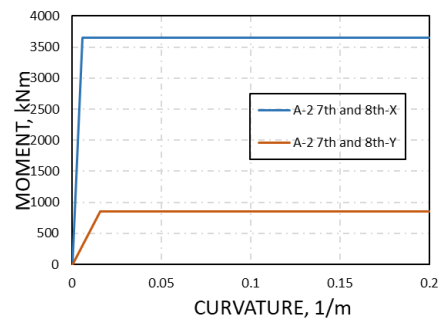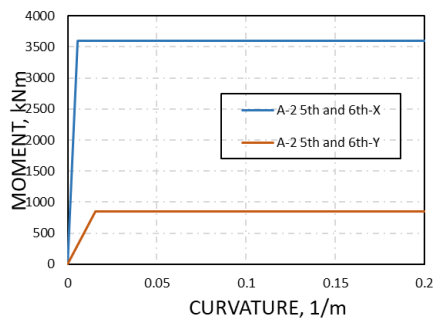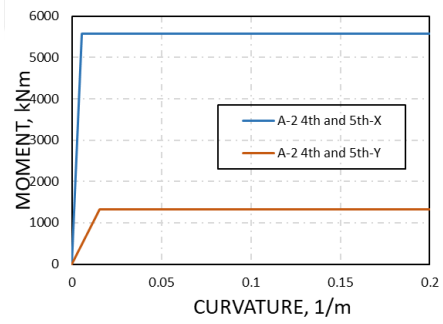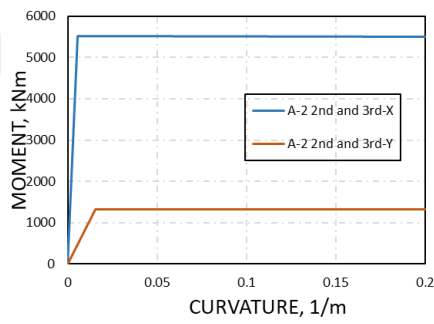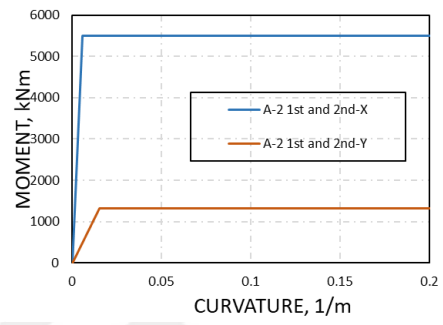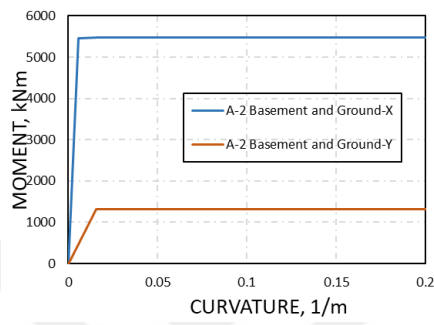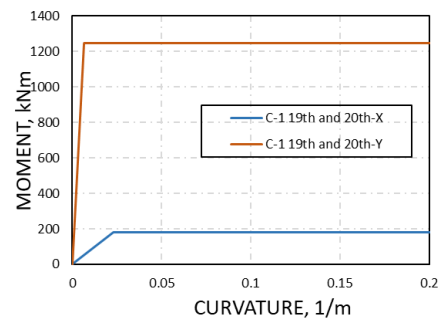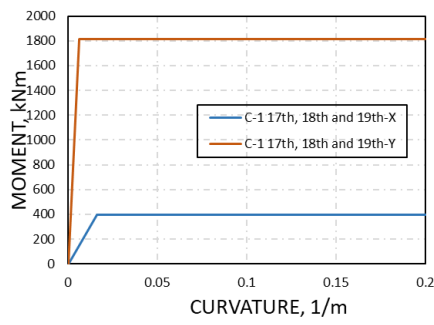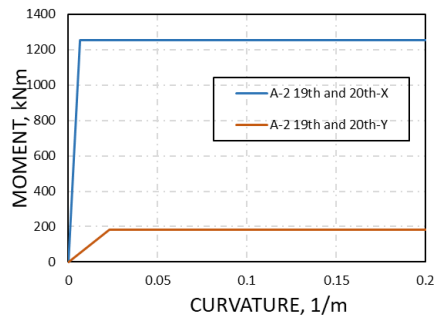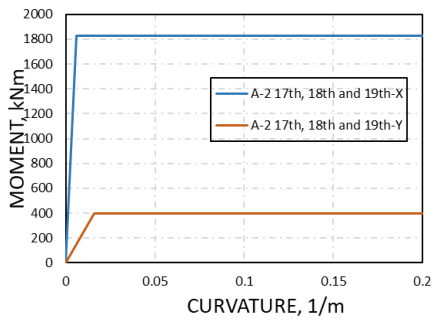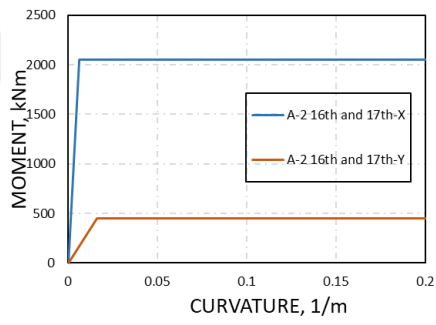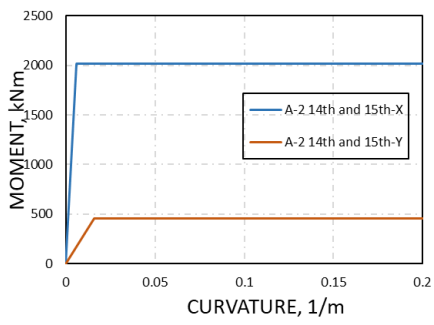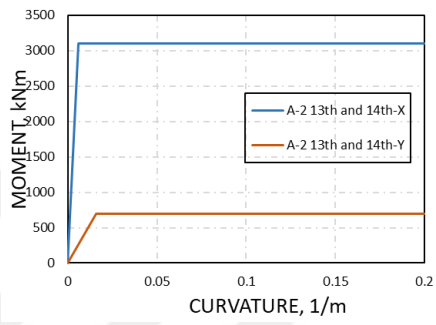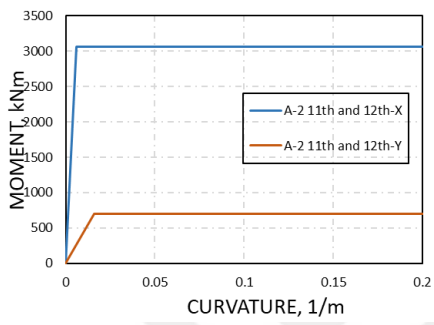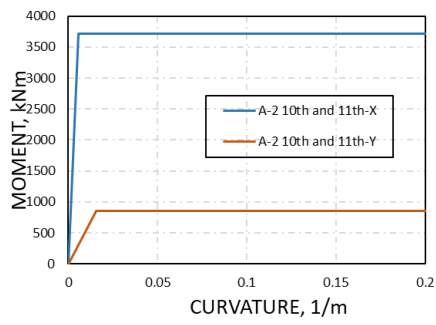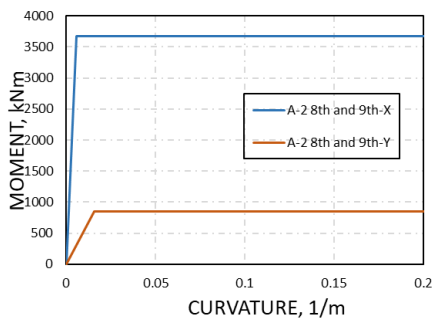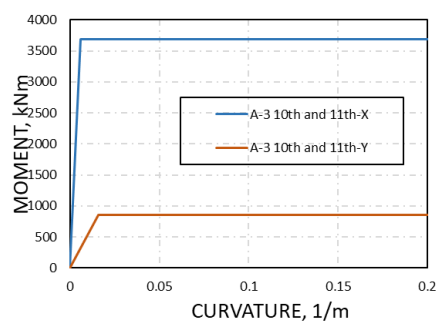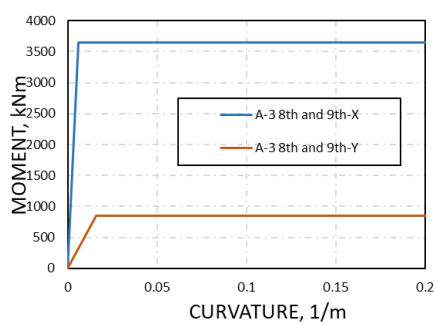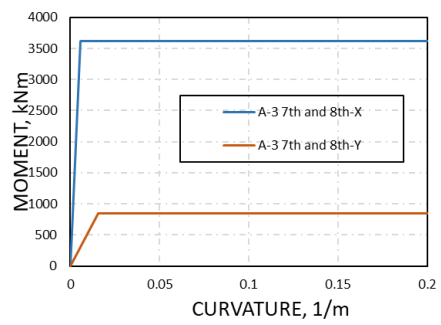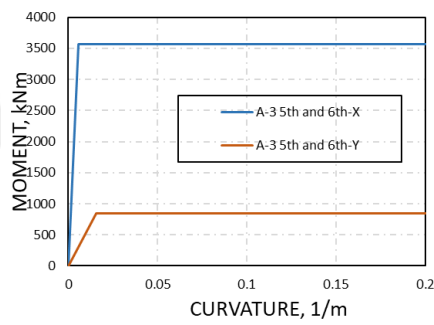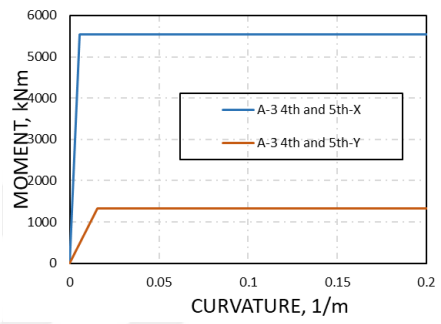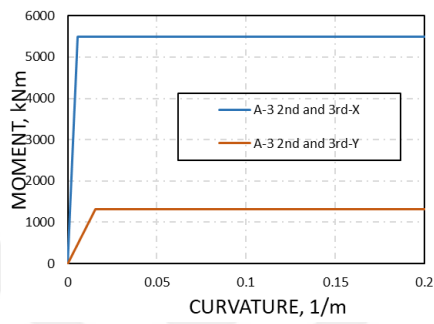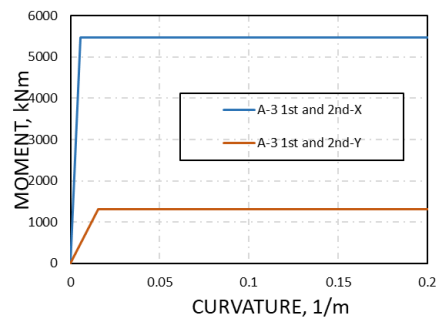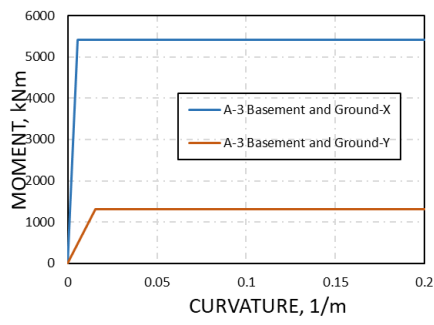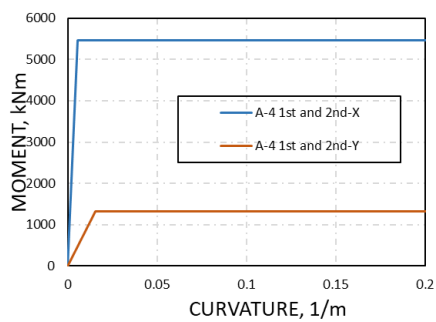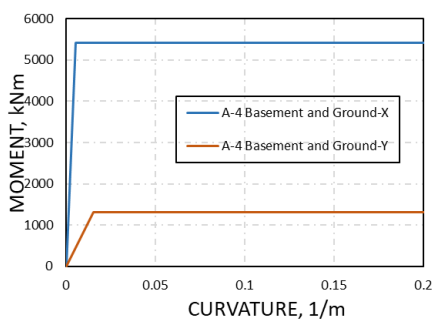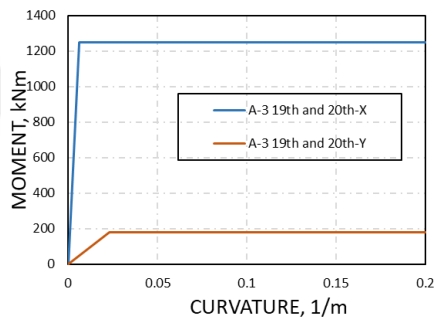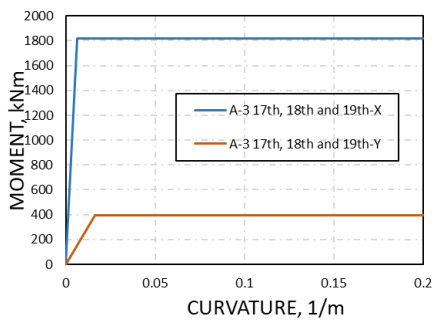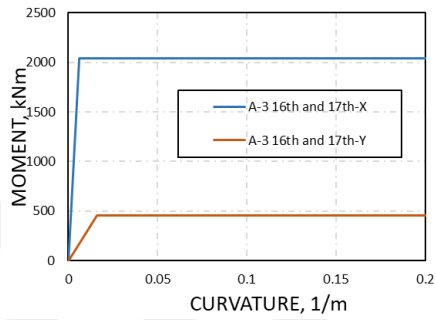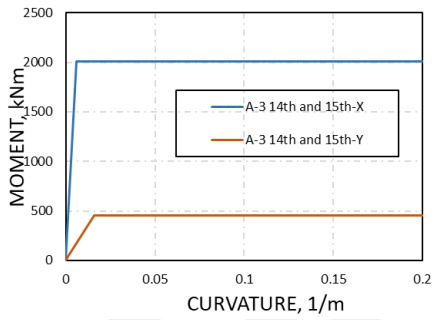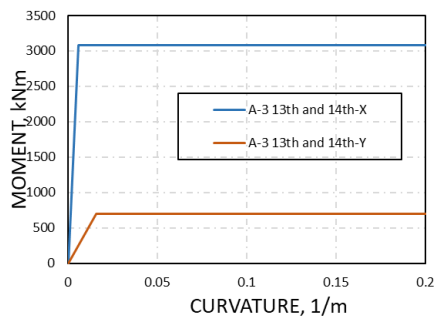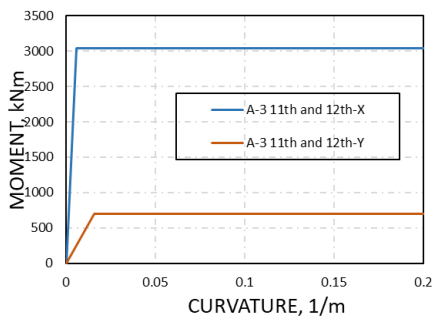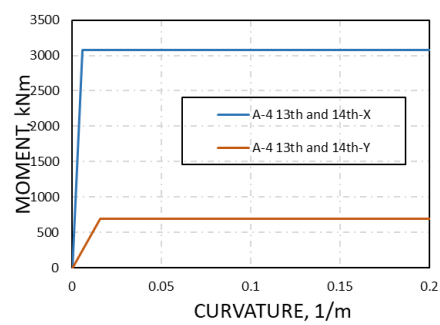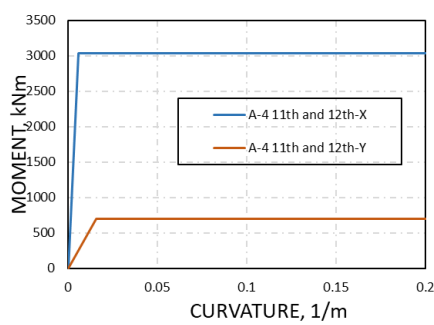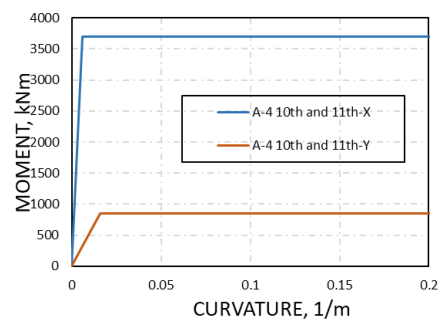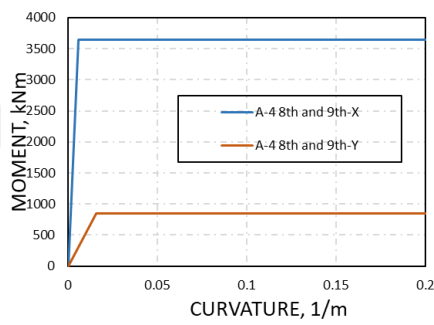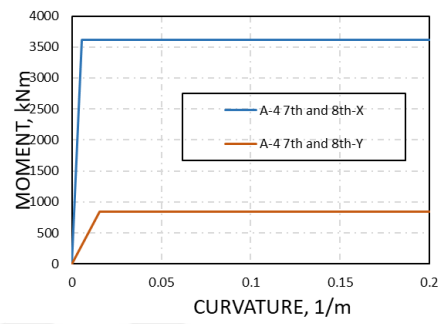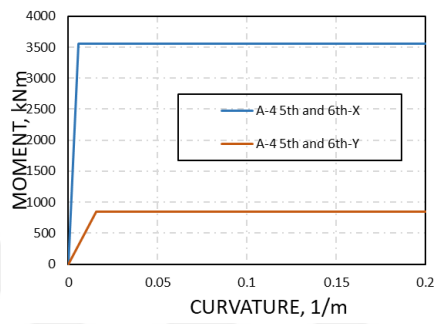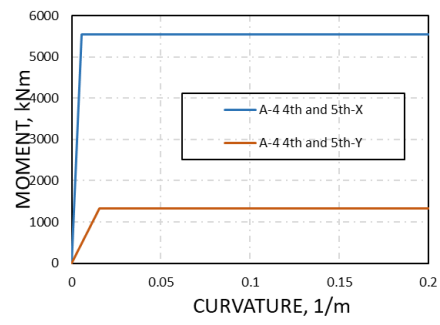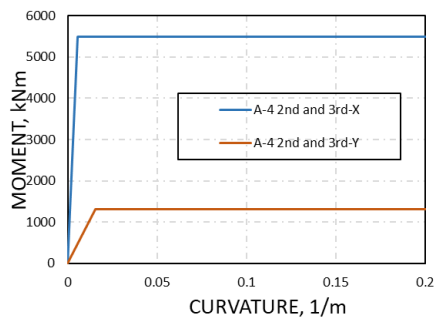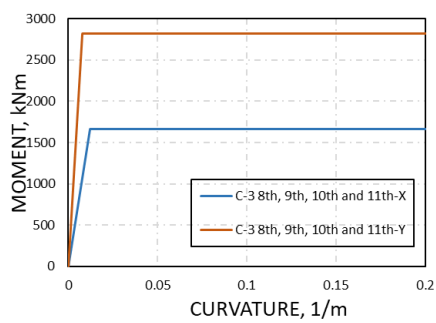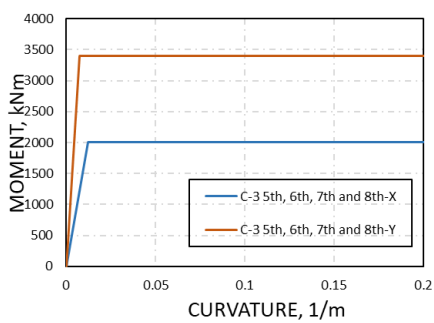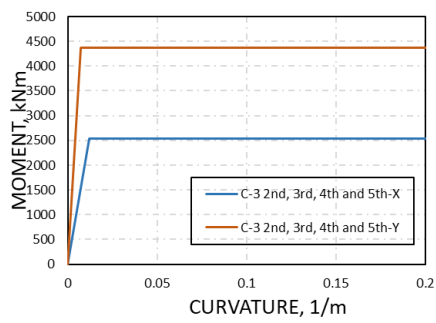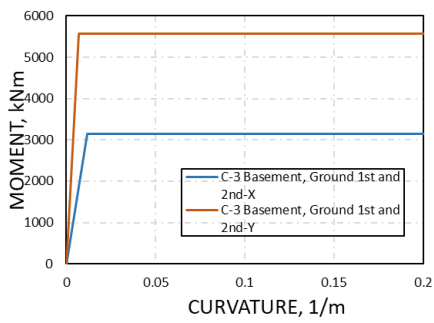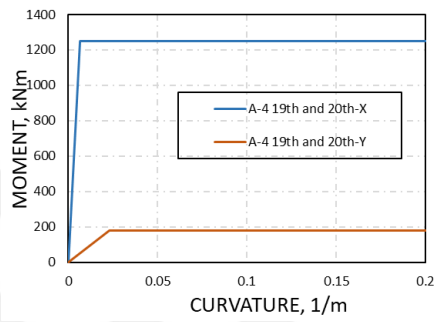
Figure C.2: Moment curvature relationship for columns.

ÖZGEÇMİŞ

Ad-Soyad   **: Özge OSMAK**

Doğum Tarihi ve Yeri   : 10.08.1994, Bakırköy

E-posta   : ozge.osmak@gmail.com

ÖĞRENİM DURUMU:

- **Lisans**   **:** 2017, İstanbul Kültür Üniversite, Mühendislik Fak., İnşaat Müh. Bölümü

MESLEKİ DENEYİM VE ÖDÜLLER: